THE ROLE OF ELECTROSTATIC INTERACTIONS IN THE PREDICTION OF PHASE EQUILIBRIUM OF DME MIXTURES USING SAFT EOS

SAIFUDDIN AHMED

CHEMICAL ENGINEERING

FEBRUARY 2015

THE ROLE OF ELECTROSTATIC INTERACTIONS IN THE PREDICTION OF PHASE EQUILIBRIUM OF DME MIXTURES USING SAFT EOS

BY

SAIFUDDIN AHMED

A Thesis Presented to the
DEANSHIP OF GRADUATE STUDIES

KING FAHD UNIVERSITY OF PETROLEUM & MINERALS

DHAHRAN, SAUDI ARABIA

In Partial Fulfillment of the
Requirements for the Degree of

MASTER OF SCIENCE

In

CHEMICAL ENGINEERING

FEBRUARY 2015

KING FAHD UNIVERSITY OF PETROLEUM & MINERALS

DHAHRAN- 31261, SAUDI ARABIA

DEANSHIP OF GRADUATE STUDIES

This thesis, written by SAIFUDDIN AHMED under the direction his thesis advisor and approved by his thesis committee, has been presented and accepted by the Dean of Graduate Studies, in partial fulfillment of the requirements for the degree of MASTER OF SCIENCE IN CHEMICAL ENGINEERING.

Dr. Mohammed Ba-Shammakh
Department Chairman

Dr. Salam A. Zummo
Dean of Graduate Studies

19/2/15
Date

Dr. Nayef M. Al-Saifi
(Advisor)

Dr. Ali Al-Matar
(Co-Advisor)

Dr. Nabeel S. M. Abo-Ghander
(Member)

Dr. Zuhair Omar Malaibari
(Member)

B. H.

Dr. Housam Binous
(Member)

DEDICATION

To my parents

and

my siblings

ACKNOWLEDGEMENTS

I use this great opportunity to express my high gratitude to my supervisor Dr. Nayef M. Al-Saifi for giving me a privilege of working with him guiding me all through my research work, for being a great support both technical and moral, motivating me through each step and I also give great appreciation and obligation to my co-advisor Dr. Ali-Al Matar and thesis committee members Dr. Nabeel Salim Abo-Ghander, Dr. Zuhair Malaibari, Dr. Housam Binous for their time and effort in evaluating my work and giving advises to improve the same.

I want to extend my sincere thanks to my friends and colleagues, Waqar Ahmad, Adeem Ghaffar Rana, Saqib Javed, Fahad Ali Rabbani, Amir Abbas, Naim Younis and Farrukh Shehzad for their high support and being a part of my life at KFUPM without them it would have been very difficult to manage this huge task.

I am highly obligated to King Fahd University of Petroleum and Minerals and ministry of higher education Saudi Arabia for providing me Full Time scholarship and monthly bursaries to pursue my master’s degree. Also I would like to thank KFUPM for providing all needed computational resources and application MATLAB® to carry out my work hassle free.

Finally I would like to thank my parent and my siblings for being a support all through my studies far away from my home.

TABLE OF CONTENTS

LIST OF TABLES

LIST OF FIGURES

LIST OF ABBREVIATIONS

2CLJ	:	2 centered Lennard Jones
AADP	:	Average absolute deviation in pressure
AADY	:	Average absolute deviation in vapor mole fraction
CK-SAFT	:	Chen Kreglewski SAFT
CPA	:	Cubic plus association
DME	:	Dimethyl Ether
EOS	:	Equation of State
GV	:	Gross and Vrabec
HE	:	Helmholtz energy
JC	:	Jog and Chapman
LHV	:	Lower heating value
LJ-SAFT	:	Lennard-Jones SAFT
PC-SAFT	:	Perturbed Chain SAFT
PVT	:	Pressure Volume Temperature
SAFT	:	Statistical Associating Fluid Theory
SSAFT	:	Simplified SAFT
SAFT-VR	:	SAFT Variable range
SRK	:	Soave Redlich Kwong
SSAFT-JC	:	Simplified SAFT Jog and Chapman
SSAFT-GV	:	Simplified SAFT Gross and Vrabec
VLE	:	Vapor liquid equilibrium

ABSTRACT

Dimethyl ether is a potential future alternative candidate due its economic and environmental advantages. Over the past years, extensive research has been conducted to develop feasible production processes. In most of the available and proposed production processes, mixtures of various components with dimethyl ether including water, alcohol, hydrocarbons, carbon dioxide and light gases are encountered. Accurate phase equilibrium data are crucial in designing separation units for dimethyl ether mixtures. Thermodynamic modeling of the involved mixtures is not trivial due to the presence of various electrostatic interactions such as dipole-dipole, association as well as to the quantum effects exhibited by very small molecules such as hydrogen. In this work, the dipole-dipole and induced association interactions are deployed using the dipole-dipole theories developed by Jog and Chapman (JC) and Gross and Vrabec (GV) into the statistical association fluid theory (SAFT) to predict VLE for dimethyl ether mixtures. The induced association interactions are studied by different approaches and compared to other proposed approaches in the literature. The effect of different number of association sites of water and alcohols is also studied to reach to an accurate model which will quantitatively predict VLE of DME-water/alcohols. Due to the variations in the accuracy of different dipolar theories, two different theories are utilized and compared. The basic model of SAFT was modified to make it applicable to DME mixtures with light gases. The results obtained indicate that inclusion of electrostatic forces significantly improves the predictive capability of the model and reduces the need for adjusting binary interaction parameter. For instance, it is possible to obtain quantitative prediction of VLE for some mixtures of DME-hydrocarbons without adjusting mixture experimental data. The model is also modified to account for interaction present in the mixtures of DME and light gases.

الخلاصة

ثنائي ميثيل الاثير هو بديل مرشح ومحتمل في المستقبل بسبب مزاياه الاقتصادية والبيئية. على مدى السنوات الماضية، أجريت بحوث مستفيضة لتطوير عمليات الإنتاج الممكنة. في معظم العمليات الإنتاجية المتاحة والمقترحة، واجهت خليط من المكونات المختلفة مع الأثير ثنائي ميثيل بما في ذلك المياه، والكحول، والهيدروكربونات، وثاني أكسيد الكربون والغازات الخفيفة. بيانات التوازن تعد مرحلة دقيقة وحاسمة في تصميم وحدات فصل لمخاليط ثنائي ميثيل الاثير. النماذج الثيرموديناميكية للمخاليط المعنية ليست تافهة بسبب وجود العديد من التفاعلات الكهربائية مثل ثنائي القطب-ثنائي القطب وتكوين الجمعيات، وكذلك لآثار الكم التي أظهرتها جزيئات صغيرة جدا مثل الهيدروجين. في هذا العمل، ولقد وظفت علاقة ثنائي القطب-ثنائي القطب والتفاعلات الناجمة عنها في الجمعية الإحصائية لنظرية السوائل (SAFT)للتنبؤ VLE لمخاليط ثنائي ميثيل الاثير. يتم دراسة التفاعلات الناجمة عن النهج المختلفة ومقارنة الأساليب الأخرى المقترحة في المراجع. وتم أيضا دراسة تأثير عدد مختلف من مواقع تجمعات المياه والكحول أيضا للوصول إلى نموذج دقيق والتي سوف تتنبأ كميا VLE في ثنائي ميثيل الاثير-الماء / الكحول. بسبب الاختلافات في دقة نظريات ثنائي القطب مختلفة، تم استخدام اثنتين من النظريات المختلفة ومقارنتها. تم تعديل النموذج الأساسي من SAFT لجعلها تنطبق على ثنائي ميثيل الاثير خلائط مع الغازات الخفيفة. النتائج التي تم الحصول عليها تشير إلى أن إدراج قوات كهرباء يحسن بشكل كبير من القدرة التنبؤية للنموذج، ويقلل من الحاجة لتعديل المتغيرات في العلاقات الثنائية. على سبيل المثال، فمن الممكن الحصول على التنبؤ الكمي لل VLEلخلطات ثنائي ميثيل الاثير الهيدروكربونات دون تعديل لبيانات الخليط. تم تعديل النموذج أيضا لحساب التفاعل الموجود في خليط من ثنائي ميثيل الاثير والغازات الخفيفة.

THESIS ORGANIZATION

Chapter 1 provides the motivation and background involved in the following work

Chapter 2 provides a detailed description of the Statistical associating Fluid theory (SAFT), including concise literature survey. Finally, a detailed Simplified SAFT version is presented along with its mathematical form which is used in this work.

Chapter 3 includes a description of electrostatic interaction, provides a detailed form of the two version of polar terms, one developed by Jog & Chapman and another by Gross & Vrabec. These terms are included to study the proposed mixtures.

Chapter 4 provides the methodology used in the present work binary VLE results for the DME + non-associating-non-polar-hydrocarbons such as various alkanes and alkenes

Chapter 5 provides the VLE of DME-Alcohols

Chapter 6 provides the proposed improvement for VLE of DME-light gases.

Chapter 7 provides the conclusion and recommendation for future work.

CHAPTER 1

INTRODUCTION

1.1 Motivation

Alternative fuel has become a subject of increasing interest due global environmental concerns, regulations on exhaust emissions and energy security [1–6]. There are alternative energy sources available such as ethanol, biodiesel, hydrogen and solar energy. Although these sources seem to be promising, they have limitations in their use. Economy, portability, limited supply, and rising environmental concerns are some of the major factors which tend to limit their adaption as a replacement for conventional fuel. However, there has lately been a growing interest towards the use of dimethyl ether as a potential alternative fuel. The use of DME has various advantages compared to other alternative fuels. The properties are comparable to conventional fuels and DME is environmentally benign. **Tables 1.1 - 1.3 and Figure 1.1** provide a brief account of these properties and benefits of dimethyl ether [7].

The use of dimethyl ether as an alternative fuel relies on the feasibility of its industrial production. The feedstock for the production of dimethyl ether could be natural gas, crude oil, residual oil, coal or waste products as shown in **Figure 1-2**. DME could then be manufactured through steam reforming or coal gasification [7–9]. After syn-gas production, the next step is to produce methanol which is then converted to dimethyl ether.

The processes for dimethyl ether production mainly differ in this step, which is the conversion of methanol to DME. Whatever the overall process is, the separation processes remain challenging and imperative tasks. Economical separation is dependent on the optimal design of separation equipment such as distillation column, extraction column and multiphase reactors. The availability of accurate thermodynamic phase equilibrium data is crucial in designing any equipment. The scope of the present work is to study and develop an accurate and predictive thermodynamic model for DME containing systems encountered in the production of DME.

Table 1-1 Properties of DME [11]

Molecular formula	C_2H_6O
Molar mass	46.07 g mol^{-1}
Appearance	Colorless gas
Odor	Typical
Density	1.97 g cm^{-3}
Melting point	−141 ◦C, 132K, −222 ˚F
Boiling point	−24 ◦C, 249K, −11 ˚F
Solubility in water	71 g dm^{-3} (at 20 ˚C)
Vapor pressure	>100 kPa

Table 1-2 Physio-Chemical property comparison table for dimethyl ether [7]

Property	**Hydrogen**	**Methane**	**Methanol**	**Dimethyl ether**	**Ethanol**	**Gasoline**	**Diesel**
Formula	H_2	CH_4	CH_3OH	CH_3OCH_3	CH_3CH_2OH	C_7H_{16}	$C_{14}H_{30}$
Molecular Weight (g mol^{-1})	2.015	16.04	32.04	46.07	46.07	100.2	198.4
Density (g cm^{-3})	0.0898[a]	0.00072[a]	0.792	0.661[b]	0.785	0.737	0.856
Normal boiling point[c] (°C)	-252.87	-162	64	-24.9	78	38–204	125–400
LHV[d] (kJ cm^{-3})	10.86	0.0346[a]	15.82	18.92	21.09	32.05	35.66
LHV (kJ g^{-1})	121	47.79	19.99	28.62	26.87	43.47	41.66
Exergy[e] (MJ L^{-1})	0.0104	0.037	17.8	20.63	23.1	32.84	33.32
Exergy[e] (MJ kg^{-1})	116.648	51.76	22.36	30.75	29.4	47.46	46.94
Carbon content[d] (wt.%)	0	74	37.5	52.2	52.2	85.5	87
Sulfur content[d] (ppm[f])	0	~7–25	0	0	0	~200	~250

a Values per cm3 of vapor at standard temperature and pressure.
b Density at P = 1 atm and T = −25 ˚C.
c Data taken from reference [12].
d Data taken from reference [13]
e Data taken from reference [14].
f Mass basis

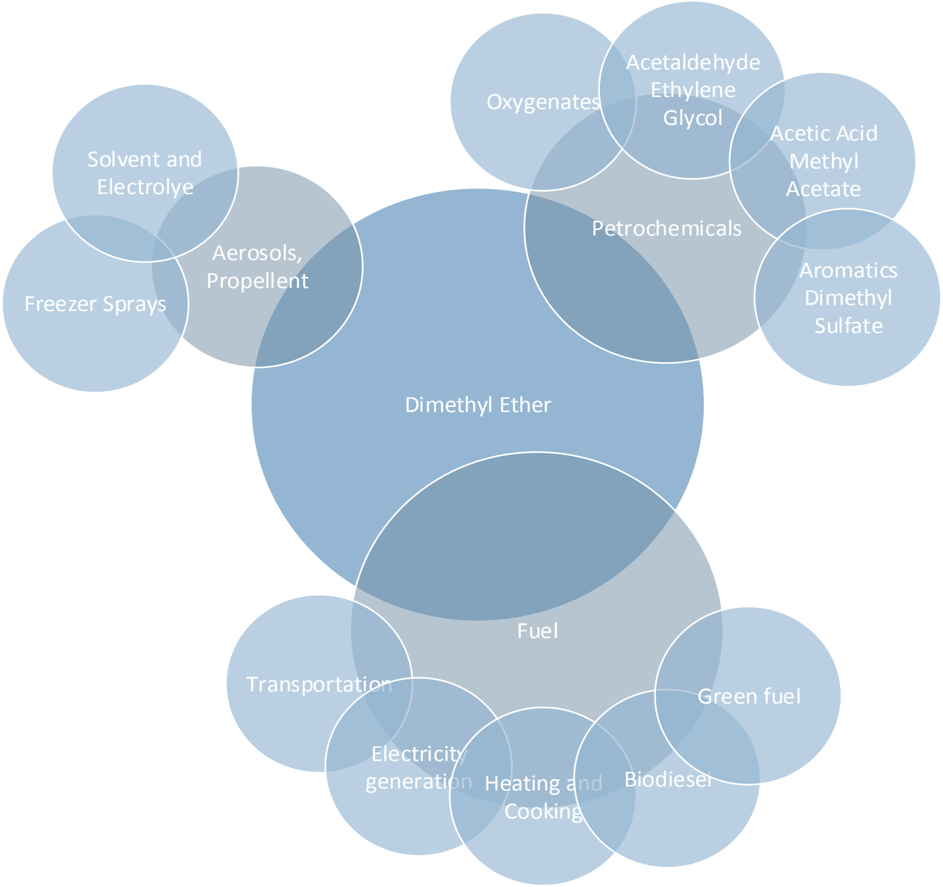

Figure 1-1 Uses of Dimethyl Ether Cloud diagram

Table 1-3 Global Warming Potentials [7]

	Time Horizon		
	20 years	100 years	500 years
Dimethyl ether[a]	1.2	0.3	0.1
Carbon dioxide[b]	1	1	1
Methane[b]	56	21	6.5
Nitrous oxide[b]	280	310	170

[a] *Data taken from reference* [15].
[b] *Data taken from reference* [13].

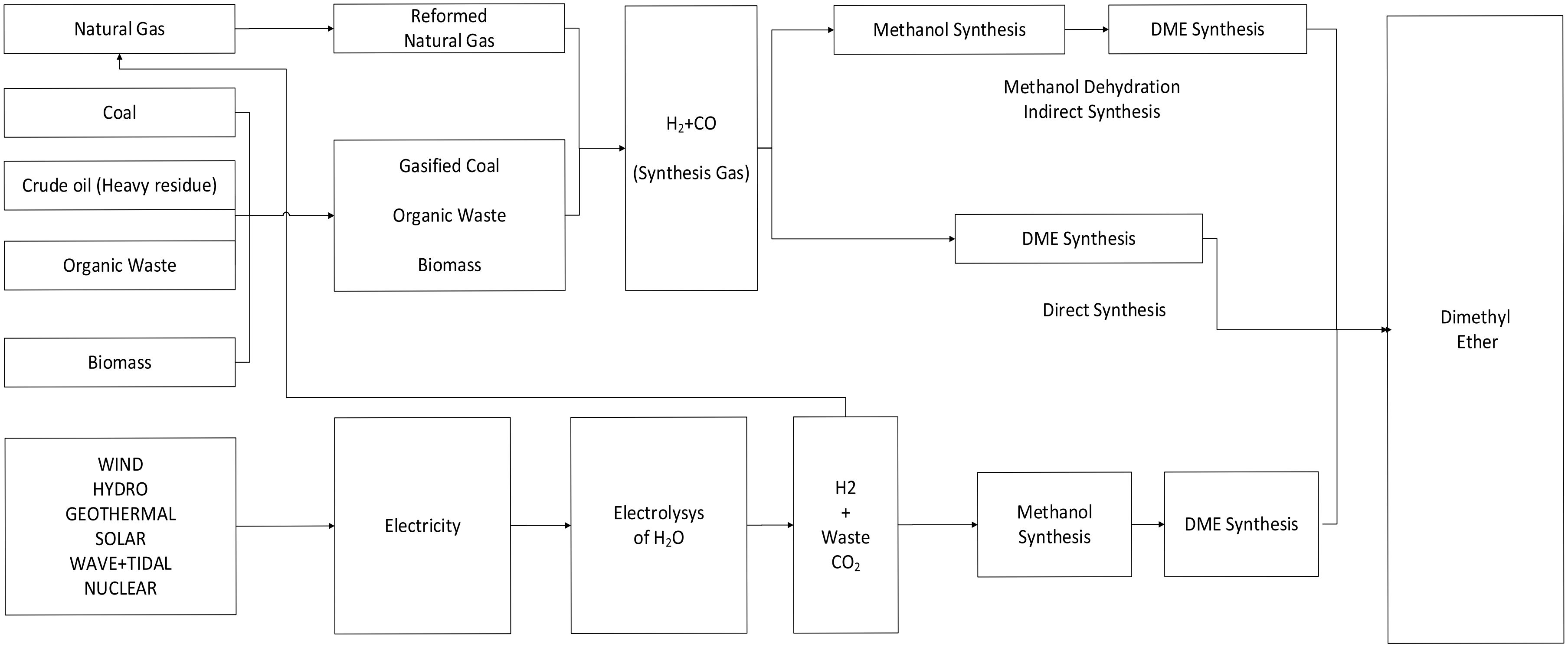

Figure 1-2 Production routes for Dimethyl Ether

There are various kinds of mixtures involved in the production of DME processes. Few examples of these DME containing mixtures include DME-hydrocarbons, DME-alcohols, DME-water, DME-carbon dioxide and DME-hydrogen. From a theoretical point of view, the study of these mixtures is not trivial. The reason is that these mixtures exhibit various molecular interactions such as, dipole-dipole, and hydrogen bonding associations, which are difficult to describe. These interactions are difficult to model using thermodynamic models. For instance, DME-methanol exhibits associations and dipole-dipole interactions that cannot be employed directly even to Statistical Associating Fluid Theory (SAFT). The reason is that the combination of DME-methanol would form induced interactions, which cannot be handled by SAFT in its current form. Furthermore, DME-light gases require very different approach because of significant quantum effects and SAFT cannot be applied directly without modification.

In this work, DME mixtures are modeled using statistical association fluid theory to predict vapor-liquid equilibrium with the emphasis on the role of long-ranged electrostatic interactions such as dipolar and quadrupolar interactions using the SAFT EOS. Furthermore, due to the failure of the SAFT for light gases that shows signification quantum effects, the SAFT is modified and applied to the mixtures of DME-light gases. VLE of the mixtures that exhibit induced interactions are studied and compared to some of the previous approaches.

1.2 Systems of interests

It is evident that in DME production processes, several DME mixtures are encountered including, water, methanol, ethanol, propanol, oxygen, nitrogen, propane and butane. Light gases such as CO_2, CO SO_2, N_2 and H_2 are also encountered in various separation processes with DME. Therefore, in this thesis, DME-hydrocarbons, DME-alcohols, DME-water, DME-light gases are the systems of interest in this work. The figure 1-3 shows a detailed list of the mixtures that are extensively studied in this work along with the molecular interactions that are employed.

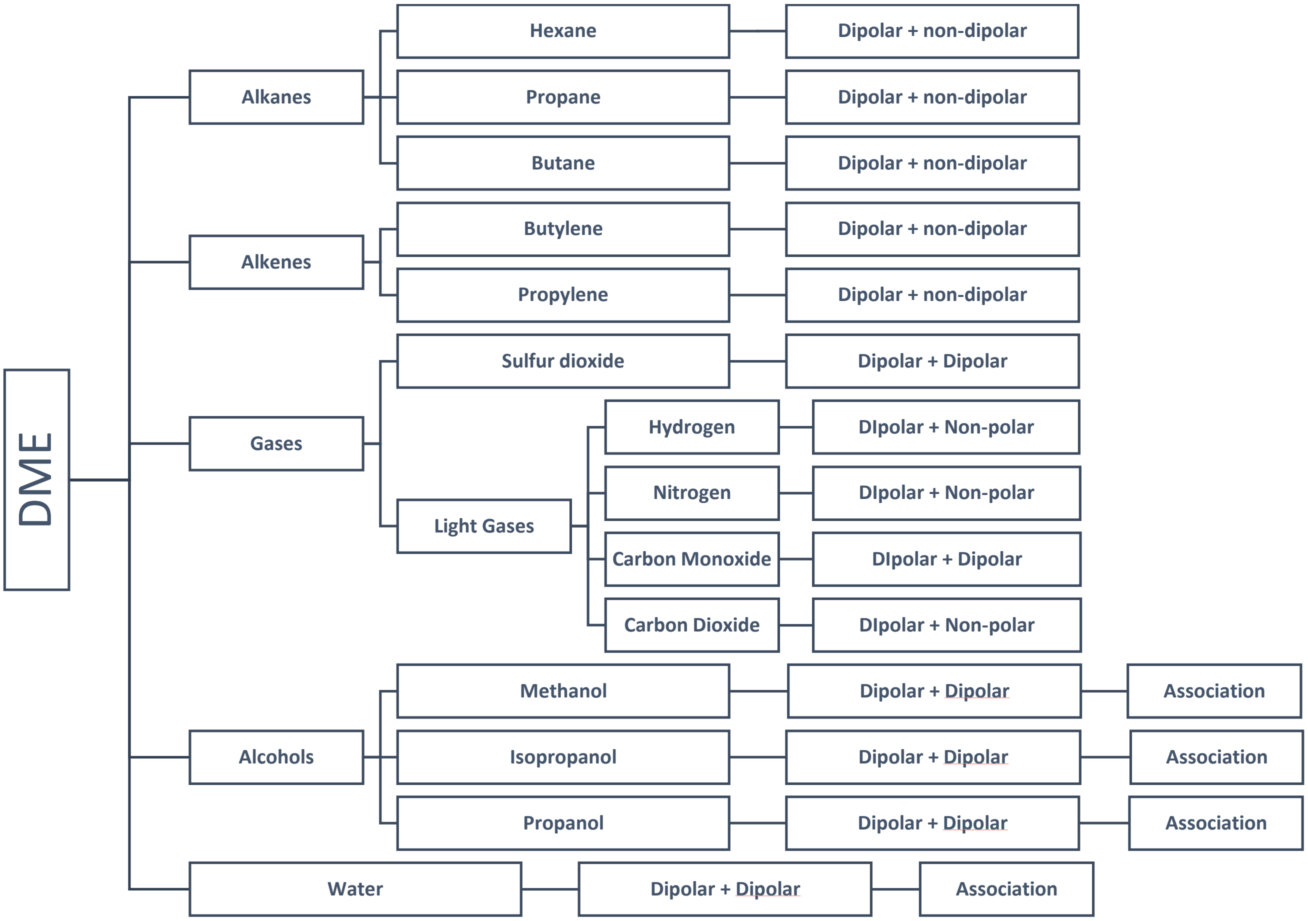

Figure 1-3 Systems of interest along with their molecular interactions

1.3 The need for thermodynamic modeling

As indicated previously, the design of separation process units and multiphase reactors are clearly dependent on the availability of accurate phase equilibrium data. One may argue that the phase equilibrium data of dimethyl ether mixtures could be obtained by experimental measurements. However, the experimental measurements are costly and time consuming. Furthermore, experimental measurements are not always possible to obtain. For instance, the determination of vapor-liquid equilibrium at high pressure is a challenging problem. Even if the experimental measurements are available for some dimethyl ether mixtures in the literature, these data might not be available at the same desired conditions for designing the separation units. As a result, it is needed to obtain phase equilibrium data from a suitable thermodynamic model.

1.4 Choice of the thermodynamic model

In the absence of experimental data, chemical engineers usually depend on thermodynamic models such as semi-empirical equations of state like Peng-Robinson [16] or activity coefficient models (Wilson 1964; Renon 1968; Anderson 1978; Kemeny 1981). Although activity coefficient models work better for liquid solutions and polar mixtures, it is limited to systems at moderate pressures. Therefore, for some mixtures such as DME-CO_2 where the pressure is expected to be high, the activity coefficient models cannot be used. On the other hand, the commonly used cubic equations of state experience weaknesses and limitations, when applied to polar and hydrogen bonding mixtures. The reason is that the cubic equations of state are generally developed without taking into consideration hydrogen bonding and polar interactions. Because of the highly complex nature of hydrogen bonding and polar interactions, many proposed empirical equations of state were unsuccessful. Furthermore, the repulsive and attractive terms in cubic equations of state are not accurate from a theoretical point of view. Indeed, it was evident that the only successful way to model complex mixtures is to take into account the molecular physics of molecules [17]. One of the models that was proposed based on theory is Statistical Associating Fluid Theory (SAFT) [18]. In this work, the SAFT equation of state is selected as a platform for predicting vapor-liquid equilibrium. Because there are several SAFT versions with varying accuracy, a specific version should be selected among them. For this work, the simplified SAFT [19] is adapted. The selection of the SSAFT is justified throughout this work. Chapter 2 is devoted to statistical association fluid theory where a detailed introduction is given about SAFT and its versions.

Most of the cubic equations of states fail if the intermolecular forces in a specific mixture are ignored. For instance there are several examples in which cubic equations of states have failed even with adjusting the binary interaction parameter. As shown in **Figures 1-4 & 1-5.** The deviations are large in the prediction for the Diethylamine-Water system which is a polar mixture using Peng Robinson equation of state. Similarly, cubic equations of state would show large deviations for propane-methanol system which is a non-polar-polar mixture. Therefore, it is clear that empirical correlations would fail to describe the phase behavior of polar and associative mixtures.

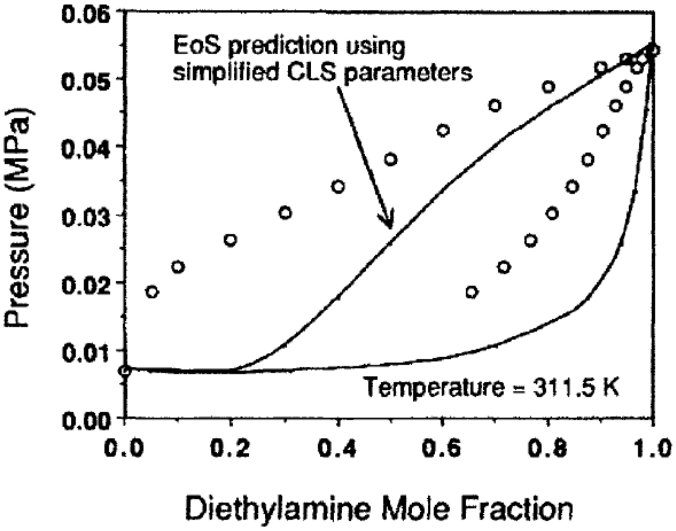

Figure 1-4 Vapor-liquid equilibrium data and calculated values from Peng-Robinson EOS for the Diethylamine-water system reproduced from Appleid paramter estimation, Englezos 2010 pp 253

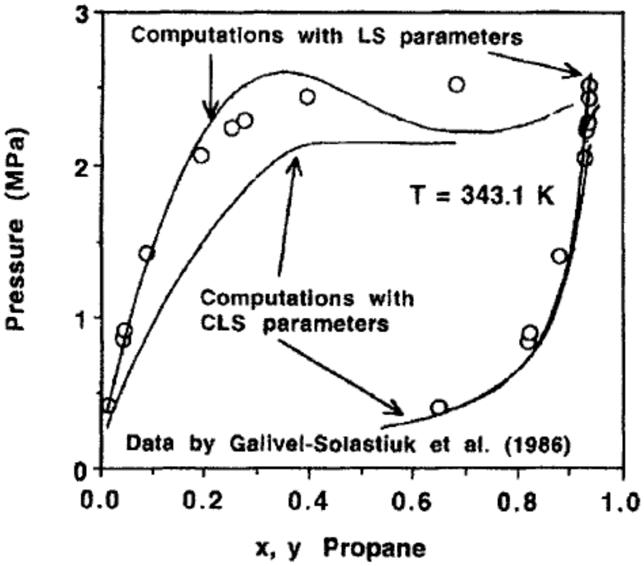

Figure 1-5 Vapor-liquid equilibrium data and calculated values from Peng-Robinson EOS for the propane - methanol system reproduced from Applied parameter estimation, Englezos 2010 pp 244

1.5 Thesis Objectives

The objective objectives of this thesis is to

- **To develop an accurate predictive thermodynamic model based on the Simplified SAFT EOS [19] including electrostatic interactions to predict VLE of DME mixtures.**

  And the specific objectives are to.

  a) Implement the dipole-dipole interactions to the SSAFT EOS using two models developed by Jog and Chapman [20] and Gross and Vrabec [21].

  b) Compare between the dipolar approaches of Jog-Chapman and Gross-Vrabec

  c) Account for hydrogen bonding association and the effect of induced cross association in predicting VLE of DME-alcohols and DME-water.

  d) Propose various schemes of association in prediction of VLE mixtures containing polar non-associating and polar associating components.

  e) Modify the SSAFT to make it applicable for VLE prediction of DME-light gases. Explore the role of electrostatic interactions in predicting the excess molar enthalpy of DME mixtures from the developed model.

CHAPTER 2

STATISTICAL ASSOCIATING FLUID THEORY

2.1 Introduction

Several developments that took place in the last century in the areas of atomistic simulation, integral equation theories, radial distribution functions, perturbation and statistical association theories have paved a way for developing statistical associating fluid theory (SAFT). **Figure 2.1** describes the backbone framework of the development of SAFT theory The SAFT EOS was proposed based on Wertheim's perturbation theory [22–25]. Perturbation theory is a mathematical theory which provides an approximate solution to a problem. The solution is obtained by adding values obtained by approximating perturbation terms to the solution of exact terms. Wertheim's perturbation theory comprises of an expansion of Helmholtz free energy into integrals of association potential and molecular distribution functions.

SAFT was developed in late 80's by Chapman as an equation of state, in the form as known today [26, 27]. Several versions of SAFT have appeared since then such as, simplified SAFT [19] and Perturbed-Chain PC-SAFT [28]. The SAFT equation of state was able to predict with fairly good accuracy the phase equilibrium of, polydisperse mixtures, non-associating and associating molecules of organic compounds, polymers and electrolyte solutions at low and high temperatures and pressures. [29–37].

In the last decade extensive research has been conducted to improve the predictive capability of SAFT and extend its applicability over a wide range of complex mixtures. (**Table 2.1** summarizes some of the well-known versions of SAFT along with their capabilities and applicability). SAFT has started to appear in process simulators such as Aspen Plus v8.

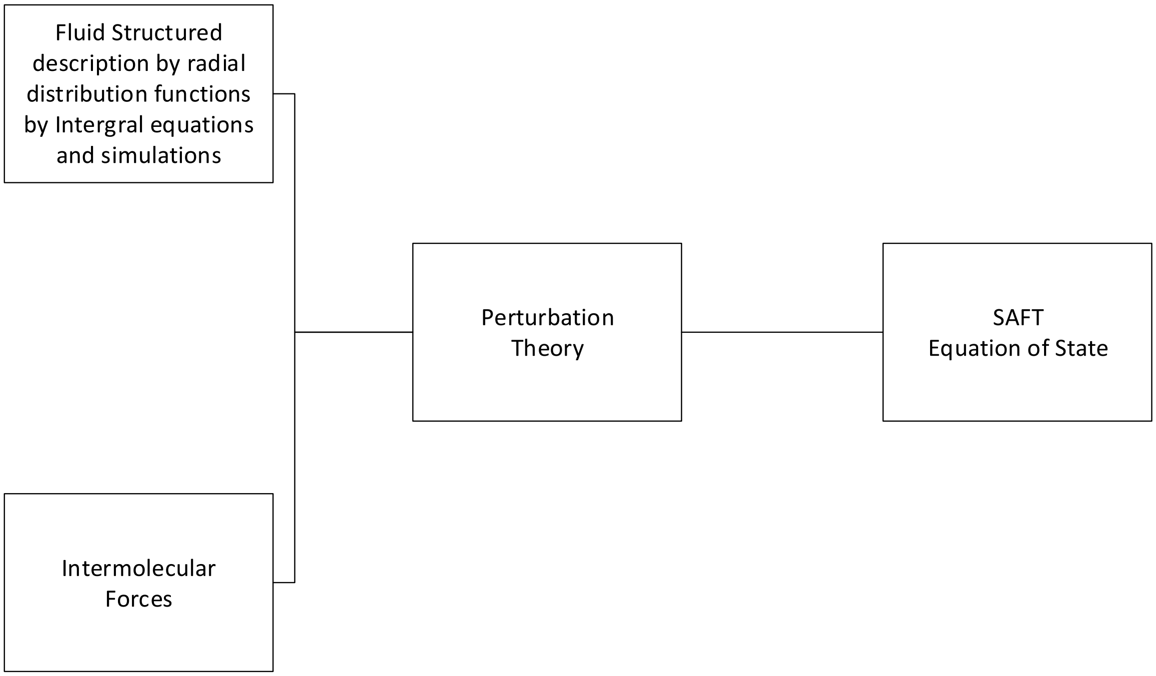

Figure 2-1 The framework for the development of SAFT

Table 2-1 References of some of the most well-known SAFT variants [38]

SAFT variant	**Reference**	**Comments**
Original SAFT	Chapman et al. [25, 35]	Mostly comparisons against simulation data Parameters for six hydrocarbons and two associating fluids are given
CK–SAFT	Huang and Radosz. [28, 29]	Parameters for 100 different fluids
Simplified SAFT	Fu and Sandler [19]	Parameters for ten non-associating and eight associating compounds
LJ–SAFT	Kraska and Gubbins [37-39]	Alkanes, alkanols, water (pure components)/mixtures of alkanes, alkanols, water
SAFT–VR	Gil-Vilegas et al. [42] McCabe et al. [43]	alkanes, perfluoroalkanes (pure components)/comparisons against simulation data
Soft SAFT	Blas and Vega [44]	
PC–SAFT	Gross and Sadowski [28]	The Gross and Sadowski [28] article contains parameters for 100 compounds and Tihic et al. [62] another 400 parameters.
Simplified PC–SAFT	Von Solms et al [46] Tihic et al [45]	comparison between PC–SAFT and simplified PC–SAFT

2.2 Further developments in the SAFT

Several developmental aspects, further extensions and improvements possibilities, of SAFT, may be classified broadly into four different categories:

1. Simplifying the chain and dispersion term by substituting it from the term present in the cubic equation of state such as, Peng Robinson and Soave-Redlich Kwong.

2. The association term of SAFT is the most computational intensive and requires significant time in solving. So, a simplified association term shall make the SAFT easily adaptable in process simulation software.
3. Improvement of various current SAFT models, by including the Helmholtz energy terms for the electrostatic interaction of long and short range order such as, dipolar, quadrupole interactions and hydrogen bonding associations. Such inclusions increases the predictive capability of the model and eliminates the need for empirical adjustment [47].
4. Developing further, the Group Contribution approach of the SAFT model (GC-SAFT). With its development, it will be easy to estimate pure component parameters of homologous compounds (**Table 2.2** gives an account of the SAFT version that uses group contribution approach).

Table 2-2 Group contribution versions of SAFT [38]

SAFT variant	**Application**	**Reference**
Original SAFT **SAFT–VR**	Alkanes, aromatics, olefins, alcohols	Tamouza et al. [48]
Original SAFT **SAFT–VR**	Alcohols Alkanes	Tamouza et al. [49]
Original SAFT **PC–SAFT + polar term** **SAFT–VR**	Esters	Thi et al. [50]
SAFT **PC–SAFT**	General	Emami et al. [51]
PC–SAFT **SAFT–VR**	H_2, CO_2 + alkanes (including a GC method for the k_{ij} parameter)	Le Thi et al. [52]
Original SAFT **PC–SAFT+ quadrupolar** **SAFT–VR**	Polycyclic Aromatic hydrocarbons	Huynh et al. [53]
PC–SAFT	General (non-associating compounds)	Tihic et al. [54]
SAFT–VR	Hydrocarbons, alcohols	Lymberiadis et al.[55]

The SAFT has widely been regarded as a potential theory, to replace conventional thermodynamic models, owing to its wide range of applicability. However, still in its infant stage, it needs rigorous research to emerge as a fully developed thermodynamic model. (Refer to **Table 2.3** below for reviews presented on various SAFT models, and **Table 2.4** discussing their applicability over a wide range of conditions and the diverse nature of components).

Table 2-3 SAFT reviews [38]

Topic	**Reference**
Electrolytes, interfaces and polymers	Paricaud et al. [56].
General, including aqueous mixtures, electrolytes, liquid crystals, polymers, oil mixtures and high pressure	Muller and Gubbins [57].
General	Economou [58], Wei and Sadus [59] Prausnitz and Tavares, [49] Tan et al. [60]
PC–SAFT applications	Arlt et al. [61]
PC–SAFT applications (strengths and limitations)	Von Solms et al. [62]
Oil applications (PC–SAFT, SAFT–VR and CPA)	De Hemptinne et al. [63]

Table 2-4 Application of SAFT (and CPA) to electrolytes [38]

SAFT variant	**Reference**	**Application**
SAFT–VR	Behzadi et al. [64]. Patel et al.[65].	Water–alkanes
PC–SAFT	Cameretti et al. [66]. Fuchs et al. [67].	Water–salts Amino acids
CPA (Peng–Robinson)	Wu and Prausnitz[17].	Water–hydrocarbons–salts
CPA (SRK)	Lin et al.[68].	Water–salts VLE, SLE

There have been many modifications, either to improve SAFT's applicability [38, 39, 68] or to simplify its nature [19, 69]. Galindo et al [55] developed a simplified version of SAFT-γ that could correlate high pressure equilibrium data for mixtures. But, SAFT still lacks accuracy in various situations, such as it is not able to predict liquid-liquid equilibria in aqueous systems at low and normal temperatures because of the significant hydrophobic effect that comes into play, which is not accounted for in SAFT. The hydrophobic effect significantly changes the molecular structure of water in a non-polar solute (e.g., methane or ethane), which is otherwise insignificant at higher temperature [71]. Moreover, SAFT fails to predict with satisfactory accuracy, the mixture phase behavior of polar associating components with polar non-associating components such as DME-Methanol because of te cross induced association interactions. These untoward limitations of SAFT has prevented its adaptability to be used as a one stop model in various process simulation software. In the present work the SAFT was improved to predict with very good accuracy, the phase behavior of mixtures of polar and associating compounds.

2.3 Proposed extensions in the current SAFT model

In this section, the extensions such as inclusion of long and short-ranged electrostatic interactions in the Simplified SAFT model [19] are discussed. Although, there have been various models which previously included such contribution for dipolar and quadrupolar interaction (as summarized in Table 2.5) However, those improvements are still largely dependent on the availability of mixture experimental data, or the models are based on such approach which is very complex and requires a large number of parameters. In a recent study, Alsaifi et al, 2008, Alsaifi and Englezos, 2011 [71, 72] was able to obtain quantitative results for water-alcohol-hydrocarbon mixtures without adjusting the mixture experimental data. Their approach has been extended to cover more complex systems, including the prediction of dissociation pressure of gas hydrates of a single compound. More recent work has shown that, the approach could also be successful with some mixtures of ketones and aldehyde [72]. The success of their work has attributed to employing the long-ranged electrostatic interactions with the SAFT (see **Table 2.5** below which summarizes some of the well know SAFT models which have included polar term).

Therefore, the objective is to model DME mixtures by employing electrostatic interactions into the SAFT, to predict phase equilibrium data without adjusting the mixture experimental data. Various complex DME mixtures will be considered such as Methanol-DME, Ethanol-DME, DME-Water, DME-Methanol-Water, DME-CO_2, DME-hydrocarbons and DME with light gases. The present study will also focus on, including hydrogen bonding associations which are a special type of electrostatic interaction, which requires specific orientation between associating molecules. Different number of association sites for hydrogen bonding components are taken into account. Before moving on further, it is imperative to present a description at the physical and mathematical form of SAFT.

Table 2-5 Polar and quadrupolar SAFT variants

SAFT variant	Additional term	Reference
CK–SAFT	Dipolar	Jog et al. [74]
PC–SAFT	Dipolar	Tumakaka and Sadowski [75, 76] Sauer and Chapman [77]
PC–SAFT	Dipolar + induced polar	Karakatsani et al. [78–80]
PC–SAFT	Dipolar	Gross and Vrabec [81]
PC–SAFT	Quadrupolar	Gross[82]
PC–SAFT	Polarizable dipoles	Kleiner and Gross[83]
PC–SAFT	Dipolar + polarizable	Karakatsani and Economou [84]

2.4 SAFT Equation of State: The Physical Picture

The physical picture of SAFT is based on statistical physics, where a molecule is perturbed and assumed to be a hard sphere. The SAFT theory is thus, a hard sphere-based model. In most SAFT versions, the dispersion interactions are considered as a perturbation term. The hard spheres are assumed to contain association and chain sites. The molecules which is initially considered as a hard spheres, is added with attractive forces, then chain sites and hence, chain molecules appear. Finally from association sites, complexes of association appear [19] (See graphical representation in **Figure 2-2** which describes the perturbation process). The representative equation for final residual Helmholtz energy is given as a follows.

$$A^{res}=\underbrace{A^{seg}}_{\text{Helmholtz energy of the segment for both hard spheres and dispersion terms}}+\overbrace{A^{chain}}^{\text{HE contribution for chain}}+A^{assoc}\ \Big\{\ \text{HE contribution for association}$$

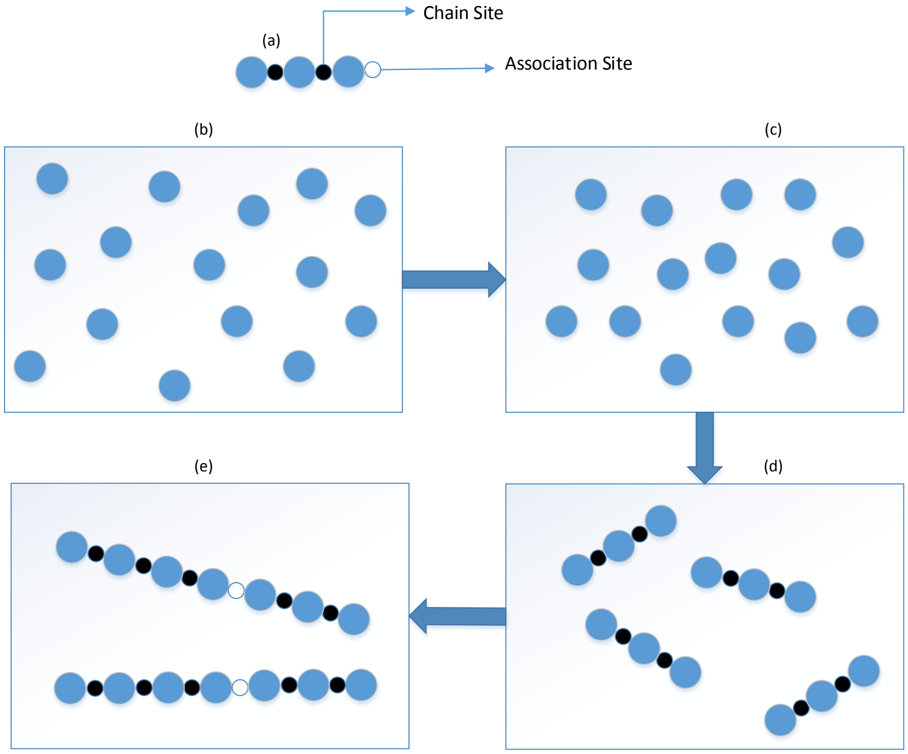

Figure 2-2 Representation to form a molecule in SAFT

Representative procedure of forming a molecule as viewed by SAFT’s perturbation approach.

(a) The molecules containing the chain and the association sites as depicted are initially assumed hard-spheres.

(b) First, the molecules are assumed to be hard-sphere and hence presence of repulsive forces are accounted.

(c) Adding attraction forces to the molecules, which are dispersive forces.

(d) Chained molecules appear, after adding the chain sites.

(e) Finally association sites are added to account for molecular association.

After realizing the physical picture, it important to describe the mathematical form of SAFT, hence the next section is devoted to describe the various mathematical formulations used in SAFT.

2.5 The SAFT Equation of State: Mathematical Representations [19]

The SAFT consists of various mathematical terms that describe, repulsion, chain, and association contribution to the residual Helmholtz energy. The next sub-section and its further sections will describe the equations developed for these various terms in SAFT, for both pure component and mixture.

2.5.1 The SAFT Equations for pure component

2.5.1.1 Hard sphere term

The hard sphere term assumes, each component to contain a chain with *m* number of segments.

$$\boldsymbol{a^{hs} = m a_0^{hs}} \tag{2-1}$$

Where a_0^{hs} represents the Helmholtz energy of a molecule which is assumed to be a hard sphere in a hard spehre fluid, that has same packing fraction as that of the chain fluid. As there are *m* number of segments, the total contribution of hard sphere helmholtz energy is ma_0^{hs}, a_0^{hs} is defined as the single hard sphere contribution for helmholtz energy, given as follows and is derived from the Carnahan Starling's (1969) expression.

$$\frac{a_0^{hs}}{RT} = \frac{4\eta - 3\eta^2}{(1-\eta)^2} \qquad \text{2-2}$$

$$\eta = \frac{\pi N_{AV}}{6} \varrho_s d^3 \qquad \text{2-3}$$

Where,

ϱ_s: The molar density of hard sphere fluid.

d : Effective hard sphere diameter of segment.

N_{AV}: Avogadro number.

R: Gas constant, T denotes the temperature.

$$\varrho_s = m\varrho \qquad \text{2-4}$$

ϱ : Molar density of the chain molecules.

$$d = \sigma \left[1 - c\, exp\left(-\frac{3u^0}{kT}\right)\right] \qquad \text{2-5}$$

c : Adjusted parameter, taken to be 0.333

u^0: Temperature independent interaction energy between the segments.

$$v^{00} = \left(\frac{\pi N_{AV}}{6\tau}\right) \sigma^3 \qquad \text{2-6}$$

The value of $\tau = 0.74048$

v^{00} : Temperature independent segment molar volume in a closed packed arrangement

2.5.1.2 Dispersion Term

The Helmholtz energy for dispersion is described as follows.

$$a^{disp} = m a_0^{disp} \qquad 2\text{-}7$$

a_0^{disp} : denotes a segment's dispersive Helmholtz energy. In the SAFT equation, original dispersive energy term was taken from Chen and Kreglewski (1997) which yields two power series with 24 coefficients.

$$\frac{a_0^{disp}}{RT} = \sum_i \sum_j D_{ij} \left[\frac{u}{kT}\right]^i \left[\frac{\eta}{\tau}\right]^j \qquad 2\text{-}8$$

D_{ij} The segment-segment attraction is assumed to be the square well potential.

However, a simplified term derived from Lee et al. (1985) which is used to describe the attractive forces in this version of SAFT (Simplified SAFT).

$$\frac{a_0^{disp}}{RT} = Z_M \ln\left(\frac{v_s}{v_s + v^* Y}\right) \qquad 2\text{-}9$$

$$Y = \exp\left(\frac{u}{2kt}\right) - 1 \qquad 2\text{-}10$$

$$u = u^0\left[1 + \left(\frac{e}{kT}\right)\right] \qquad 2\text{-}11$$

Where

v_s : the molar volume for one segment.

u : depth of the square well potential

Z_M : represents the maximum coordination number which is taken to be 36 in simplified version of the perturbed hard chain theory(SPHCT) [85]

$^{e}/_{k}$ =10 K based on fitting the vapor pressure and molar liquid volumes of ethane is a universal constant for SSAFT.

v^*: closed packed molar volume of a segment

$$v^* = \frac{N_{AV} d^3}{\sqrt{2}} \qquad 2\text{-}13$$

2.5.1.3 Chain term

The chain term used in this model is approximated by making the association energy infinite in the Wertheim's association theory and it is given as follows [19].

$$\frac{a^{chain}}{RT} = (1 - m) \ln \frac{1-1/2\eta}{(1-\eta)^3} \qquad 2\text{-}14$$

$$g^{hs}(d) = \frac{1-1/2\eta}{(1-\eta)^3} \qquad 2\text{-}15$$

$g^{hs}(d)$: The radial distribution function for the hard sphere.

2.5.1.4 Association term

The association term in the equation is given as follows the same term also applies to the hydrogen bonding interaction [19].

$$\frac{a^{assoc}}{RT} = \sum_{A_i} \left[\left(\ln X^A - \frac{X^A}{2} \right) + \frac{1}{2} M \right] \qquad 2\text{-}16$$

$$X^A = [1 + N_{AV} \sum_B \varrho \, X^B \Delta^{AB}]^{-1} \qquad 2\text{-}17$$

$$\Delta^{AB} = g^{hs}(d) \left[\exp\left(\frac{\varepsilon^{AB}}{kT} \right) - 1) \right] d^3 k^{AB} \qquad 2\text{-}18$$

Where

$$g^{hs}(d) = \frac{1-1/2\eta}{(1-\eta)^3} \qquad 2\text{-}18$$

$g^{hs}(d)$: The radial distribution function for the hard sphere.

X^A : The fraction of un-bonded associations sites A

M: The number of association sites in a molecule.

Δ^{AB}: The association strength between two sites A and B.

The two adjustable parameters are ε^{AB} association energy and k^{AB} association volume respectively. In the present Simplified SAFT version, they are only applied to associating components for instance, oxygenated hydrocarbons.

2.5.1.5 Final form in terms of compressibility factor

The final form of the SAFT EOS for pure fluids in terms of compressibility factor is, the sum of the various compressibility factors of each perturbed term obtained from the derivative w.r.t volume of the Helmholtz free energy.

$$Z = \frac{Pv}{RT} = Z^{hs} + Z^{disp} + Z^{chain} + Z^{assoc} + 1 \qquad \text{2-19}$$

$$Z^{hs} = m\left[\frac{4\eta - 2\eta^2}{(1-\eta)^3}\right] \qquad \text{2-20}$$

$$Z^{disp} = -mZ_M\left(\frac{v^*Y}{v_s + v^*Y}\right) \qquad \text{2-21}$$

$$Z^{chain} = (1-m)\frac{\left(\frac{5}{2}\right)\eta - \eta^2}{(1-\eta)(1-(\frac{1}{2})\eta)} \qquad \text{2-22}$$

$$Z^{assoc} = \varrho \sum_A \left[\frac{1}{X^A} - \frac{1}{2}\right]\frac{\partial X^A}{\partial \varrho} \qquad \text{2-23}$$

Finally the various terms described so far in the Simplified SAFT version, has three tunable parameters for non-associating components and five parameters for associating components.

The following three parameters are applicable for both associating and non-associating components

u^0: Temperature independent square well depth

v^{00}: The segment molar volume in a close packed arrangement

m: The number of segments

The next two parameters are applicable only for associating components

k^{AB}: Association volume

ε^{AB}: Association energy

To obtain pure component parameters in the above equations, they are optimized against the experimental PVT data. These parameters are unique for each component, even for homologues in the same series, but once they are obtained, can be used anywhere in the stated range of temperature and pressures (refer to **Chapter 4** for detailed description of methodology employed in this work). So, this brings us to favorable situation in which, if a large database for the pure components is developed, it becomes robust to use them for mixtures. However, there are shortcomings, the simpler it looks is not that simple. The mixtures tend to show varying trends than assumed, because of the various intermolecular interactions that comes into play, such as, short and a long range electrostatic interactions and hydrogen bonding associations (refer to **Section 2.3, 2.6 and 3.1)**. These various situation must be accounted before estimating the parameters for pure components. The next section is devoted to mathematical representation of Helmholtz energy in mixture after which, a general idea would be clear in terms of predicting the thermodynamic phase equilibrium data.

2.5.2 The SAFT equation for mixtures

The total residual Helmholtz Energy (HE) is given by the following equation which is similar to that developed for the pure component.

$$A^{res} = A^{disp} + A^{hs} + A^{chain} + A^{assoc} \qquad 2\text{-}24$$

The mixture is assumed to be a hard sphere mixture which are based on hard spheres results of Mansoori et al. 1971.

$$\frac{a^{hs}}{RT} = \frac{6}{\pi N_{AV}\rho}\left[\frac{(\zeta_2)^3 + 3\zeta_1\zeta_2\zeta_3 - 3\zeta_1\zeta_2(\zeta_3)^2}{\zeta_3(1-\zeta_3)^2} - \left[\zeta_0 - \frac{(\zeta_2)^3}{(\zeta_3)^2}\right]\ln(1-\zeta_3)\right] \qquad 2\text{-}25$$

Where,

$$\zeta_k = \frac{\pi N_{AV}}{6}\sum_i x_i m_i (d_{ii})^k \qquad k = 0,1,2,3 \qquad 2\text{-}26$$

ρ: represents the total molar density of molecules

x_i : is the mole fraction of component i

m_i : number of segments per molecule i

d_{ii} : Temperature dependent segment diameter

Considering the attractive forces between the segments, assuming the attractive potential to be the square-well and extending the equation based on derivation from Lee et al., similar to what was done for the case of pure components, the dispersive Helmholtz energy term for mixtures are thus obtained and given below.

$$\frac{a^{disp}}{RT} = mZ_M \ln\left(\frac{v_s}{v_s+\langle v^*Y\rangle}\right) \quad 2\text{-}27$$

v_s: the total molar volume of a segment and is $1 / \rho m$

Z_M=36 Maximum coordination number 2-28

$$m = \sum_i x_i m_i \quad 2\text{-}29$$

$$\langle v^*Y\rangle = \frac{\sum_i \sum_j x_i x_j m_i m_j \left(\frac{{d_{ij}}^3}{\sqrt{2}}\right)\left[\exp\left(\frac{u_{ij}}{kt}\right)-1\right]}{\sum_i \sum_j x_i x_j m_i m_j} \quad 2\text{-}30$$

$$u_{ij} = \left(1-k_{ij}\right)\sqrt{u_i u_j} \quad 2\text{-}31$$

$$d_{ij} = \frac{d_{ii}+d_{jj}}{2} \quad 2\text{-}32$$

k_{ij}: adjustable binary interaction parameter

$$\frac{a^{chain}}{RT} = \sum_i x_i(1-m_i)\ln({g_{ii}}^{hs}(d_{ii})) \quad 2\text{-}33$$

${g_{ii}}^{hs}(d_{ii})$: pair correlation function for hard spheres in the mixture for the segments of same diameter.

$${g_{ii}}^{hs}(d_{ii}) = \frac{1}{1-\zeta_3} + \frac{3d_{ii}d_{jj}}{d_{ii+}d_{jj}}\frac{\zeta_2}{(1-\zeta_3)^2} + 2\left[\frac{d_{ii}d_{jj}}{d_{ii+}d_{jj}}\right]^2\frac{{\zeta_2}^2}{(1-\zeta_3)^3} \quad 2\text{-}34$$

$$\frac{a^{assoc}}{RT} = \sum_i x_i\left[\sum_{A_i}\left(\ln X^{Ai} - \frac{X^{Ai}}{2}\right) + \frac{1}{2}M_i\right] \quad 2\text{-}35$$

M_i: denotes the total number of association sites in a component i.

X^{Ai}: represents the mole fraction of unbonded sites A_i

$$X^{Ai} = \left[1 + N_{Av}\sum_j \sum_{Bj} \rho_j X^{Bj}\Delta^{AjBj}\right]^{-1} \quad 2\text{-}36$$

ρ_j: denotes the molar density of component j

$$\Delta^{A_iB_j}= {d_{ij}}^3 {g_{ij}}^{hs}\left(d_{ij}\right)^{seg}\kappa^{AiBj}\left[exp\left(\varepsilon^{AiBj}/kT\right)-1\right] \qquad 2\text{-}37$$

ε^{AiBj}, κ^{AiBj} and $\Delta^{A_iB_j}$ represents, the association energy, association volume and association strength for an interaction site between site A$_i$ and B$_j$ .These terms are obtained based on certain mixing rules which are described later in this chapter in the **Section 2.6**. The final form of SAFT equation of state for mixtures in terms of compressibility factor is given as

$$Z = Z^{hs} + Z^{disp} + Z^{chain} + Z^{assoc} + 1 \qquad 2\text{-}38$$

$$Z^{hs} = \frac{6}{\pi N_{AV}\rho}\left[\frac{\zeta_0\zeta_3}{1-\zeta^3} + \frac{3\zeta_1\zeta_2}{(1-\zeta_3)^2} + \frac{3{\zeta_2}^3}{(1-\zeta_3)^3} - \frac{3\zeta_3{\zeta_2}^3}{(1-\zeta_3)^3}\right] \qquad 2\text{-}39$$

$$Z_{disp} = -m\,\mathrm{Z}_M\left(\frac{\langle v^*Y\rangle}{v_s+\langle v^*Y\rangle}\right) \qquad 2\text{-}40$$

$$Z_{chain} = \sum_i x_i\,(1-m_i)\left(\frac{\rho}{g_{ii}^{hs}}\frac{\partial g_{ii}^{hs}(d_{ii})}{\partial\rho}\right) \qquad 2\text{-}41$$

$$Z_{assoc} = \sum_i x_i\left[\sum_{A_i}\left(\frac{1}{X^{A_i}}-\frac{1}{2}\right)\frac{\partial X^{A_i}}{\partial x\rho}\right] \qquad 2\text{-}42$$

Before moving on to describe the central idea of this work, the electrostatic contributions, it is important to demonstrate the various association schemes by which components may associate, in the mixture phase and in the pure form.

2.6 The various Association schemes Explained

The associating components are mainly oxygenated compounds such as, alcohols, aldehydes, ketones, acids, esters and so on. The presence of oxygen, which is an electronegative element and accepts protons, tends to associate with a proton donor sites, on self or a different compound. However, the trend of association is not general, but particular and hence, different association possibilities exist. One has to look into different association cases, to accurately predict which one would exist but the guidelines are simple. Association sites will exist only in between a proton donor and proton acceptor sites such as a hydrogen atom and an electron pair. Although, the spectroscopic data may give an indication to number of association sites, at times it is seen to deviate from the inference.

It is better to visualize the association sites and hence the illustration is given in **Figure 2-3** & **Figure 2-4.** To explain the different association brief explanation of **Figure 2-3** is provided, which describes the association scenario in an alcohol-dimethyl ether mixture (methanol-DME). It has both cross-association i.e. association between the different molecules of different components and self-association i.e. association between molecules of same components. The description of the illustrations **Figure 2-3** goes as follows.

Initially, the molecule of alcohol has two lone pair of electrons on its oxygen atom, that acts as proton acceptor and it has one hydrogen atom that acts as proton donor. Similarly, the dimethyl ether molecule has two lone pair of electrons, but no proton donor site. For the sake of brevity, the sites are labelled as A1 and B1 for the first lone pair and second lone pair of electron on oxygen atom and C1 for the hydrogen atom as proton donor.

site. Similarly, the sites on dimethyl ether are labelled as A2 and B2. It may be noted that this convention is not standard, one may have its own nomenclature however it should be kept in mind that such a nomenclature should clearly indicate different sites on different components

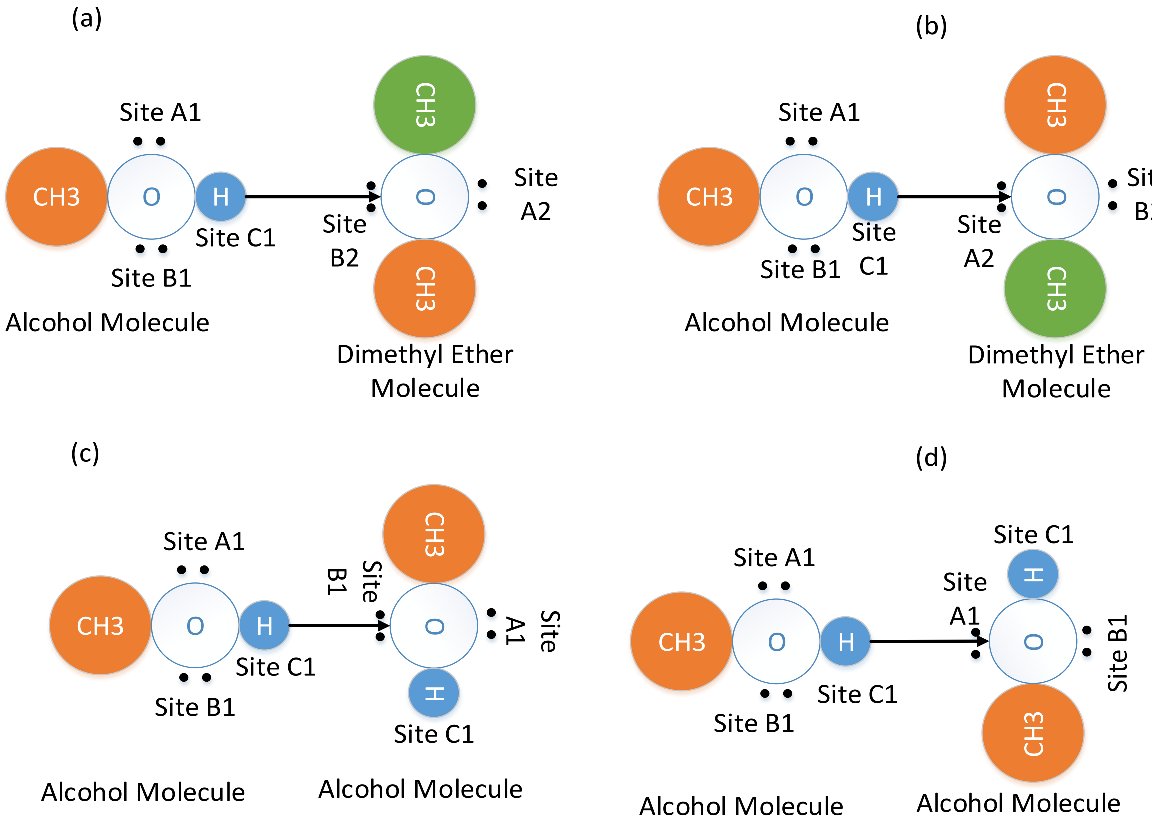

Figure 2-3 Illustration for the types of association for Methanol-Dimethyl Ether mixure using 3 association sites for methanol and 2 for DME

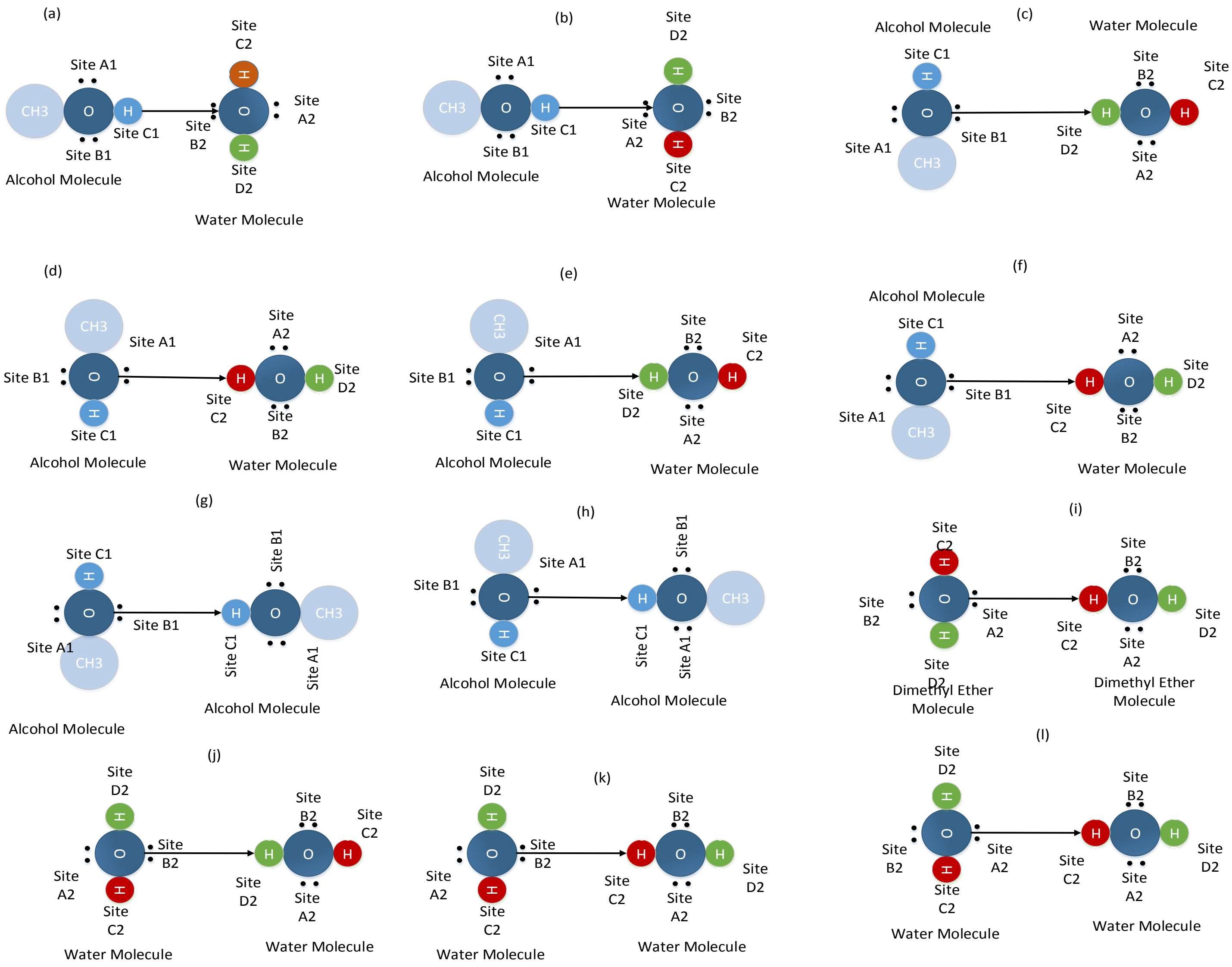

Figure 2-4 Illustration showing association between alcohol with 3 association sites and Water with 4 association sites

The various cases shown in the figure are described below. Cases (a) and (b) denotes cross-association and (c) and (d) denotes self-association.

a) In this case, the methanol shares it hydrogen atom on site C1 with the oxygen on site B2 of dimethyl ether, forming a hydrogen bond.
b) This case is similar to the case (a) but this time, methanol shares its hydrogen with the different site A2 (second lone pair of electron on oxygen at DME).
c) The hydrogen of the methanol is shared to form hydrogen bond with oxygen of another molecule of same component methanol.
d) The same case as (c) but this time the site is different.

It is important to note here that, the methanol should also be investigated with 2 association sites unlike 3, for which the illustration is described in **Figure 2-3** because sometimes methanol can have only have its 2 association sites available depending on various conditions such as steric effect, conformational configurations temperature and pressure which tend to effect the association. Moreover the dimethyl ether should also be investigated for 1 association site for the same reason.

Hence, there will be many association scenarios for the same type of mixture for investigation like, for Alcohol-DME (3-2, 2-2, 2-1, 3-1) association cases may exist. However 1-1 association site and 1-0 association may be omitted based on experience and on the fact that Dimethyl Ether has strong tendency to associate with hydrogen and methanol at least has 2 association site available, always.

Finally, after investigating the possible association scenarios, the equation for association, mentioned in section 2.5.2 are expanded for each and every case, refer to appendix A1 for sample case of expansion for equations and appendix A2 for similar illustration for Water-Alcohol as shown above.

After describing the Statistical Associating Fluid Theory, both by its mathematical and physical form, in this chapter along with the description of association scenarios in DME mixtures. It is necessary to devote the next chapter based on the electrostatic contribution.

2.7 Summary of SAFT and proposed improvements

The discussion that is made until now, proves that the accurate phase equilibrium data for mixtures and pure components is very critical for efficient and optimal design. For this purpose, many thermodynamic models have been derived to predict quantitative phase equilibria such as, PR, SRK, and activity coefficient models. But, because of their empirical nature i.e. reliance on experimental data to produce quantitative results, they have been lacking on their reliability and adaptability. As the experiments are both costly and time consuming, and these so-called thermodynamic models have been failing so far. The development of a reliable, robust and accurate method, for predicting the phase equilibria of the complex systems is a need of the hour. Many of the newer thermodynamic EOS are built on statistical mechanical theories. These theories are able to predict the phase equilibrium data with increased accuracy and reliability. But, still these theories are unable to produce satisfactory prediction for, associating and polar species especially, small sized molecules where the polar interactions are predominant (described in detail in **Chapter 2**).

Originating from the development of molecular simulation tools, a new equation of state using the concepts of statistical thermodynamics, have been developed. One of these theories is the SAFT EOS. The idea behind this theory is, to construct a model based on the physical description of the real fluids. In, the last ten years tremendous focus was made to improve the predictive capability of these models. Many modified theories were proposed such as, original SAFT, Chen-Kreglewski SAFT (CK-SAFT), Simplified SAFT, Lennard Jones SAFT (LJ-SAFT), Soft SAFT, and Variable Range SAFT (SAFT–VR), Perturbed Chain SAFT (PC-SAFT) (refer to **Table 2.1** for description). The main modifications in these theories can be grouped into, either a different choice of reference system or the choice of describing attractive/ repulsive interaction. Unarguably, the best modification were those in which, there were inclusion of the polar interaction between the molecules (see **section 2.3** for description). But, the extension of electrostatic/ coulombic interactions resulted in more complex equation of state and hence, these modifications were being avoided so far, despite of adjusting the binary interaction parameter with the experimental data. Such a choice leads in, rendering these SAFT equations, unable to predict results without experimental data availability. It has been observed that, the inclusion of the dipolar term in the present SAFT theories could enable them, to produce quantitative results without the need of adjusting binary interaction parameter [21, 74, 77, 86–90]. The next section is devoted to the developments leading to the dipolar contribution applicable to SAFT.

CHAPTER 3

THE LONG-RANGED POLAR INTERACTIONS

3.1 Introduction

As discussed in the previous chapters, the need for including long-ranged electrostatic interactions in the current model of SAFT. A definitive basis is formed that electrostatic interactions cannot be ignored if SAFT model needs improvements.

Electrostatic forces exist between molecules that exhibit polarity. The polar molecules tend to align themselves for greater attraction to reduce potential energy. Polarity is the segregation of positive and negative charges separated by a distance in molecules. The following illustration shows how DME molecules exhibit dipole-dipole attraction. The negative end of O (δ-) attracts the positive end of CH_3 (δ+). The molecule is held together by these attractive forces which significantly changes the phase behavior of the compound.

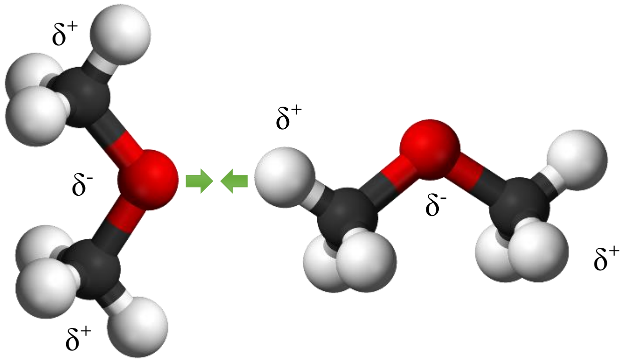

Figure 3-1 Dipolar attraction between dimethyl ether molecule

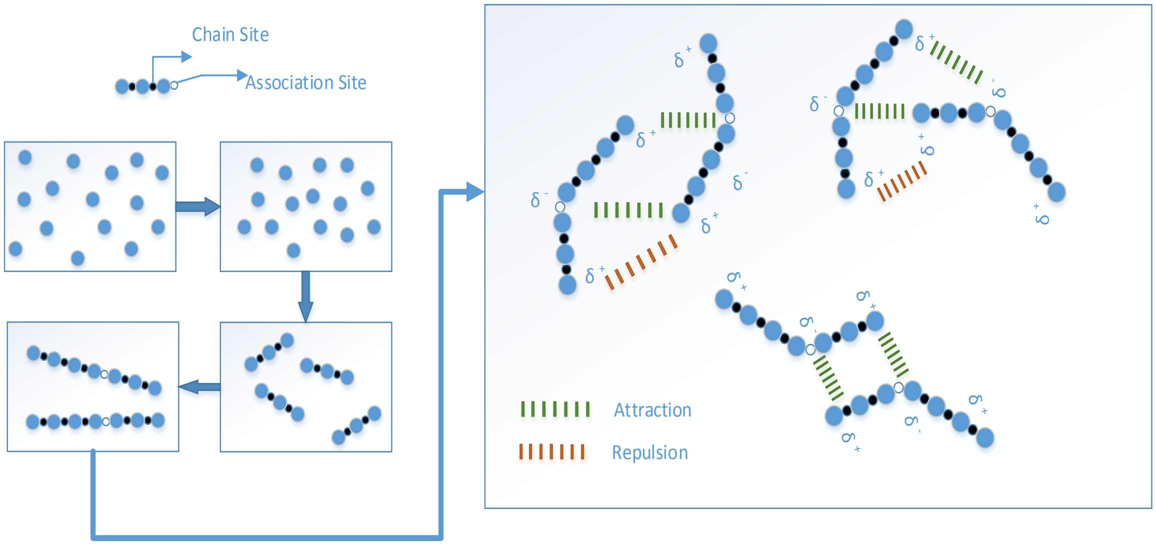

Figure 3-2 Dipolar forces as viewed in SAFT

In the present chapter, the discussions are made to account for polar contributions in SAFT. **Section 3.2** describes the background and developments that lead to include polar contributions in the SAFT model. Two polar theories that are employed into Simplified SAFT (SSAFT) are discussed in detail in **Section 3.3 and 3.4,** namely Gross & Vrabec (GV) and Jog & Chapman (JC) dipolar theories. The mathematical formulations are also provided alongside in those sections. Finally **Section 3.5** provides the detailed equations for hydrogen bonding association, which is a special case of electrostatic interactions.

3.2 Development of polar contribution for SSAFT

There are two ways to include polar interactions in SAFT. First method which was suggested by the integral equations and the second by perturbation theories, where the dipolar contribution of the intermolecular interactions are defined as a perturbation to a known non-polar reference fluid. Rushbrooke et al [91] proposed a dipolar term using mean spherical approximation theory, that involved pair correlation function for a fluid that exhibits hard sphere repulsions, which was later modified to account for ionic charges by Henderson et al. [92]. Gubbins and Twu [93] proposed a simple expression along with Lennard Jones potential, for a fluid exhibiting dipolar and quadrupolar interactions for non-spherical components and their mixtures. Since then, several modification relating to the Statistical Associating Fluid Theory have come, a dipolar term developed by Chapman et al [74] was developed which uses perturbation theory of first order to model polar fluids. Later, Gross and Sadowski [94] developed the polar Perturbed-Chain Statistical associating fluid theory (PPC-SAFT) EOS, accounting for quadrupolar term developed by Saager and Fischer [95]. Later boublik [96] studied the polar contribution for non-spherical molecules, considering using the radial distribution function. Luposki & Monson [97] and Mc Guinen [98] later included polar interactions and did a thorough investigations on elucidating the structure and the vapor-liquid equilibrium, which was in agreement with the molecular simulation data.

Among these mentioned models, most of them used the molecular simulation data for structural properties (pair correlation function). Another approach that gave good results was suggested Saager and Fischer et al [99] and Saager et al [100], performed molecular simulations for VLE and obtained dipole and quadrupole terms by regressing them against the macroscopic properties, rather than using macroscopic properties from molecular simulations. The simulations were performed on the 2-center Lennard-Jones (LJ) point-dipole fluids, by fixing the molecular elongation. But, such expressions were not useful for asymmetrical mixtures as these were empirical in nature. Of these mentioned dipolar contribution approaches, we find the one developed by Jog & Chapman and another by Gross & Vrabec, suitable to be included in the current model of simplified SAFT because of their non-empirical nature and their basis on perturbation theory, which is consistent with the overall SAFT model. These two dipolar modification are proposed in this present work, which successfully predicted the phase data, without the adjustment of binary interaction parameter. Hence, the model was successfully included with the electrostatic interactions. In the preceding section, the Gross & Vrabec dipolar term and Jog & Chapman dipolar term are discussed in detail, along with their mathematical representation.

3.3 The Gross & Vrabec (GV) Dipolar Term [21]

The Gross and Vrabec dipolar term which is based on the third order perturbation theory, is derived for non-spherical molecules, accounting for dipolar contribution. The model is written in Pade approximation and the constants were regressed to comprehensive experimental phase equilibrium data, of pure 2CLJ (2 centered-Lennard-Jones) plus point dipoles fluids.

The 2CLJ plus pointdipole consist of two Lenard Jones site located at a distance L apart and pointdipolar site placed at geometric center along the molecular axis as shown in the **Figure 3-3** (pointdipolar representation) and **Figure 3-4**.

The intermolecular potential, can thus be divide into a contribution from the 2CLJ fluid and the contribution from the dipolar forces u^{2CLJ} and u^{DD}.

$$u\left(r_{ij,}\omega_{i,}r_{j,}\right) = u^{2CLJ}\left(r_{ij,}\omega_{i,}r_{j,}\right) + u^{DD}\left(r_{ij,}\omega_{i,}r_{j,}\right) \qquad 3\text{-}1$$

Where r_{ij} the vector from the first pointdipole's molecular center, to the other and ω_i denotes a set of two molecular orientation angles {θ$_i$ and φ$_i$}. The part of the potential, of the pure 2CLJ fluid can conveniently be written as.

$$u^{2CLJ}\left(r_{ij,}\omega_{i,}r_{j,}\right) = \sum_{\alpha=1}^{2}\sum_{\beta=1}^{2} 4\varepsilon\left[\left(\frac{\sigma}{r_{\alpha\beta}}\right)^{12} - \left(\frac{\sigma}{r_{\alpha\beta}}\right)^{6}\right] \tag{3-2}$$

Where $\sigma \; and \; \varepsilon$ are the Lennard Jones segment size and segment energy parameters and $r_{\alpha\beta}$ is the distance between two LJ sites of different molecules i and j. The dipolar contribution can therefore be written as.

$$u^{DD}\left(r_{ij,}\omega_{i,}r_{j,}\right) = -\mu_i\mu_i\left|r_{ij}\right|^{-3} \times \left[2\cos\theta_i\cos\theta_j - sin\theta_i\sin\theta_j\cos(\varphi_j - \varphi_i)\right] \tag{3-3}$$

Where μ_i is the dipole moment the θ_i is the polar angle of the dipole formed with the vector $r_{ij} \; and \; \varphi_i$ is the azimuthal angle thereof. By applying the perturbation theory for the intermolecular potential, the equation 3.1 results in an EOS given in the azimuthal angle thereof in terms of residual Helmholtz energy A^{res}.

$$\frac{A^{res}}{NkT} = \frac{A^{2CLJ}}{NkT} + \frac{A^{DD}}{NkT} \tag{3-4}$$

Where,

A^{2CLJ} is the residual Helmholtz energy of the 2CLJ reference fluid.

A^{DD} is the contribution from the dipole-dipole interaction

N denotes the total number of molecules and

k is the Boltzmann constant.

$$\frac{A^{2CLJ}}{NkT} = m\frac{A^{LJ}}{NkT} + (1-m)[g^{LJ}(\sigma)] \qquad 3\text{-}5$$

A^{LJ} : the Lennard Jones's monomer Helmholtz energy.

$g^{LJ}(\sigma)$: represents the pair correlation for a system of LJ spherical molecules at a radial distance σ.

A simple scheme is adapted where the segment size parameter σ for both the models is equal and thus [21]

$$\sigma = \sigma^{2CLJ} \qquad 3\text{-}6$$

$$\in = \frac{4}{m^2} \in^{2CLJ} \qquad 3\text{-}7$$

$$\mu^{*^2} = \frac{m}{4}(\mu^{*^{2CLJ}})^2 \qquad 3\text{-}8$$

$$T^* = \frac{m^2}{4} T^{*2CLJ} \qquad 3\text{-}9$$

$$P^* = \frac{m^3}{4} P^{*2CLJ} \qquad 3\text{-}10$$

Dimensionless molecular elongation, $L^* = L/\sigma$ is related to equivalent segment number m, to the simulation data of the 2CLJ fluid from Stoll et al. The relation between elongation $L^*$and the segment number m is then given by,

$$m = 1 + 0.1795L^* + 3.3283L^{*2} - 3.8855L^{*3} + 1.3777L^{*4} \qquad 0 \le L^* \le 1 \quad 3\text{-}9$$

After applying the Pade approximation [101], we obtain.

$$\frac{A^{DD}}{NkT} = \frac{A_2/NkT}{1-A_{3/}A_2} \qquad 3\text{-}10$$

Where A_2 and A_3 are the the 2nd order 3rd order perturbation terms respectively.

$$\frac{A_2}{NkT} = -\pi\rho \sum_i \sum_j x_i x_j \frac{\varepsilon_{ii}}{kT} \frac{\varepsilon_{jj}}{kT} \frac{{\sigma_{ii}}^3 {\sigma_{jj}}^3}{{\sigma_{ij}}^3} n_{\mu i} n_{\mu j} \mu_i^{*2} \mu_i^{*2} J_{2,ij}^{DD} \tag{3-11}$$

and

$$\frac{A_3}{NkT} = -\frac{4\pi^2}{3} \rho^2 \sum_i \sum_j \sum_k x_i x_j x_k \frac{\varepsilon_{ii}}{kT} \frac{\varepsilon_{jj}}{kT} \frac{\varepsilon_{kk}}{kT} \frac{{\sigma_{ii}}^3 {\sigma_{jj}}^3 {\sigma_{kk}}^3}{\sigma_{ij} \sigma_{ik} \sigma_{jk}} n_{\mu i} n_{\mu j} n_{\mu k} \mu_i^{*2} \mu_i^{*2} \mu_k^{*2} J_{3,ij}^{DD} \tag{3-12}$$

$$J_{2,ij}^{DD} = \sum_{n=0}^{4} \left(a_{n,ij} + b_{n,ij} \frac{\varepsilon_{ij}}{kT} \right) \eta^n \tag{3-13}$$

$$J_{3,ij}^{DD} = \sum_{n=0}^{4} c_{n,ij}\, \eta^n \tag{3-14}$$

Where x_i represent the mole fraction of component i.

μ_i^{*2} : squared dimensionless dipole moment of component u and is given as

$$\mu_i^{*2} = \frac{\mu^{*2}}{m_i \varepsilon_{ii} {\sigma_{ii}}^3} \tag{3-15}$$

The terms $J_{2,ij}^{DD}, J_{3,ij}^{DD}$ represent the intergral on the 2- body and 3-body correlation function and ref-fluid correlation function for the dipolar fluids respectively.

η: Dimensionless density.

The coefficients of the equation 3-13 and 3-14 are dependent on the length of the chain. For detailed descriptions, reader are encouraged to refer to [21], [88]. The next section is similarly devoted to Jog and Chapman dipolar term.

3.4 The Jog & Chapman (JC) dipolar term [20]

3.4.1 Introduction

Jog and Chapman gave a term that was able to successfully describe the associating interaction nature of electrostatic nature within the systems, it was based on the Wertheim's thermodynamic perturbation theory of first order. The SAFT term describing the change in free energy contributing to the dipolar interaction, is taken by dissolving all bonds in a chain and forming a mixture of non-bonded segments of both polar and non-polar segments.

The first order perturbation theory of Wertheim, is applied to polar hard sphere chains, tangentially. Let us assume a hard sphere chain with alternated dipolar segments as shown below in the figure 3-1 and 3-2

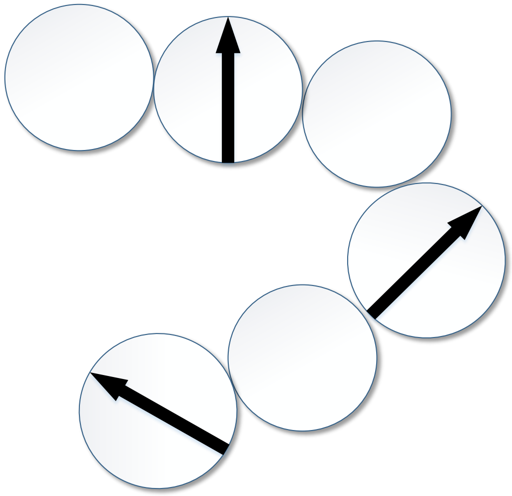

Figure 3-3 Model for the dipolar chain molecules. Orientation of dipolar segments point-dipolar site

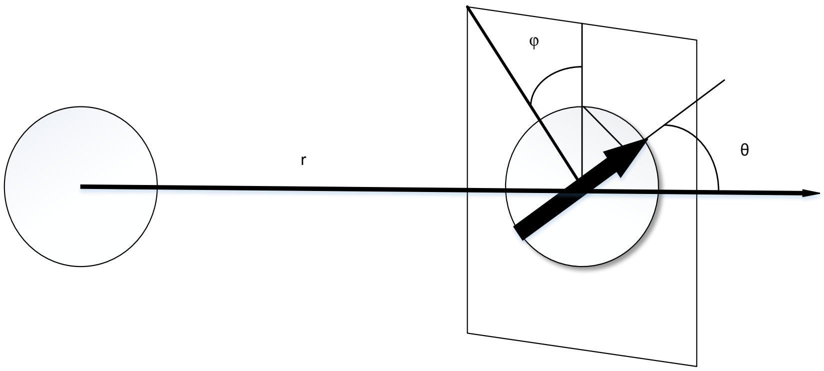

Figure 3-4 The dependence of the pair correlation function g=g(r, θ, φ) on the orientation of the dipolar segment.

$$\mu^{*} = \mu/(\sigma^{3}kT)^{1/2} \qquad 3\text{-}15$$

σ : Hard sphere diameter

μ: Dipole moment.

Here the contribution of the dipole moment can be obtained as single parameter as evident from the interaction potential. The dipole moment in this model, is assumed to be perpendicular, to the line vector which joins the segment, which bears the dipole to the last segment. This model is developed for chain molecules that bear polar substituent groups. The model is thus formed by assuming a mixture of non-polar and dipolar hard spheres reference fluid.

The pair potential u_{ij} is thus written as.

$$u_{22}(r,\Omega_1,\Omega_2) = u_{HS}(r) - \frac{\mu^2}{r^3}[3(\hat{u}_1\hat{r})(\hat{u}_2\hat{r}) - \hat{u}_1\hat{u}_2] \qquad 3\text{-}16$$

Where $\hat{r}$ the unit vector is parallel to the axis and û is the unit vector which is parallel to the dipole moment of the molecule.

After shedding adequate light, on the physical picture of the Jog and Chapman dipolar term, it is apparently evident, to continue developing its mathematical formulation which can thence be integrated into Simplified SAFT (SSAFT) model.

3.4.2 Developing the EOS for the JC dipolar term

For the reason of predicting the Pressure, Volume, Temperature (PVT) behavior of the polar chains, it is necessary to use Statistical mechanical EOS, for these proposed polar spheres. It is thus ultimately required, to calculate the compressibility factor of these reference fluids (mixture containing equal number of moles of dipolar and non-polar hard spheres). The term for Helmholtz energy and other thermodynamic properties are obtained analytically through the u-expansion particularly for the mixtures. [91, 102]

$$u_{\alpha\beta}(\boldsymbol{r},\boldsymbol{\Omega_1},\boldsymbol{\Omega_2}) = u^0_{\alpha\beta}(\boldsymbol{r}) + u^a_{\alpha\beta}(\boldsymbol{r},\boldsymbol{\Omega_1},\boldsymbol{\Omega_2}) \qquad 3\text{-}17$$

$$u^0_{\alpha\beta}(\boldsymbol{r}) = \langle u_{\alpha\beta}(\boldsymbol{r},\boldsymbol{\Omega_1},\boldsymbol{\Omega_2})\rangle_{\boldsymbol{\Omega_1},\boldsymbol{\Omega_2}} \qquad 3\text{-}18$$

There are 3 pair interactions (1-1, 1-2, 2-2). Because of the orientational average and the dipole-dipole potential being 0, the isotropic potential can be assumed to be the hard-sphere potential. Finally the Helmholtz free energy is expanded through powers of $u_{\alpha\beta}/kT$.(Rushbrooke, G. S. Stell, G., Hoye, 1973) [74]

$$A = A_0 + A_2 + A_3 \ldots \qquad 3\text{-}19$$

A_1 term in this Helmholtz energy equation is discarded because of the choice made in deciding reference fluid potential.[102]

The other terms in the equation 3-19 are described as follows.

$$A_2 = -\frac{1}{4kT}\sum_{\alpha\beta} \rho_\alpha \rho_\beta \int d\boldsymbol{R_1}\, d\boldsymbol{R_2} \times \langle u^a_{\alpha\beta}(\boldsymbol{R_{12}}, \boldsymbol{\Omega_1}, \boldsymbol{\Omega_2})^2\rangle_{\boldsymbol{\Omega_1},\boldsymbol{\Omega_2}} g^0_{\alpha\beta}(R_{12}) \tag{3-20}$$

$$A_3 = A_{3A} + A_{3B} \tag{3-20}$$

$$A_{3A} = -\frac{1}{12(kT)^2}\sum_{\alpha\beta} \rho_\alpha \rho_\beta \int d\boldsymbol{R_1}\, d\boldsymbol{R_2} \times \langle u^a_{\alpha\beta}(\boldsymbol{R_{12}}, \boldsymbol{\Omega_1}, \boldsymbol{\Omega_2})^3\rangle_{\boldsymbol{\Omega_1},\boldsymbol{\Omega_2}} g^0_{\alpha\beta}(\boldsymbol{R}_{12}) \tag{3-21}$$

$$A_{3B} = -\frac{1}{6(kT)^2}\sum_{\alpha\beta\gamma} \rho_\alpha \rho_\beta \rho_\gamma \int d\boldsymbol{R_1}\, d\boldsymbol{R_2} d\boldsymbol{R_3} \times \langle u^a_{\alpha\beta}(\boldsymbol{R_{13}}, \boldsymbol{\Omega_1}, \boldsymbol{\Omega_3}) \times$$

$$u^a_{\alpha\gamma}(\boldsymbol{R_{23}}, \boldsymbol{\Omega_2}, \boldsymbol{\Omega_3}) u^a_{\beta\gamma}(\boldsymbol{R_{23}}, \boldsymbol{\Omega_2}, \boldsymbol{\Omega_3})^3\rangle_{\boldsymbol{\Omega_1},\boldsymbol{\Omega_2},\boldsymbol{\Omega_3}} g^0_{\alpha\beta}(\boldsymbol{R}_{12}\boldsymbol{R}_{13}\boldsymbol{R}_{23}) \tag{3-22}$$

After applying the Pade approximation to the different terms of the Helmholtz energy viz. A_2 A_3, the following simpler equations are obtained. These obtained terms are finally integrated into final Helmholtz energy equation of the current SSAFT model.

$$a^{polar} = \frac{a_2{}^{polar}}{1 - a_3^{polar}/a_2^{polar}} \tag{3-23}$$

$$a_2^{polar} = -\frac{2\pi}{9}\frac{\rho}{(kT)^2}\sum_i \sum_j x_i x_j m_i m_j x_{pi} x_{pj} \frac{\mu_i^2 \mu_j^2}{d_{ij}^3} I_{2,ij} \tag{3-24}$$

$$a_3^{polar} = -\frac{15}{9}\pi^2 \frac{\rho^2}{(kT)^3}\sum_i \sum_j \sum_k x_i x_j x_k m_i m_j m_k x_{pi} x_{pj} x_{pk} \frac{\mu_i^2 \mu_j^2 \mu_k^2}{d_{ij} d_{jk} d_{ik}} I_{3,ijk} \tag{3-25}$$

For the reference fluid which is considered here the other variables are defined as

$$y = \frac{4\pi}{9}\frac{\rho}{2}\frac{\mu^2}{kT} \tag{3-26}$$

$$\rho^* = \rho\sigma^3 \tag{3-27}$$

$$T^* = \frac{kT\sigma^3}{\mu^2} \tag{3-28}$$

The integrals in the above equations are defined as follows.

$$I_2(\rho^*) = \frac{3\sigma^3}{4\pi}\int g_{HS}(r,\rho^*)\frac{1}{r^6}\,d\boldsymbol{r} \tag{3-29}$$

$$I_3(\rho^*) = \frac{3\sigma^3}{5\pi^2}\int g_{HS}(123,\rho^*)u(123)\,d\boldsymbol{r_2}d\boldsymbol{r_3} \tag{3-30}$$

$$u(123) = \frac{1+3cos\alpha_1 cos\alpha_2 cos\alpha_3}{(r_{12}r_{13}r_{23})^3} \tag{3-31}$$

$$I_2(\rho^*) = \frac{1-0.3618\rho^* - 0.3205{\rho^*}^2 + 0.1078{\rho^*}^3}{(1-0.5236\rho^*)^2} \tag{3-32}$$

$$I_3(\rho^*) = \frac{1+0.62370\rho^* - 0.11658{\rho^*}^2}{1-0.59056\rho^* + 0.80059{\rho^*}^2} \tag{3-33}$$

Finally the Helmholtz free energy is given as

$$\frac{A-A_0}{kT} = \frac{-\frac{2\pi}{9}\left(\frac{1}{T^*}\right)^2\rho^* x_p^2 I_2(\rho^*)}{1+\frac{5\pi}{36}\left(\frac{1}{T^*}\right)\rho^* x_p \frac{I_2(\rho^*)}{I_3(\rho^*)}} \tag{3-34}$$

Here x_p denotes the mole fraction of the polar hard spheres.

In the previous **sections 3.2** and **3.3** we have provided a detailed description of the Gross and Vrabec (GV) and Jog and Chapman (JC) dipolar terms. These electrostatic contribution are based on perturbation theory, the same theory on which SAFT is based. Describing the picture of dipolar molecules, as point-dipole and obtaining the final expression for residual Helmholtz energy based on perturbation, makes the final model more simplistic and consistent.

Before moving on to the evaluation and prediction from the developed model it necessary to summarize the equation for associative components.

3.5 Equations for the associative components

Although, written previously in section 2.5.2 it is still however necessary, to summarize them for a clearer understanding. These are derivative equation in terms of Helmholtz energy which are expanded based on the description provided in **Section 2.6**, for the various schemes of association. (Refer to **appendix B** for a sample case of expansion)

$$H = \frac{a^{assoc}}{RT} = \sum_i X_i \left[\sum_{Ai} \left[lnX^{Ai} - \frac{X^{Ai}}{2}\right] + \frac{1}{2} M_i\right] \qquad \text{3-34}$$

$$X^{Ai} = \left[1 + \rho \sum_i \sum_{Bj} X_j X^{Bj} \Delta^{A_i B_j}\right]^{-1} \qquad \text{3-35}$$

$$\Delta^{A_i B_j} = \left(\sigma_{ij}\right)^3 \kappa^{A_i B_j} g_{ij}(d_{ij})[exp(\epsilon^{A_i B_j}/kT) - 1] \qquad \text{3-36}$$

$$(H)_\rho = \frac{\partial H}{\partial \rho} = \sum_i X_i \left[\sum_{Ai} \left[\frac{1}{X^{Aj}} - \frac{1}{2}\right] \left(X^{Ai}\right)_\rho\right] \qquad \text{3-37}$$

$$(H)_\rho = \frac{\partial H}{\partial X_k} = \left[\sum_{Ak} \left[lnX^{Ak} - \frac{X^{Ai}}{2}\right] + \frac{1}{2} M_k\right] + \sum_i X_i \left[\sum_{Ai} \left[\frac{1}{X^{Ai}} - \frac{1}{2}\right] \left(X^{Ai}\right)_{X_k}\right] \qquad \text{3-38}$$

$$\left(X^{Ai}\right)_\rho = -\left(X^{Ai}\right)^2 \left[\sum_j \sum_{B_j} X_j X^{Bj} \Delta^{A_i B_j} + \rho \sum_j \sum_{Bj} X_j (X^{Bj})_\rho \Delta^{A_i B_j} + \right.$$

$$\left. \rho \sum_j \sum_{Bj} X_j (X^{Bj}) (\Delta^{A_i B_j})_\rho \right] \qquad \text{3-39}$$

$$(\Delta^{A_i B_j})_\rho = \left(\sigma_{ij}\right)^3 \kappa^{A_i B_j} \left(g_{ij}\right)_\rho (d_{ij})[exp(\epsilon^{A_i B_j}/kT) - 1] \qquad \text{3-40}$$

$$\left(X^{Ai}\right)_{X_k} = -\left(X^{Ai}\right)^2 [\sum_j \sum_{B_k} X_j X^{Bk} \Delta^{A_i B_k} + \rho \sum_j \sum_{Bj} X_j (X^{Bj})_{X_k} \Delta^{A_i B_j} +$$

$$\rho \sum_j \sum_{Bj} X_j (X^{Bj}) (\Delta^{A_i B_j})_{X_k}] \qquad \text{3-41}$$

$$(\Delta^{A_iB_j})_{X_k} = \left(\sigma_{ij}\right)^3 \kappa^{A_iB_j} \left(g_{ij}\right)_{X_k} (d_{ij}) [exp(\epsilon^{A_iB_j}/kT) - 1] \qquad 3\text{-}42$$

After presenting description about the Statistical Associating Fluid Theory followed by the proposed modifications using long ranged electrostatic interaction and short ranged hydrogen binding associations. It is obvious to present Vapor Liquid Equilibrium (VLE) predictions from the developed model. The succeeding chapters are going to present the results of VLE for DME containing mixtures such as DME-hydrocarbons, DME-alcohols, DME-light gases. The methods and various challenges presented along with the results.

CHAPTER 4

PREDICTION OF VLE FOR DME-HYDROCARBONS WITH THE POLAR SSAFT EOS

This chapter presents the methodology and results of vapor-liquid equilibrium prediction from polar SSAFT model for DME-hydrocarbon mixtures. The long-ranged dipole-dipole interactions of DME are employed using Jog and Chapman approach (JC) as well as Gross and Vrabec approach (GV). Various kinds of hydrocarbons are considered including alkanes and alkenes. The role of the electrostatic interactions in VLE prediction is studied and compared to the non-electrostatic case. This chapter is organized as follows. **Section 4.1** gives a brief introduction on how the adjustable parameters are obtained for both dipolar and non-polar components. Then, the prediction of VLE for various DME-hydrocarbon mixtures using JC term is demonstrated and compared to the non-electrostatic case (**Section 4.2**). In **Section 4.3**, a comparison is made between JC and GV approaches. Finally, the conclusions obtained from the role of electrostatic dipole-dipole interactions in the VLE prediction of DME-hydrocarbon are highlighted in **Section 4.4**.

4.1 Adjustable parameters for pure compounds

The SSAFT equation of state has only 3 adjustable parameters for non-polar compounds. They are the temperature independent square well depth (u^0), the segment molar volume in a close packed arrangement (v^{00}) and the number of segments (m). For associating compounds such as alcohols and water, there are two more parameters, namely the association volume (k^{AB}) and the association energy ($\in^{AB}$). An additional parameter might be added if the polar forces are included depending on which polar term is used. For example, an adjustable parameter is used to represent the fraction of dipolar segment in a molecule (x_p) if Chapman term is utilized. However, Gross term does not have any adjustable parameter for polar compounds.

These adjustable parameters are estimated by regressing against the experimental data of pressure-volume-temperature (PVT). In particular, an objective function is minimized based on the experimental and calculated liquid density and vapor pressure:

$$obj = \sum \left[\left(\frac{P_{cal} - P_{exp}}{P_{exp}} \right)^2 + \left(\frac{\rho_{cal}^L - \rho_{exp}^L}{\rho_{exp}^L} \right)^2 \right]$$

The Average Absolute Deviation in Pressure (% AADP) and Average Absolute Deviation in Liquid Density (% AADL) are calculated for vapor pressure and liquid density based on the following equations:

$$AADP\ (\%) = \left(\sum \left| \frac{P_{exp} - P_{cal}}{P_{exp}} \right| / N \right) \times 100$$

$$AADL\ (\%) = \left(\sum \left| \frac{\rho_{exp}^L - \rho_{cal}^L}{\rho_{exp}^L} \right| / N \right) \times 100$$

Where N represents the number of data points P is vapor pressure, ρ_{cal}^L is calculated saturated liquid density and ρ_{exp}^L is experimental Saturated liquid density.

The calculated saturated density and vapor pressure are determined by satisfying the three equilibrium conditions, namely, thermal, mechanical and chemical equilibrium. A brief procedure for VLE calucation is provided in Appendix C. For minimizing the objective function, Nelder-Mead simplex direct search is utilized [103].

Table 4.1 provides the estimated pure component parameters of various compounds including hydrocarbons, DME, water and alcohols. These pure parameters are used for all calculations presented in this thesis. For associating components, various association schemes are used such as two and three association sites which were discussed in detail previously in **Section 2.6**. Electrostatic interactions are accounted for polar compounds. It should be noted that JC is used to indicate Jog & Chapman dipolar term while GV is used to denote the Gross & Vrabec term. The table also lists the values of dipole and quadrupole moments. The average absolute deviations are also reported for vapor pressure and liquid density. The sources of the experimental PVT data are also given for each component.

Sandler et al gave general expressions for the determination of pure component parameters based on small alkanes using least squares analysis. It was observed that the number of segments (m) increases linearly with increasing molecular weight and is given by the following expression.

$$m = 0.047M_W + 0.511 \qquad 4\text{-}1$$

Similar expressions were obtained for segment molar volume (v^{00}) and temperature independent square well depth (u^0/k) as follows:

$$mv^{00} = 0.835M_W + 8.206 \qquad 4\text{-}2$$

and

$$mu^0/k = 4.912M_W + 30.318 \qquad 4\text{-}3$$

The previous three correlations should be used only for hydrocarbons.

To explore the accuracy of the estimation of the pure parameters, a comparison of the SSAFT and dipolar SSAFT are compared with experimental data. **Figures 4-1 and 4-2** shows vapor-liquid equilibrium coexistence curve. The vapor pressure vs. temperature is plotted for few pure components using the proposed model against experiment. As seen in the figures, the polar SSAFT is in excellent agreement with the experimental data and performs better than the non-polar SSAFT. The average absolute deviation for pure DME in vapor pressure is 0.99 % and in liquid density is 0.88 % using SSAFT-JC. On the other hand, the non-polar SSAFT has average absolute deviations of 1.61 % in vapor pressure and 1.13 % in liquid density.

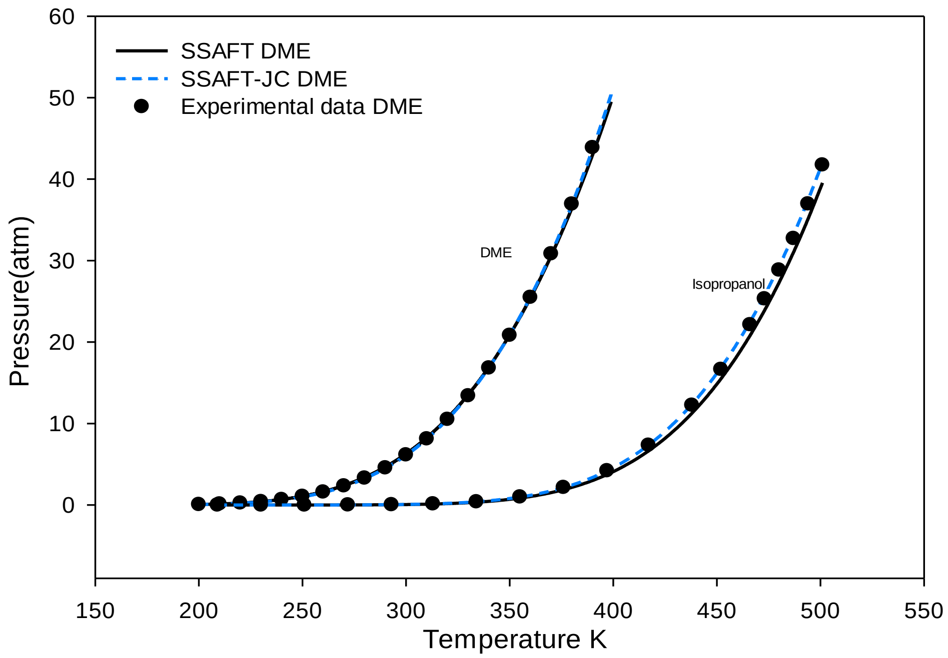

Figure 4-1 Pressure-Temperature curve for pure compounds

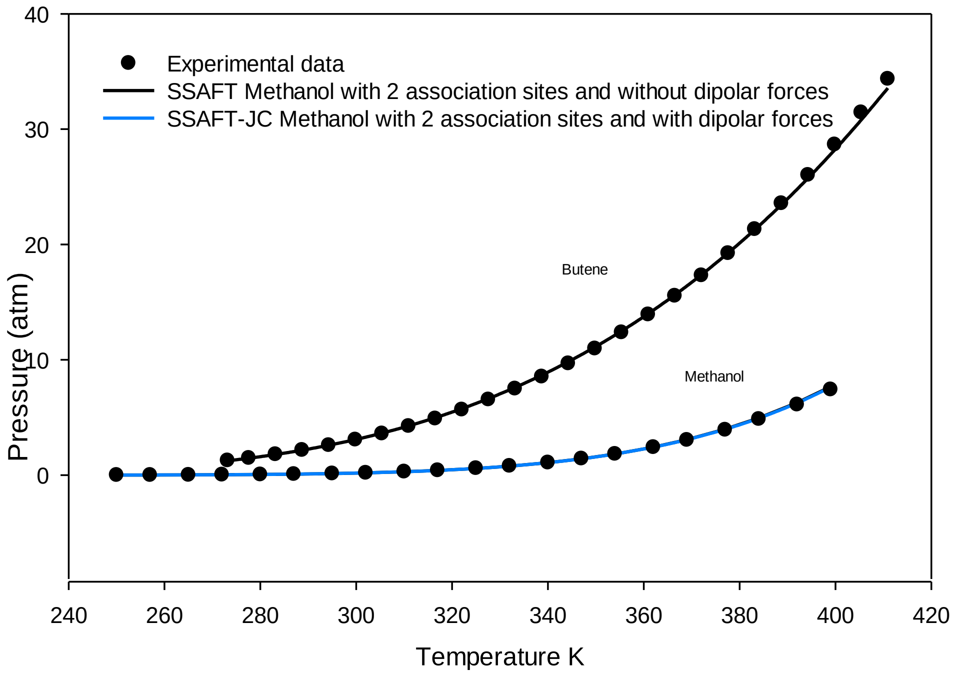

Figure 4-2 Pressure-Temperature curve for pure compounds black line is from SSAFT without polar forces while blue line is from SSAFT-JC including polar forces.

Table 4-1 Estimated parameters for pure components

Compound Class	Compound	Polar Term	Polar form[a]	M g mol^{-1}	m	v^{00}(mL)	u^0/k (K)	$1000\kappa^{AB}$	ε^{AB}/k (K)	x_p
Alkanes	propane	-	-	44.10	2.7350	16.507	92.571	-	-	-
	Butane	-	-	58.12	2.9620	19.263	102.823	-	-	-
	Hexane	-	-	88.18	4.5480	17.657	99.724	-	-	-
	Decane	-	-	142.28	7.4677	17.022	99.329	-	-	-
Alkenes	1-Propene	-	-	42.0	2.3949	17.003	98.715	-	-	-
	1-Butene	-	-	56.11	3.6005	14.708	90.937	-	-	-
DME	DME	JC	DD	46.07	3.6274	11.116	77.519	-	-	0.2757
	DME	JC	DD	46.07	2.8936	13.897	89.644	-	-	1/m
	DME	GV	DD	46.07	3.3547	11.380	89.14	-	-	-
	DME	-	-	46.07	3.4688	10.935	88.634			-
Gases	Nitrogen	-	-	28.02	3.1041	6.2622	30.746	-	-	-
	SO2	JC	DD	64.06	3.9676	7.7962	65.439	-	-	0.2
	SO2	-	-	64.06	4.0652	6.5166	88.952	-	-	
	SO2	GV	DD	64.06	3.5573	7.6797	88.659	-	-	

Alcohols	Methanol[d]	-	-	32.04	1.9408	15.000	147.67	0.036970	1435.2	-
	Methanol[e]	JC	DD	32.04	1.9845	15.000	139.24	0.045392	1408.5	0.2
	Methanol[f]	-	-	32.04	1.9890	14.000	89.135	0.119107	2710.4	-
	Methanol[g]	JC	DD	32.04	2.0842	14.000	75.487	0.136710	2734.4	0.2
	Ethanol[f]	-	-	46.08	2.5400	16.000	93.131	0.056634	2802.7	-
	Ethanol[g]	JC	DD	46.08	2.7935	15.000	84.234	0.068407	2716.7	0.2
	1-Propanol[f]	-	-	60.10	3.3160	16.000	104.651	0.041420	2511.7	-
	1-Propanol[g]	JC	DD	60.10	3.5874	15.000	99.891	0.049516	2257.0	0.2
	2-Propanol[f]	-	-	60.10	4.7501	10.582	80.460	0.117350	2383.2	-
	2-Propanol[g]	JC	DD	60.10	4.6300	12.303	66.520	0.131790	2214.9	0.2
	2-Propanol[g]	JC	DD	60.10	4.7187	10.706	80.163	0.11750	2380.9	0.035962
	2-propanol[f]	-	-	60.10	3.5257	15.000	94.508	0.042354	2518.4	-
	2-propanol[g]	JC	DD	60.10	3.6622	15.000	85.449	0.055923	2518.1	0.2
Water	Water[h]	-	-	18.015	2.0000	6.5600	188.231	0.119930	825.90	-
	Water[i]	-	-	18.015	1.5000	9.1362	189.74	0.101780	925.75	-
	Water[j]	JC	DD	18.015	1.3209	10.254	233.69	0.055765	580.40	0.2

Table 4-1 Continued.

Compound Class	Compound	μ (D)	AAD (%) Pressure	AAD (%) Density	Temperature range(K)	Data Ref.
Alkanes	Propane	0	1.13	1.56	189.5-367.18	[104]
	Butane	0	0.27	0.83	213.15-323.15	[104]
	Hexane	-	2.06	0.89	243.1-503.15	[104]
	Decane	0	2.89	1.31		[104]
Alkenes	1-Propene	0	3.16	0.71	277.15-333.15	[105]
	1-Butene	0	1.02	0.58	273.15 -410.93	[106]
DME	DME	1.3	0.05	0.07	250-399	Yaws Handbook 2003
	DME	1.3	0.99	0.98	200-399	Yaws Handbook 2003
	DME	1.3	0.07	0.08	200-399	Yaws Handbook 2003
	DME	1.3	1.61	1.13	200-399	Yaws Handbook 2003
Gases	Nitrogen	0	1.61	0.22	253.15-303.15	[107]
	SO2	1.62	1.53	1.10	200-420	[108]
	SO2	-	2.24	1.10	200-420	[108]
	SO2	1.62	1.78	0.97	200-420	
Alcohols	Methanol[d]	1.69	1.51	0.88	250-399	WebBook NIST
	Methanol[e]	1.69	1.65	1.05	253.15-493.15	[109]
	Methanol[f]	1.69	1.38	1.05	250-399	WebBook NIST
	Methanol[g]	1.69	1.40	1.08	250-399	WebBook NIST
	Ethanol[f]	1.66	1.21	0.56	250-399	[110]

	Ethanol[g]	1.66	1.05	0.61	250-399	[110]
	1-Propanol[f]	1.68	0.22	1.52	260-530	[111]
	1-Propanol[g]	1.68	3.58	2.29	210-500	[111]
	2-Propanol[f]	1.66			209-501	Yaws Handbook 2003
	2-Propanol[g]	1.66			209-501	Yaws Handbook 2003
	2-Propanol[g]	1.66			209-501	Yaws Handbook 2003
	2-propanol[f]	1.66			209-501	Yaws Handbook 2003
	2-propanol[g]	1.66			209-501	Yaws Handbook 2003
Water	Water[h]	1.85	2.22	3.30	283-613	[104]
	Water[i]	1.85	2.09	2.66	274-394	[104]
	Water[j]	1.85	1.96	2.51	274-394	[104]

[a] *Represents the polar term either Dipolar-Dipolar (DD) Quadrupolar-Quadrupolar (QQ)*
[b] *Quadrupolar moment given in the unit electron-barns*
[c] *Quadrupole moment value taken from (J.M. Junquera-Hernandez J. Sanchez-Mar, 2002)*
[d] *Alcohol with 3 association but without including dipolar forces*
[e] *Alcohol with 3 association including dipolar forces*
[f] *Alcohol with 2 association but without including dipolar forces*
[g] *Alcohol with 2 association including dipolar forces*
[h] *Water with 3 association sites but without including dipolar forces*
[i] *Water with 4 association sites but without including dipolar forces*
[j] *Water with 4 association including dipolar forces*
- The term or the value is not used.

4.2 VLE predictions for DME-Hydrocarbon mixtures

After the estimation of pure component parameters, the next task is to predict vapor-liquid equilibrium of binary mixtures. The calculations are carried out based on flash calculations. The calculated vapor-liquid equilibrium is compared with the experimental data to observe the accuracy in the prediction from the model. The experimental data are taken from the literature. The study of VLE is conducted with and without the addition of long-ranged dipole-dipole interactions for DME. Two different dipolar approaches are utilized with SSAFT, namely Gross & Vrabec (SSAFT-GV) and Jog & Chapman (SSAFT-JC). In this chapter, the focus is on DME-hydrocarbon mixtures. While, the next chapter covers DME-alcohols that exhibit cross association along with polar interactions.

The vapor-liquid equilibrium for DME mixtures with hydrocarbons, such as DME-Hexane, DME–Butane, DME-Propane, DME-Butene, and DME-propene are thoroughly studied, by incorporating the dipolar interactions in dimethyl ether. These systems have one polar non-associating component (DME) and another non-polar-non-associating component (alkanes, alkenes). In the prediction of VLE of these mixtures, it was observed that by including the dipolar forces to SSAFT (SSAFT-JC), the prediction was improved significantly compared to the non-polar case (SSAFT). As will be shown for several mixtures, quantitative results are obtained without adjusting binary interaction parameter (kij=0) .Such an enhancement makes possible to free the SAFT from the dependency on availability of experimental data.

As depicted in **Figure 4-3**, the VLE prediction of SSAFT-JC for dimethyl ether and hexane at 308.13K is in excellent agreement with experimental data. This quantitative prediction is not possible without incorporating dipole-dipole interactions to DME. It is clear from the figure that the non-polar SAFT is unable to give quantitative prediction unless binary interaction parameter is introduced (k_{ij}=0.0457). It is also interesting to note that the SSAFT-JC is more accurate than the adjusted non-polar SSAFT. This is evident from noticing the average absolute deviations in pressure given in **Table 4.2** for the two cases. As seen in the table, the average absolute deviations in pressure for SSAFT-JC (k_{ij}=0) and SSAFT (k_{ij}=0.0458) are 1.84 and 2.2 %; respectively. Therefore, it is clear that the inclusion of the dipole-dipole interactions makes a significant improvement to the SSAFT for this mixture.

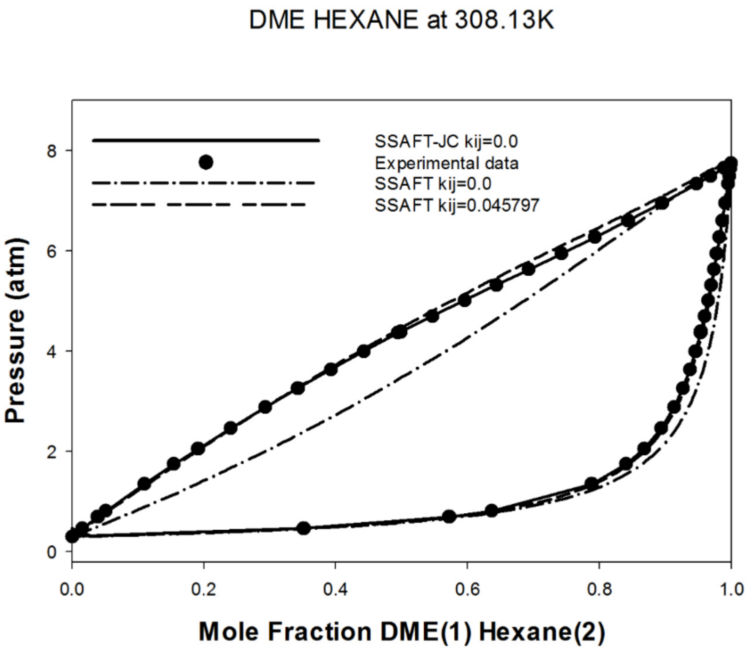

Figure 4-3 Prediction of DME-Hexane VLE at 308.13K as a comparison between three different approaches using (1) SSAFT model with Jog and Chapman dipolar term (SSAFT-JC) without adjusting binary interaction parameter, k_{ij}=0.0 (2) Using SSAFT model without dipolar contribution and k_{ij}=0.0 (3) using the SSAFT model without dipolar contribution but adjusted binary interaction parameter k_{ij}=0.045797.Experimental data is obtained from (Sundberg et al, 2011)

VLE prediction for DME-Hexane at 335.66K is shown in **Figure 4-4** which exhibits a similar trend like the previous one. The prediction from the SSAFT-JC is excellent and significantly improved than SSAFT without dipolar interactions. The average absolute deviations for SSAFT-JC at k_{ij}=0 are 0.59 and 0.06 % in pressure and vapor mole fraction respectively while for SSAFT at kij=0 these are 14.59 % and 0.13 %. The value of binary interaction parameter is adjusted for SSAFT (k_{ij}=0.0466) and then deviations are 1.42 and 0.06 % in pressure and vapor mole fraction respectively. There are however very slight unnoticeable deviations with SSAFT-JC at k_{ij}=0.0. The reason can be attributed to the fact that polar forces begin to weaken at higher temperatures because of increase in kinetic energy of the molecules.

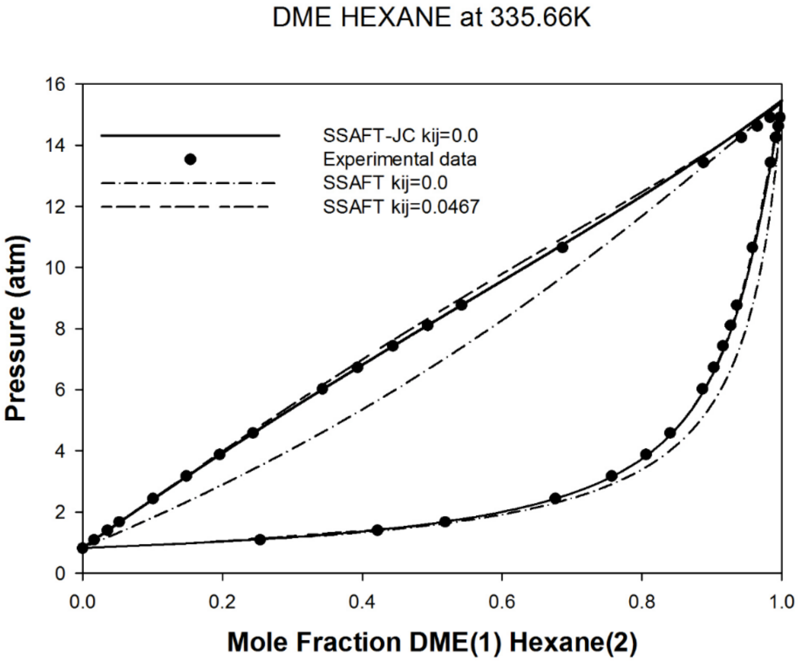

Figure 4-4 Prediction of DME-Hexane VLE at 335.66K as a comparison between three different approaches using (1) SSAFT model with Jog and Chapman dipolar term (SSAFT-JC) without adjusting binary interaction parameter, k_{ij}=0.0 (2) Using SSAFT model without dipolar contribution and k_{ij}=0.0 (3) using the SSAFT model without dipolar contribution but adjusted binary interaction parameter k_{ij}=0.0467. Experimental data is obtained from (Sundberg et al, 2011)

Figure 4-5 shows a VLE prediction for the dimethyl ether and propane at 323.15 K. The prediction can be deemed as very accurate. The SSAFT-JC model at k_{ij}=0 is successfully able to provide very good predictions. Improvements from SSAFT-JC are significant and deviations are small as compared to its non-polar counterpart, AADP is 1.92% and AADY is 0.01% using SSAFT-JC k_{ij}=0.0 whereas for SSAFT k_{ij}=0.0 it is 7.30% and 0.05% respectively. However, there are slight deviation from the experimental data using SSAFT-JC. The value of binary interaction parameter is adjusted in this case. It is observed that k_{ij} for SSAFT-JC is a very small number as compared to the kij for original non polar SSAFT.

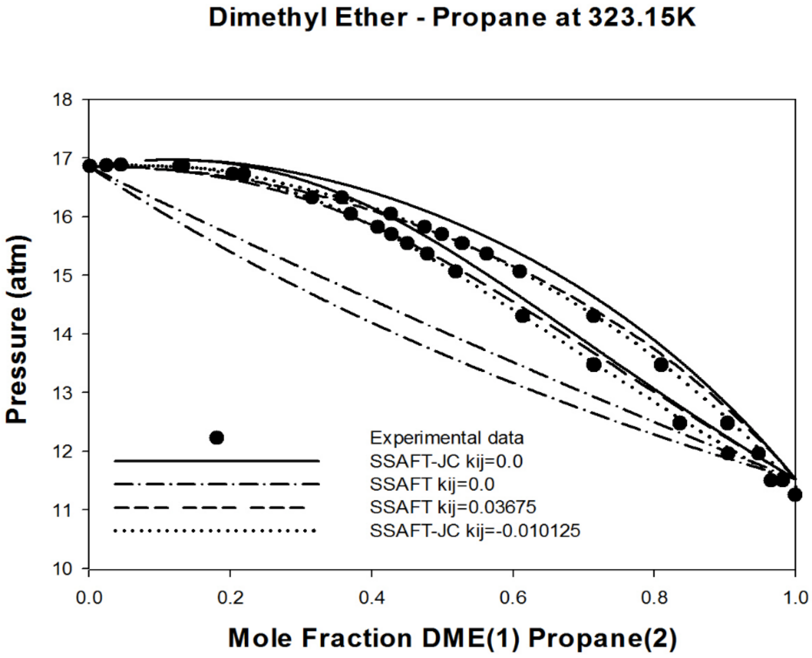

Figure 4-5 Prediction of DME-Propane VLE at 323.15K as a comparison between four different approaches using (1) SSAFT model with Jog and Chapman dipolar term (SSAFT-JC) without adjusting binary interaction parameter, k_{ij}=0.0 (2) Using SSAFT model without dipolar contribution and k_{ij}=0.0 (3) using the SSAFT model without dipolar contribution but adjusted binary interaction parameter kij=0.03675 (4) using the SSAFT model with dipolar contribution but adjusted binary interaction parameter k_{ij}= -0.010125. Experimental data is obtained from (Horstmann et al , 2004)

In **Figure 4-6** which is very accurate prediction for DME-Propane at 273.15K. The average absolute deviation using SSAFT-JC at k_{ij}=0.0 are 1.05 and 0.012 % for pressure and vapor mole fraction, whereas in case of SSAFT at k_{ij}=0.0 these deviations are 0.41 and 0.14 respectively. There are some very slight deviation from the data which can be improved by adjusting the binary interaction parameter for SSAFT-JC. Evidently the value of k_{ij} for SSAFT-JC is a very small number as compared to SSAFT.

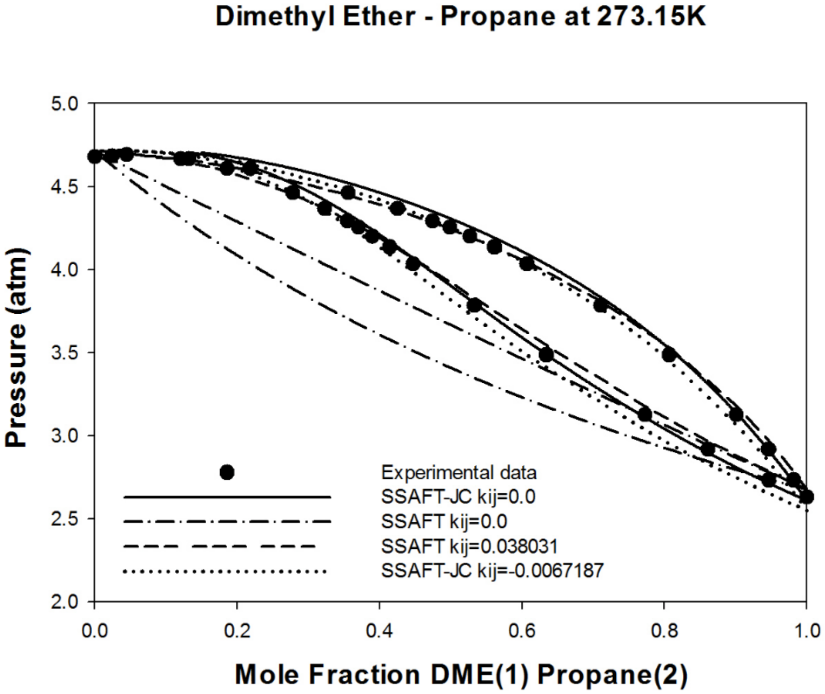

Figure 4-6 Prediction of DME-Propane VLE at 273.15K as a comparison between four different approaches using (1) SSAFT model with Jog and Chapman dipolar term (SSAFT-JC) without adjusting binary interaction parameter, k_{ij}=0.0 (2) Using SSAFT model without dipolar contribution and k_{ij}=0.0 (3) using the SSAFT model without dipolar contribution but adjusted binary interaction parameter k_{ij}=0.038031 (4) using the SSAFT model with dipolar contribution but adjusted binary interaction parameter k_{ij}= -0.0067187. Experimental data is

Figure 4-7, 4-8 shows the graphical representation of VLE of the DME-butane mixture at two different temperatures. The deviation are small and improvements are significant when polar forces are accounted in the SSAFT model. The similar trend could be observed, as in the previous cases. The predictions are very accurate, in fact the adjusted kij for SSAFT-JC is a very small number in comparison to SSAFT. The most accurate case is exhibited by employing electrostatic interactions using Jog & Chapman dipolar term. The value of binary interaction parameter is adjusted to compensate for small deviations. The deviations for SSAFT-JC kij=0.00215 are 0.51 and 0.25 % in AADP and AADY respectively. These small deviation describes the high accuracy of the model after including electrostatic interactions.

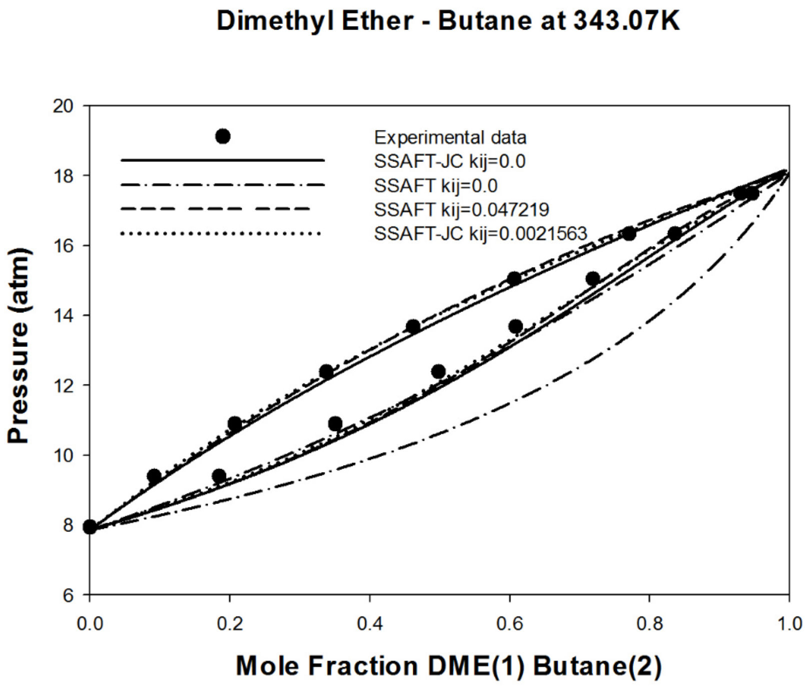

Figure 4-7 Prediction of DME-Butane VLE at 343.07 K as a comparison between four different approaches using (1) SSAFT model with Jog and Chapman dipolar term (SSAFT-JC) without adjusting binary interaction parameter, kij=0.0 (2) Using SSAFT model without dipolar contribution and kij=0.0 (3) using the SSAFT model without dipolar contribution but adjusted binary interaction parameter kij=0.047219 (4) using the SSAFT model with dipolar contribution but adjusted binary interaction parameter kij= 0.0021563. Experimental data is obtained from [116]**.**

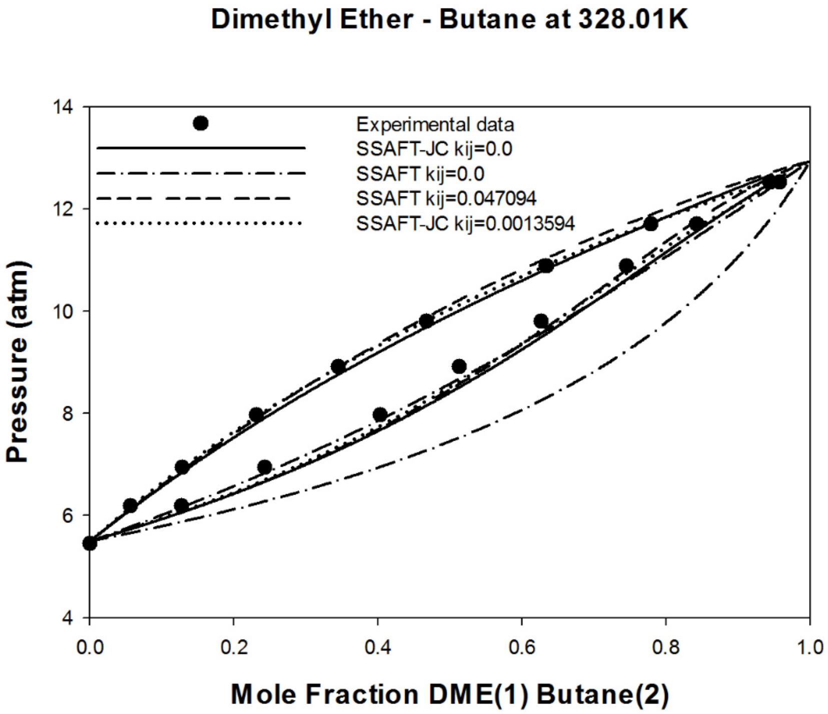

Figure 4-8 Prediction of DME-Butane VLE at 328.01K as a comparison between four different approaches using (1) SSAFT model with Jog and Chapman dipolar term (SSAFT-JC) without adjusting binary interaction parameter, k_{ij}=0.0 (2) Using SSAFT model without dipolar contribution and k_{ij}=0.0 (3) using the SSAFT model without dipolar contribution but adjusted binary interaction parameter k_{ij}=0.047094 (4) using the SSAFT model with dipolar contribution but adjusted binary interaction parameter k_{ij}= 0.0013594. Experimental data is obtained from [116]**.**

Figure 4-9 shows a combined VLE prediction for DME-butane at various temperatures. A general trend could be observed that, polar forces are, predominant as dipolar-dipolar interaction in the DME, however they are not present in butane. The SSAFT-JC model begins to deviate slightly at increasing temperatures, this is because the polar interaction begins to weaken at higher temperatures. However, these forces are still present and their effect is predominant enough and must be accounted in the model.

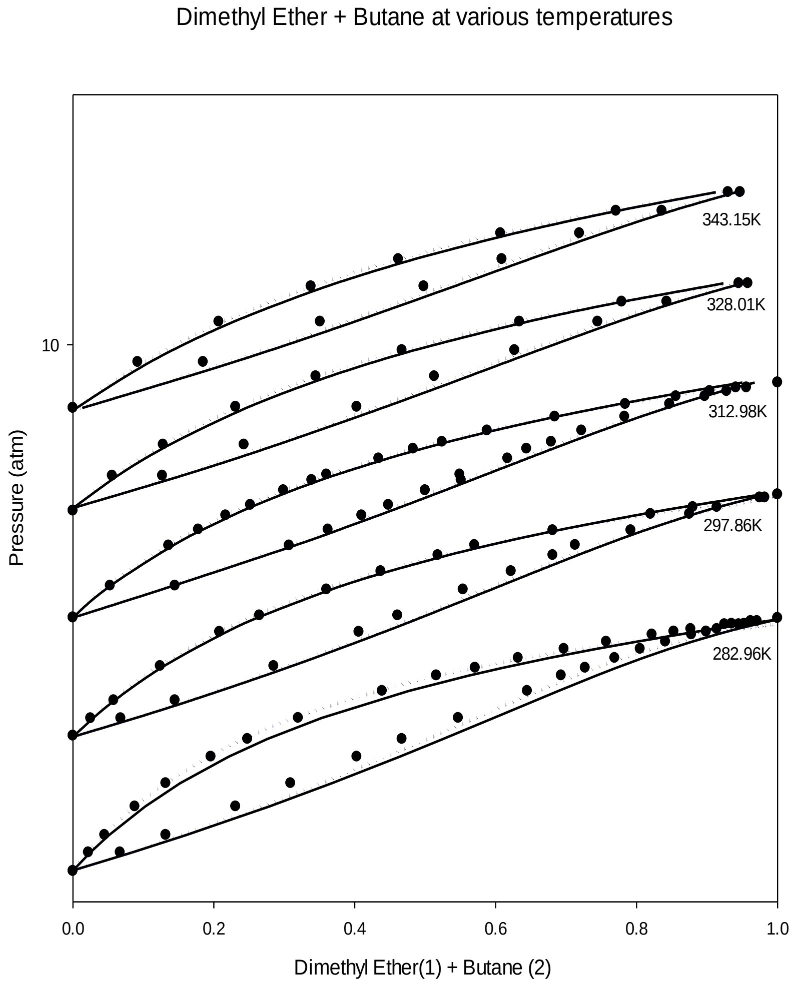

Figure 4-9 Prediction of DME-Butane VLE at various temperatures using Simplified SAFT model and Jog and Chapman dipolar without adjusting binary interaction parameter k_{ij}=0.0. in comparison to adjusting k_{ij} for same model. Experimental data is obtained from [116]**. Solid line represents prediction from SSAFT-JC and dotted line represents prediction with SSAFT-JC fitted k_{ij}.**

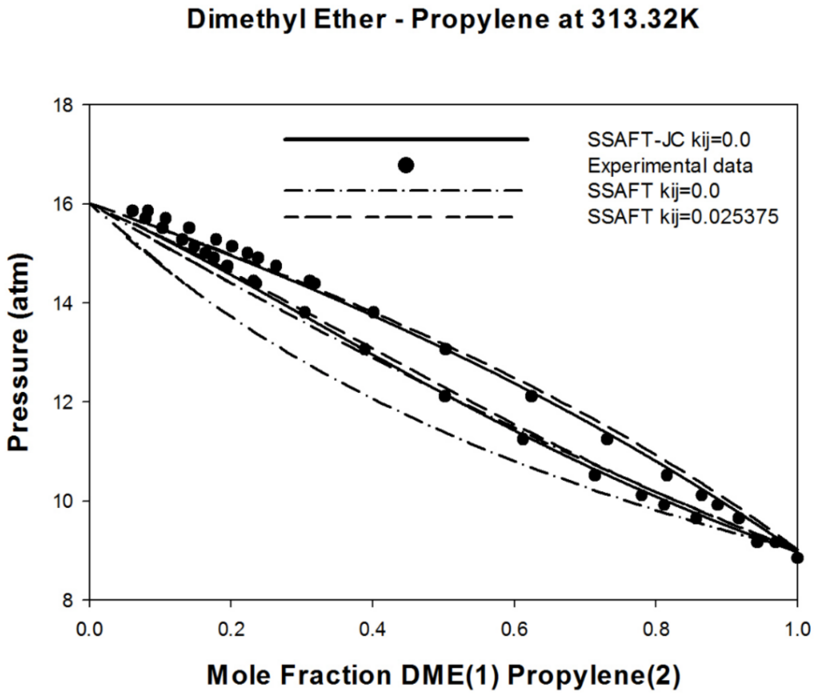

Figure 4-10 Prediction of DME-Propylene VLE at 313.32K as a comparison between three different approaches using (1) SSAFT model with Jog and Chapman dipolar term (SSAFT-JC) without adjusting binary interaction parameter, k_{ij}=0.0 at mx_p=0.7 for DME (2) Using SSAFT model without dipolar contribution and k_{ij}=0.0 (3) using the SSAFT model without dipolar contribution but adjusted binary interaction parameter k_{ij}=0.0253754. Experimental data is obtained from (Horstmann et al , 2004)

Figures 4-10 and 4-11 depicts the VLE of DME alkene mixture viz. (DME-propylene and DME-Butene). The predictions are accurate and the inclusion of dipolar forces have shown, improved results. The deviations from polar SSAFT are significantly more less than its non-polar counterpart. In **Figure 4-10 & 4-11** VLE of DME-Propylene and DME-Butene are predicted using three different approaches. SSAFT-JC was able to give very accurate predictions at mx_p=0.7. The reason is that alkenes are unsaturated hydrocarbon containing double bonds. SAFT is conceived using single bond molecules.

The double bonded compounds tend to show varying behavior which SAFT does not account, because it views molecules as single bonded hard spheres.

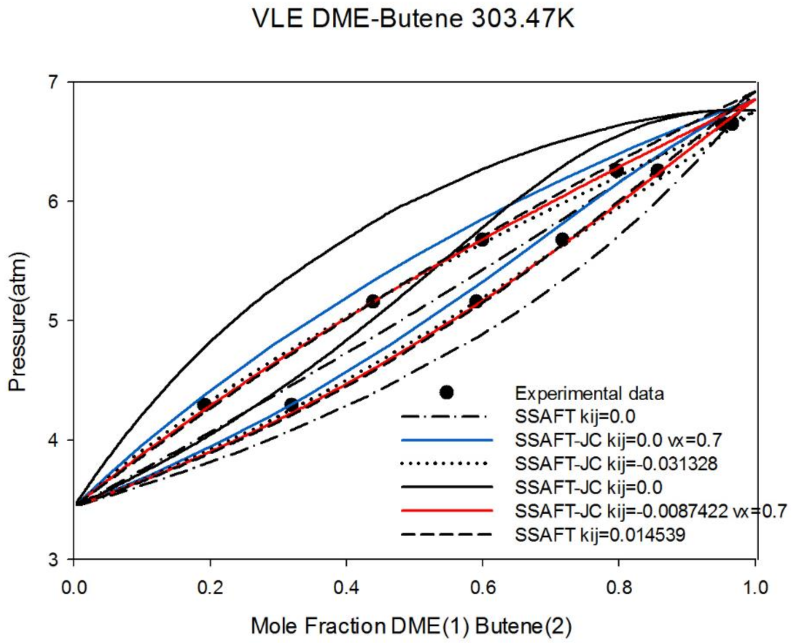

Figure 4-11 Prediction of DME-Propylene VLE at 303.47K as a comparison between six different approaches using (1) SSAFT model with Jog and Chapman dipolar term (SSAFT-JC) without adjusting binary interaction parameter, kij=0.0 at mx_p=0.7 for DME (2) Using SSAFT model without dipolar contribution and kij=0.0 (3) using the SSAFT model without dipolar contribution but adjusted binary interaction parameter kij=0.014539 (4) using the SSAFT with dipolar contribution but adjusted binary interaction parameter kij=-0.031328 (5) using the SSAFT with dipolar contribution kij=0.0 (6) using the SSAFT with dipolar contribution but adjusted binary interaction parameter kij=-0.0087422 at mx_p=0.7 for DME. Experimental data is obtained from [116]**.**

Average absolute deviation in pressure and vapor phase mole fraction for the prediction for DME-hydrocarbons is listed in Table 4-2. Binary interaction parameters are also adjusted in cases where there are small but noticeable deviation.

Table 4-2 Average Absolute Deviation (AAD) in pressure and vapor mole fraction from experimental data using various approaches

Mixture	T (K)	Model	AADP (%)	AADY (%)
DME-Hexane	335.65	SSAFT-JC kij=0.0	0.59	0.06
DME-Hexane	335.65	SSAFT kij=0	14.59	0.13
DME-Hexane	335.65	SSAFT kij=0.0466	1.42	0.06
DME-Hexane	308.13	SSAFT-JC kij=0.0	1.84	0.01
DME-Hexane	308.13	SSAFT kij=0.0457	2.20	0.01
DME-Hexane	308.13	SSAFT kij=0.0	18.20	0.05
DME-Butane	343.07	SSAFT-JC kij=0.0	1.43	0.23
DME-Butane	343.07	SSAFT kij=0.0	9.48	0.14
DME-Butane	343.07	SSAFT-JC kij=0.00215	0.51	0.25
DME-Butane	343.07	SSAFT kij=0.47219	0.94	0.24
DME-Butane	328.01	SSAFT-JC kij=0.0	1.12	0.25
DME-Butane	328.01	SSAFT kij=0.0	9.37	0.16
DME-Butane	328.01	SSAFT-JC kij=0.00135	0.31	0.27
DME-Butane	328.01	SSAFT kij=0.47219	0.99	0.25
DME-Butane	297.86	SSAFT kij=0.0	9.36	0.15
DME-Butane	297.86	SSAFT JC kij=0.0	0.75	0.20
DME-Butane	297.86	SSAFT JC kij=0.000031	0.39	0.22
DME-Butane	282.96	SSAFT kij=0.0	9.99	0.14
DME-Butane	282.96	SSAFT JC kij=0.00525	0.89	0.20
DME-Butane	282.96	SSAFT JC kij=0.0	1.78	0.16

DME-Propane	323.15	SSAFT JC kij=0.0	1.92	0.01
DME-Propane	323.15	SSAFT kij=0.0	7.30	0.05
DME-Propane	323.15	SSAFT kij=0.0367	0.82	0.01
DME-Propane	323.15	SSAFT-JC kij=-0.0102	0.28	0.00
DME-Propane	273.15	SSAFT-JC kij=0.0	1.06	0.01
DME-Propane	273.15	SSAFT-JC kij=-0.00671	0.89	0.02
DME-Propane	273.15	SSAFT kij=0.0	8.41	0.14
DME-Propane	273.15	SSAFT-kij=0.0380	0.69	0.02
DME-Propene	313.32	SSAFT-JC kij=0.0	1.14	0.01
DME-Propene	313.32	SSAFT kij=0.0	4.43	0.06
DME-Propene	313.32	SSAFT kij=0.0253	1.44	0.02
DME-Butene	303.47	SSAFT-JC kij=0.0	8.47	0.06
DME-Butene	303.47	SSAFT kij=0.0	3.80	0.02
DME-Butene	303.47	SSAFT kij=0.014539	1.02	0.02
DME-Butene	303.47	SSAFT JC vx=0.7 kij=-0.00874	0.48	0.01
DME-Butene	303.47	SSAFT-JC kij=0.0 m.xp=0.7	2.47	0.02
DME-Butene	303.47	SSAFT-JC kij=-0.031328	0.34s	0.01

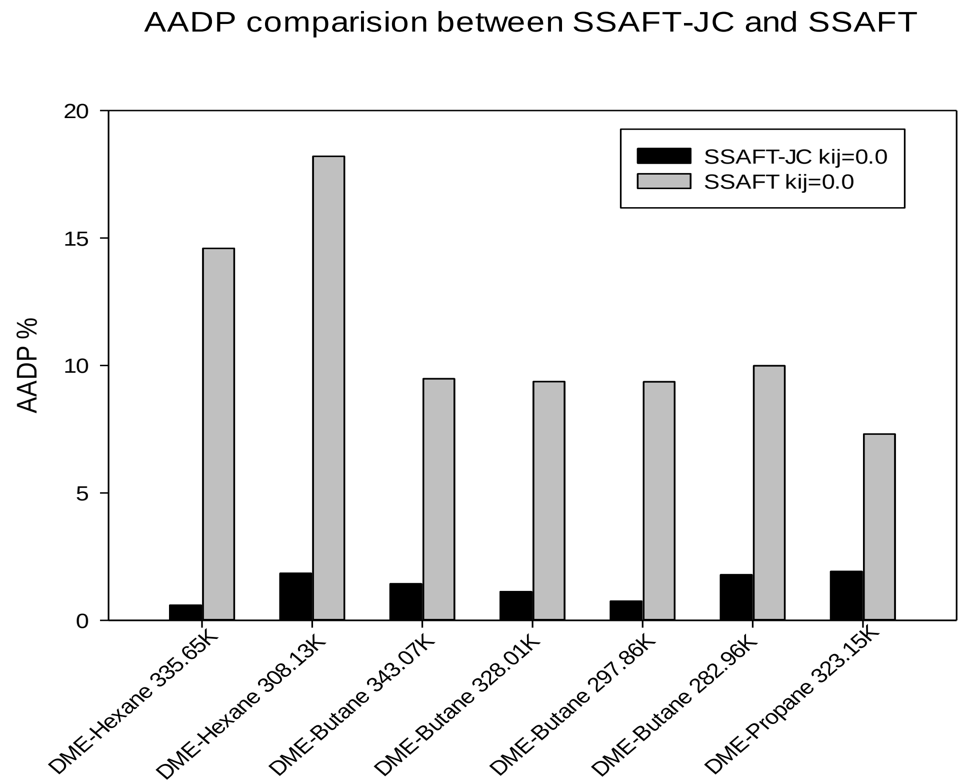

Figure 4-12 Comparison of AADP between SSAFT-JC and SSAFT at kij=0.0

4.3 Comparison with different dipolar terms

The following section presents a comparison between, Jog & Chapman (JC) and Gross & Vrabec Term (GV). The value of mx_p in the JC term has been set to 1(refer to **section 3.4**), in order to draw appropriate comparison. The value of binary interaction parameter is set to 0.0 in both the cases.

As illustrated in **Figure 4-13** VLE of DME-Butane at 282.96K using SSAFT model with two different dipolar terms, SSAFT-JC and SSAFT-GV, the former gives more accurate predictions as compared to latter. The absolute average deviation in pressure and vapor mole fraction are 0.38 and 0.19 respectively whereas similar deviations for SSAFT-

GV are 8.55 and 0.14 respectively. The increased deviations are an evidence that Gross term fails to describe the accurate phase behavior for DME-hydrocarbons. Similar trend can be observed clearly in **Figures 4-14 – 4-20. Table 4-3** provides the average absolute deviations for the comparison between the two dipolar terms in the prediction of DME-hydrocarbons. **Figure 4-21** provides a comparison between the deviations from the two dipolar terms JC (Jog & Chapman) and GV (Gross and Vrabec) applied to SSAFT. Apparently SSAFT-JC appears to be more accurate than SSAFT-GV.

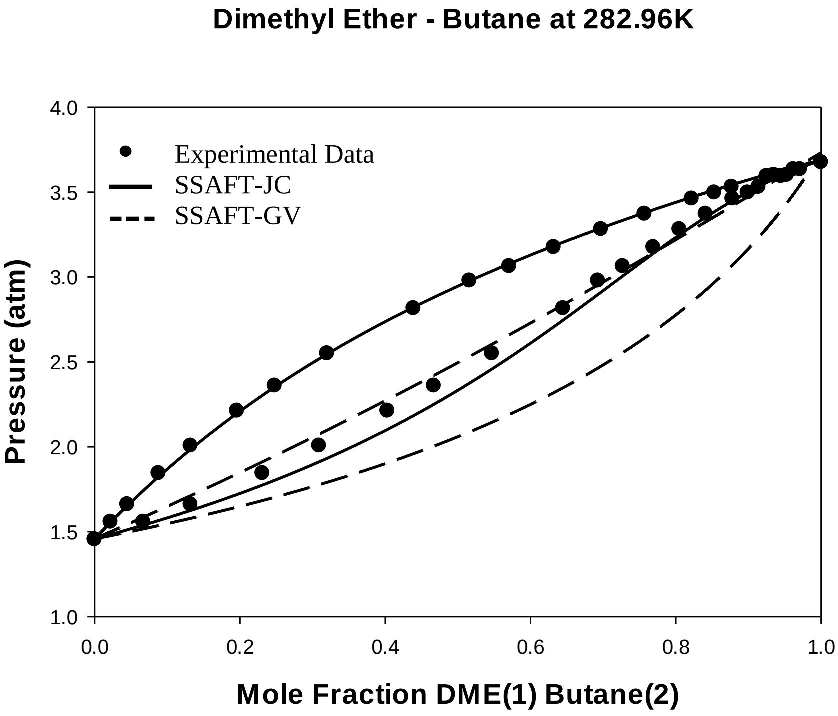

Figure 4-13 Prediction of DME-Butane VLE at 297.86K using Simplified SAFT model and Jog and Chapman(JC) and Gross and Vrabec (GV) dipolar without adjusting binary interaction parameter kij=0.0. Experimental data is obtained from [116]**.**

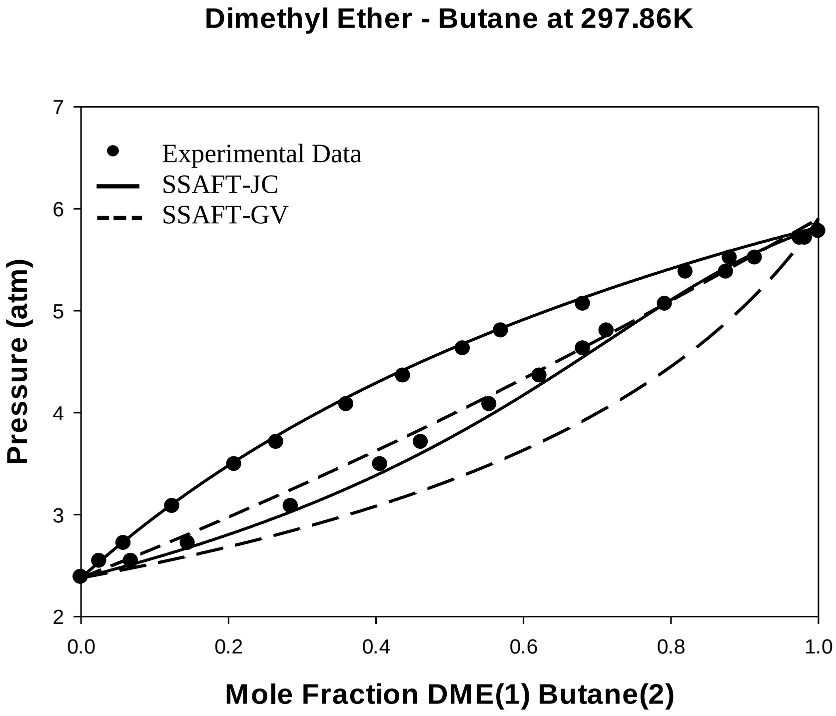

Figure 4-14 Prediction of DME-Butane VLE at 297.86K using Simplified SAFT model and Jog and Chapman(JC) and Gross and Vrabec(GV) dipolar without adjusting binary interaction parameter kij=0.0. Experimental data is obtained from [116]**.**

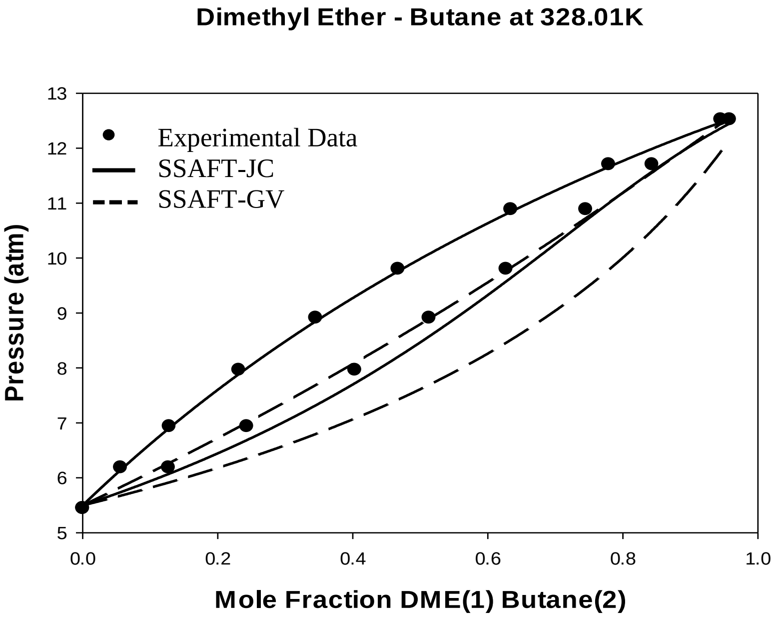

Figure 4-15 Prediction of DME-Butane VLE at 328.01K using Simplified SAFT model and Jog and Chapman(JC) and Gross and Vrabec(GV) dipolar without adjusting binary interaction parameter kij=0.0. Experimental data is obtained from [116]**.**

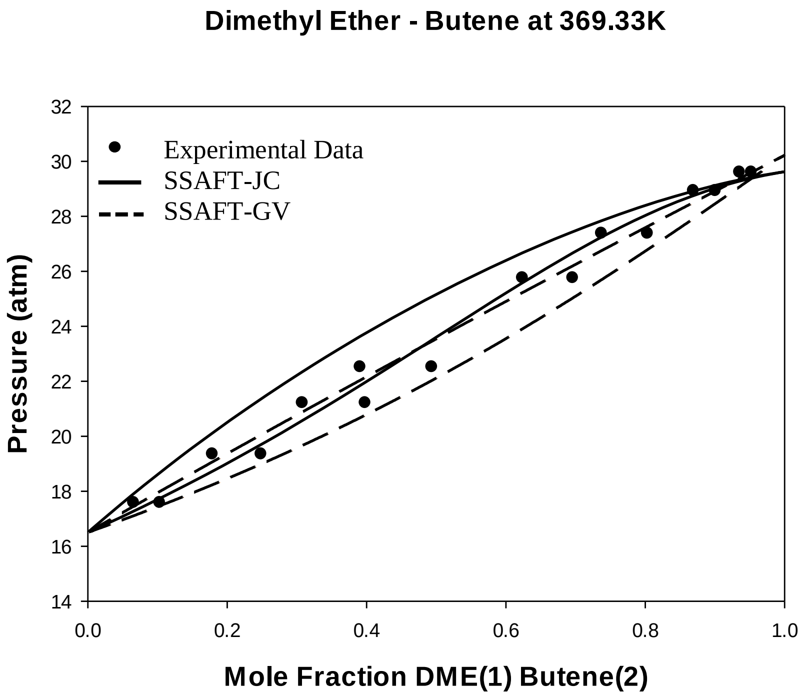

Figure 4-16 Prediction of DME-Butene VLE at 369.33K using Simplified SAFT model and Jog and Chapman (JC) and Gross and Vrabec(GV) dipolar without adjusting binary interaction parameter kij=0.0. Experimental data is obtained from [116]**.**

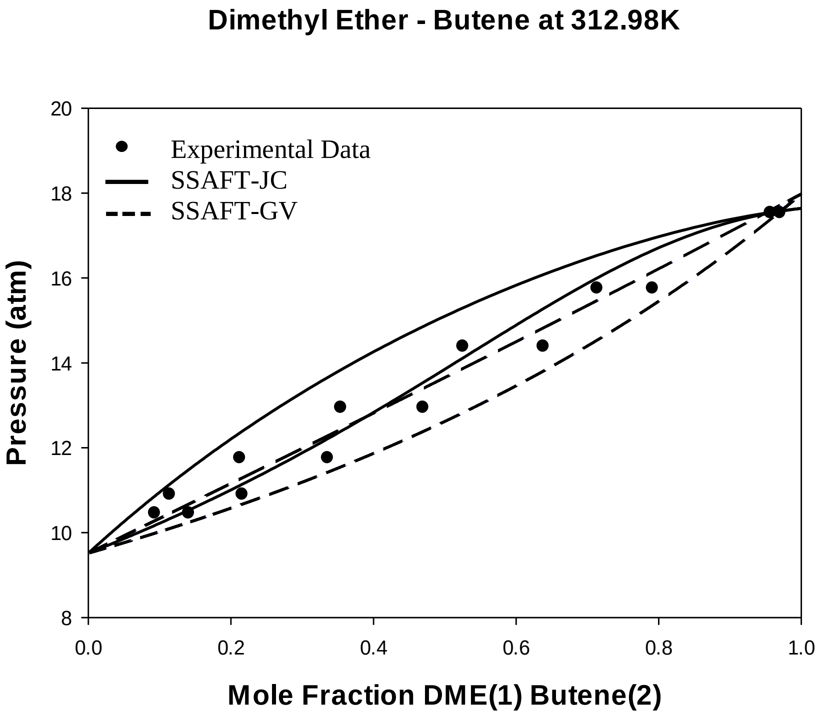

Figure 4-17 Prediction of DME-Butene VLE at 312.98 K using Simplified SAFT model and Jog and Chapman (JC) and Gross and Vrabec(GV) dipolar without adjusting binary interaction parameter kij=0.0. Experimental data is obtained from [116]**.**

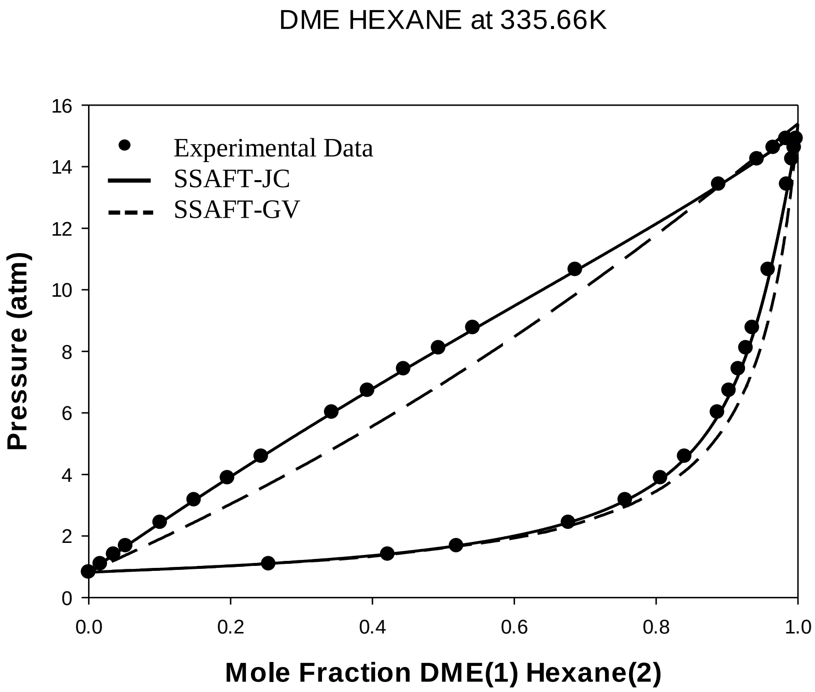

Figure 4-18 Prediction of DME-Hexane VLE at 335.66 K using Simplified SAFT model and Jog and Chapman(JC) and Gross and Vrabec(GV) dipolar without adjusting binary interaction parameter kij=0.0. Experimental data is obtained from (Sundberg et al, 2011)

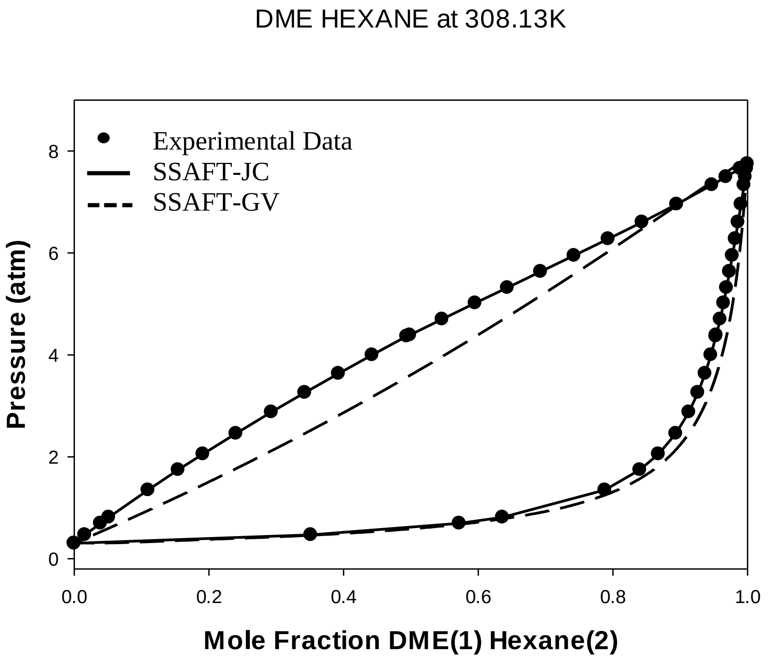

Figure 4-19 Prediction of DME-Hexane VLE at 308.13 K using Simplified SAFT model and Jog and Chapman(JC) and Gross and Vrabec(GV) dipolar without adjusting binary interaction parameter kij=0.0. Experimental data is obtained from (Sundberg et al, 2011).

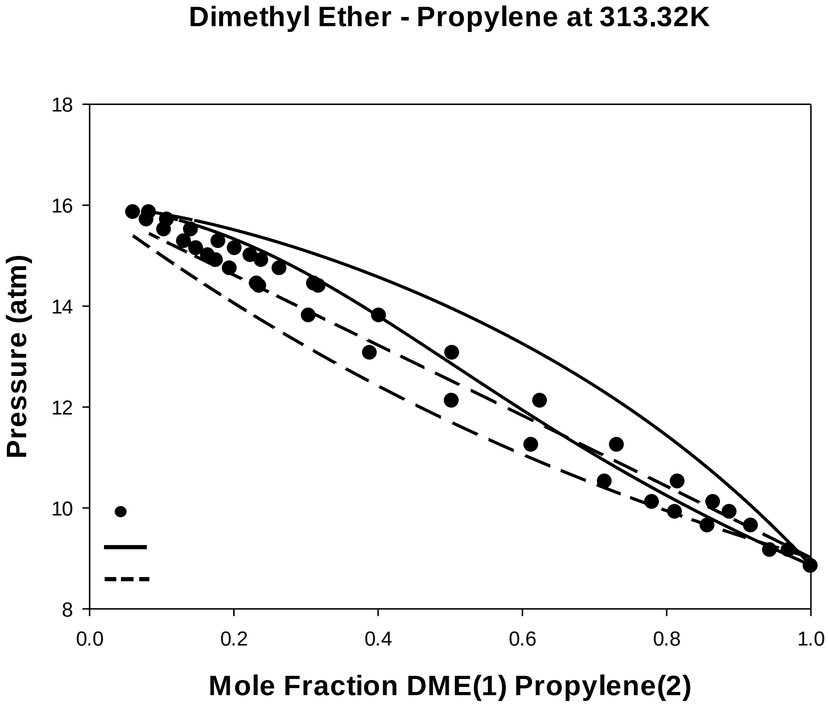

Figure 4-20 Prediction of DME-Propylene VLE at 313.32 K using Simplified SAFT model and Jog and Chapman (JC) and Gross and Vrabec(GV) dipolar without adjusting binary interaction parameter kij=0.0. Experimental data is obtained from (Horstmann et al , 2004)

Table 4-3 provides the average absolute deviation for DME-hydrocarbons as a comparison between two different approaches SSAFT-JC and SSAFT-GV.

Table 4-3 AADs for DME-Hydrocarbon as a comparison between SSAFT-JC and SSAFT-GV

Mixture	Model	Temp	AADP (%)	AADY (%)
DME-Butane	SSAFT-JC	282.96	0.38	0.19
DME-Butane	SSAFT-GV	282.96	8.55	0.14
DME-Butane	SSAFT-JC	297.86	0.94	0.23
DME-Butane	SSAFT-GV	297.86	8.06	0.14
DME-Butane	SSAFT-JC	343.07	1.38	0.27
DME-Butane	SSAFT-GV	343.07	9.14	0.17
DME-Butane	SSAFT-JC	328.01	0.64	0.26
DME-Butane	SSAFT-GV	328.01	8.03	0.15
DME-Butene	SSAFT-JC	369.33	2.73	0.04
DME-Butene	SSAFT-GV	369.33	2.93	0.02
DME-Propene	SSAFT-JC	313.32	1.72	0.20
DME-Propene	SSAFT-GV	313.32	4.40	0.06
DME-Hexane	SSAFT-JC	335.65	0.27	0.06
DME-Hexane	SSAFT-JC	335.65	12.60	0.11
DME-Hexane	SSAFT-JC	308.13	2.08432	0.006
DME-Hexane	SSAFT-JC	308.13	17.13	0.05

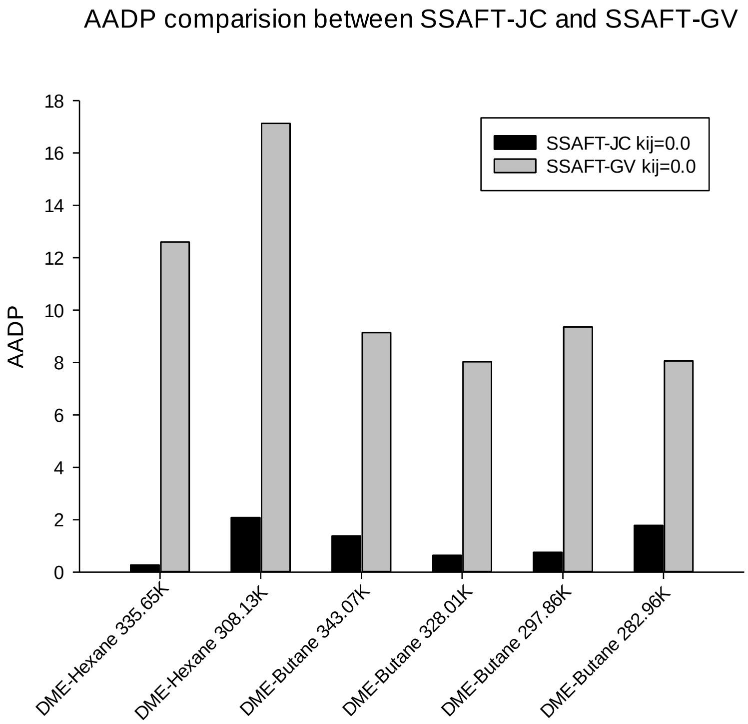

Figure 4-21 AAD comparison between SSAFT-JC and SSAFT-GV for various DME-hydrocarbon mixtures.

4.4 Conclusion

The present chapter covered the prediction of vapor liquid equilibrium of DME-Hydrocarbons. dipole-dipole interaction were employed to predict the phase behavior of mixtures of polar DME and non-polar hydrocarbons. It is observed that by inclusion of electrostatic interaction the improvements in the prediction are significant, as compared in **Figure 4-12**. Moreover, in many cases the need for adjusting the binary interaction parameter was eliminated and even at kij=0.0 for SSAFT-JC the model agrees fairly accurate with the experimental data. For some systems in which there were slight deviation binary interaction parameter was adjusted which evidently appeared to be a very small number in comparison to non-polar version of SSAFT. Two different dipolar terms were employed to study the phase equilibrium behavior of these system. It was found that the

Jog & Chapman dipolar term performed better that the Gross & Vrabec dipolar term, as illustrated in **Figure 4-21**. It is thus concluded without doubt that inclusion of long ranged electrostatic interactions resulted in significant improvements and accurate phase equilibrium predictions. The model is closer to real behavior of the mixtures and need for empirical adjustments are eliminated.

CHAPTER 5

VLE PREDICTION OF DME – ALCOHOLS

5.1 Introduction

In the previous chapter, the predictions of vapor-liquid equilibrium involving mixtures of DME (polar) and hydrocarbons (non-polar) were studied. It was found that Jog & Chapman dipolar term works much better than Gross and & Vrabec dipolar term. Thus, in this chapter, an extensive study is presented for the VLE of mixtures of -DME with associating compounds such as DME-Alcohols and DME-Water using Jog & Chapman dipolar term. The study of phase behaviors of these mixtures is not trivial. The problem of VLE prediction gets difficult when association interactions are involved, Hydrogen bonding associations are covered in detail in **Section 2.6** with illustrations.

Alcohols are a class of oxygenated hydrocarbons which contains parent alkane chain and hydrogen bonded on the two sides of oxygen (R-O-H). Oxygen in alcohol contains two lone pair of electrons and is a highly electronegative element capable of forming hydrogen bonds. DME, on the other hand, is a polar but non-associating compound in the pure form. However if the DME mixes with alcohols, induced association interactions arise between DME and alcohols. Therefore, the system of DME-alcohol would have association interactions between alcohol particles as well as induced association interactions between DME and alcohols. This makes it difficult to predict phase behavior using any thermodynamic model.

The SSAFT is unable to predict accurately the VLE of for DME-Alcohols without careful consideration of association interactions. In the present chapter, DME-Alcohol mixtures are thoroughly studied by employing these association interactions using several configurations along with dipole-dipole interaction for DME. The present chapter provides an in-depth study of DME-alcohols using different cross association schemes including electrostatic interactions in SSAFT.

The present chapter is divided into the following sections. **Section 5.2** presents the details of cross induced associations. The VLE predication for DME-Alcohols is presented from **Sections 5.3 - 5.5** for 2 association sites for alcohol and 2 association sites for DME. **Section 5.6** presents VLE prediction for methanol-DME using 3 and 2 association sites; respectively. VLE prediction of DME-Water is also presented in **section 5.7**. Finally, **section 5.9** provides the prediction of excess molar enthalpy for methanol-DME.

5.2 Induced cross associations

DME is a non-self-associating compound, but has a strong tendency to form cross association interactions with alcohols. Alcohols have both long-range electrostatic and association interactions. . In a mixture of DME and alcohols, cross-association begins to play a crucial role (refer to **section 2.6**). It becomes ambiguous to decide the value of association parameters for the non-associating component. The reason is that polar-non-associating component such as DME does not have association parameters in the pure phase. But, these components begin to associate with associating components in the mixture phase when there is a possibility to form hydrogen bond. Such types of interactions are called induced association interactions. The SAFT in its current structure is unable to treat induced interactions. In these cases, adjusting the association parameters in the mixture phase could be proposed to overcome this problem, another way to overcome the problem of induced association is to use the approach developed by Sadowski et al (2007). This approach utilized in the present study along with the other proposed approaches.

5.2.1 Sadowski approach to account for induced association interactions in polar systems

Sadowski approach is based on the study of mixtures in which there is one polar component which does not self-associate, but has a tendency to form hydrogen bonds in the mixture phase. The Sadowski's approach is first based on using Wolbach and Sandler mixing rules for the cross-association. Then, the following two assumptions are proposed only for the pure parameters:

a) the association volume parameter ($k^{A_iB_j}$) of the non-associating component is set equal to that of associating compound
b) the association energy parameter ($\varepsilon^{A_iB_j}$) for non-associating compound is set to zero.

In their work, based on these assumptions, various mixtures were studied using PC-SAFT model to predict phase equilibrium. In the next section the other induced association schemes are explained.

5.2.2 Adjusting the association parameters for non-associating component

Apart from the Sadowski approach, there are other approaches that are proposed in this work and extensively tested in modeling mixtures of non-associating components with associating components. One is the adjustment of association parameters over experimental data. Although this approach is empirical, it yields appropriate results. Another approach is similar to Sadowski's second assumption but the association energy parameter is made half that of the value of the associating component. In the next sections, these approaches will be implemented and compared by studying VLE for DME-alcohols/water mixture in which induced association interactions are involved.

5.3 Isopropanol – DME (2 Association sites for Alcohol -2 Association sites for DME)

The vapor liquid equilibrium results of DME - Isopropanol are given in **Table 5.1** and also demonstrated in **Figure 5.1,** to show the behavior of SSAFT and SSAFT-JC using various approaches of induced interactions. The Sadowski approach, in these predictions does not seem to give accurate predictions without adjusting binary interaction parameter and hence it can be concluded that it is extremely necessary to include polar interactions in such systems. It was observed that the best approach so far was, including dipolar interaction between the molecules of the two components and adjusting the association parameters for the polar-non-associating component. The SSAFT-JC at kij=0.0 with adjusted association parameters deviates by only 3.13 and 0.417 % respectively for AADP and AADY and in case of adjusted kij=0.0195, these deviation are 4.48 and 0.289 % respectively.

Table 5-1 Prediction of VLE of Isopropanol – DME using various approaches at 373.15K

Case #	**Approach**	**κ^{AB}**	**ε^{AB}/k**	**k_{ij}**	**Dipolar forces**	**AADP**	**AADY**
Case 1	Sadowski approach without dipolar and binary interaction parameter set to 0	0.042354	10^{-7}	0.0	Not Included	32.25	0.296
Case 2	Sadowski approach without dipolar forces and fitted binary interaction parameter	0.042354	10^{-7}	-0.0980	Not Included	5.50	0.356
Case 3	Setting ε^{AB}/k = 1/2 ε^{AB}/k for Alcohol without dipolar forces or adjusting binary interaction parameter	0.042354	1259.2	0.0	Not Included	10.55	0.200
Case 4	Sadowski approach with dipolar and binary interaction parameter set to 0	0.04234354	10^{-7}	0.0	Included	17.14	0.234
Case 5	Adjusted ε^{AB}/k and κ^{AB} ignoring dipolar forces and binary interaction parameter set to 0	0.043254	1322.16	0.0	Not Included	9.20	0.216
Case 6	Adjusted ε^{AB}/k and κ^{AB} with dipolar forces and fitting binary interaction parameter	0.046137	1311.66	0.0195	Included	4.48	0.289
Case 7	Adjusted ε^{AB}/k and κ^{AB} with dipolar forces and binary interaction parameter set to 0	0.044424	1305.70	0.0	Included	3.13	0.417

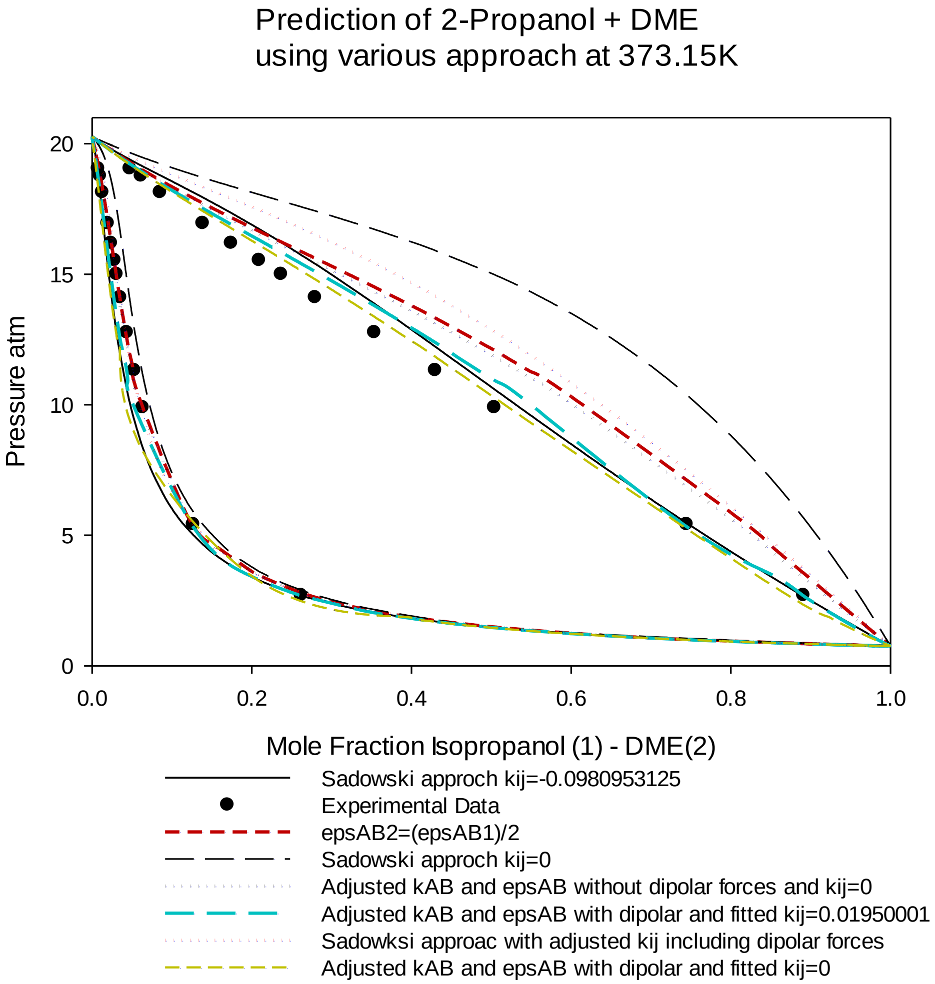

Figure 5-1 Prediction of DME-2-Propanol VLE at 373.15 K using Simplified SAFT model and Jog and Chapman (JC) dipolar by various approaches. Experimental data was obtained from [117]

5.4 Methanol- DME (2 Association sites for Alcohol -2 Association sites for DME)

The VLE prediction of methanol-DME is given in **Table 5-2** and in **Figure 5-2.** Two association sites for methanol and two induced cross-association sites for dimethyl ether are assumed (refer to **Section 4.2.1** for details). A comparison between induced association interactions assumptions show that the best approach among all is the adjusted cross-association parameters approach along with the polar interactions. Average absolute deviations in SSAFT-JC at kij=0.0 are 5.08 and 0.177 in pressure and vapor phase mole fraction; respectively. In case of adjusted kij=0.0463, these deviations reduce to 5.07 and 0.114 %; respectively. For simplicity, the results of all cases are summarized in the **Table 5-2 and Figure 5.2**

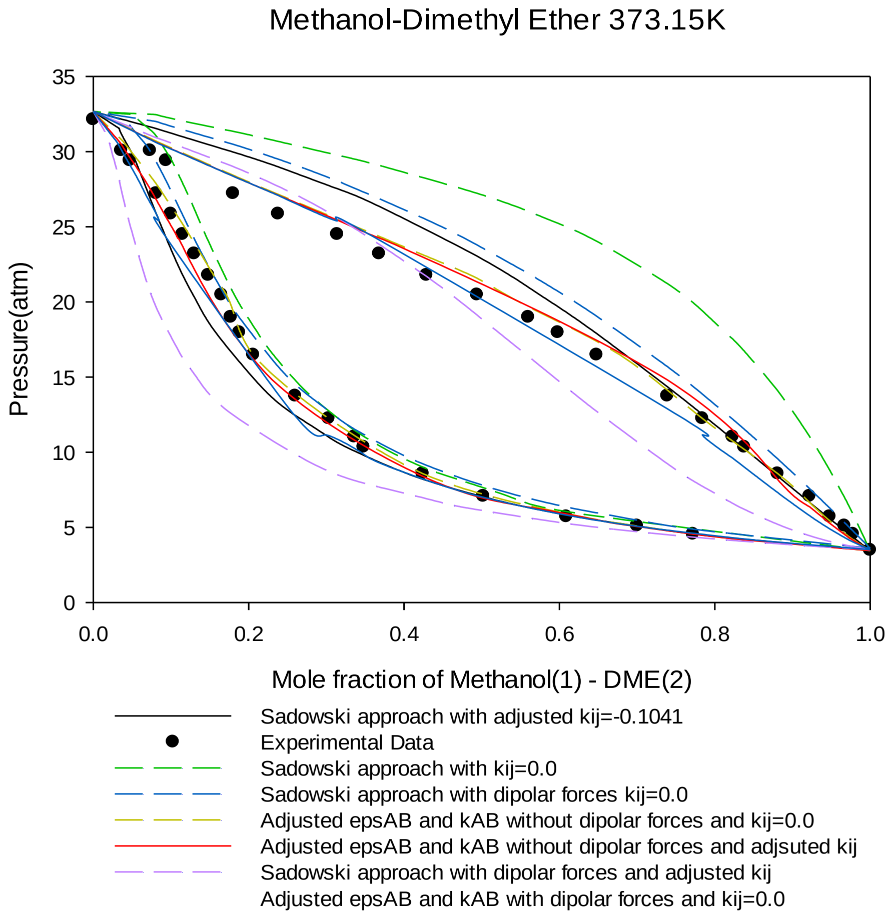

Figure 5-2 Prediction of DME-2-Methanol VLE at 373.15 K using Simplified SAFT model and Jog and Chapman (JC)) dipolar by various approaches. Experimental data was obtained from [118]

Table 5-2 Prediction of VLE of Methanol – DME using various approaches at 373.15K

	Approach	κ^{AB}	ε^{AB}/k	k_{ij}	**Dipolar forces**	**AADP (%)**	**AADY (%)**
Case 1	Sadowski approach without dipolar forces and fitted binary interaction parameter	0.119107	10^{-7}	-0.1041	Not Included	6.38	0.186
Case 2	Sadowski approach without dipolar and binary interaction parameter set to 0	0.119107	10^{-7}	0.0	Not Included	34.80	0.280
Case 3	Sadowski approach with dipolar and binary interaction parameter set to 0	0.136710	10^{-7}	0.0	Included	10.43	0.128
Case 4	Adjusted ε^{AB}/k and κ^{AB} with dipolar forces and binary interaction parameter set to 0	0.119812	1405.68	0.0	Not Included	5.08	0.177
Case 5	Adjusted ε^{AB}/k and κ^{AB} with dipolar forces and adjusted binary interaction parameter	0.096265	1742.93	0.0463	Not Included	5.07	0.114
Case6	Sadowski approach with dipolar forces and fitted binary interaction parameter	0.136710	10^{-7}	-0.1927	Included	18.84	0.365
Case7	Adjusted ε^{AB}/k and κ^{AB} without dipolar forces and binary interaction parameter set to 0	0.1254054	1215.94	0.0	Included	8.23	0.218

5.5 Propanol DME (2 Association sites for Alcohol -2 Association sites for DME)

The prediction of Propanol-DME, tabulated in **Table 5-3** and shown in **Figure 5-3** are in good agreement with the argument presented for the presented for the previous prediction of DME-Alcohol. Unarguable the best approach still remains to be the prediction by including dipolar forces and adjusting the association parameters. SSAFT-JC at $k_{ij}=0.0$ deviated by only 6.67 and 0.604 % in AADP and AADY respectively.

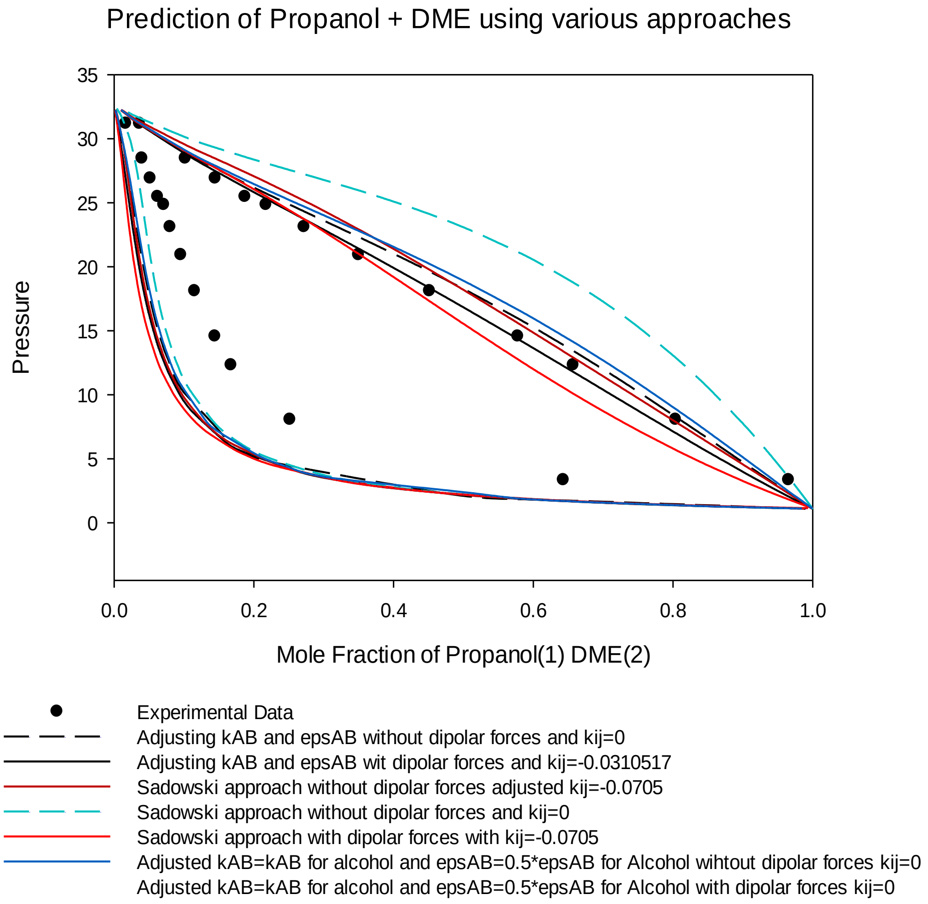

Figure 5-3 Prediction of DME-2-Ethanol VLE at 373.15 K using Simplified SAFT model and Jog and Chapman (JC) dipolar by various approaches. Experimental data was obtained from [119]

Table 5-3 Prediction of VLE of Propanol – DME using various approaches at 373.15K

	Approach	κ^{AB}	ε^{AB}/k	**k**$_{ij}$	**Dipolar forces**	**AADP (%)**	**AADY (%)**
Case 1	Adjusted ε^{AB}/k and κ^{AB} *without dipolar forces and binary interaction parameter set to 0*	0.042083	1390.74	0.0	Not Included	16.64	0.737
Case2	Adjusted ε^{AB}/k and κ^{AB} *without dipolar forces and adjusted binary interaction parameter*	0.527455	380.42	-0.0310	Not Included	5.35	0.621
Case 3	Sadowski approach without dipolar forces but adjusted *binary interaction parameter*	0.041420	10^{-7}	-0.0705	Not Included	8.14	0.614
Case 4	*Sadowski approach* without dipolar *and binary interaction parameter set to 0*	0.041420	10^{-7}	0.0	Not Included	23.36	0.556
Case 5	*Sadowski approach* with dipolar *and fitted binary interaction parameter*	0.049516	10^{-7}	-0.0705	Included	10.34	0.616
Case 6	*Adjusted* $\kappa^{AB} = \kappa^{AB}$ *for Alcohol* $\varepsilon^{AB}/k = 0.5*\varepsilon^{AB}/k$ *for Alcohol without dipolar forces kij=0.0*	0.041420	1255.84	0.0	Not Included	24.33	0.664
Case 7	*Adjusted* $\kappa^{AB} = \kappa^{AB}$ *for Alcohol* $\varepsilon^{AB}/k = 0.5*\varepsilon^{AB}/k$ *for Alcohol with dipolar forces kij=0.0*	0.049516	1128.50	0.0	Included	6.67	0.604

5.6 Methanol-DME (3 Association sites for Methanol - 2 Association sites for DME)

Figure 5-4 represents the vapor liquid equilibrium prediction of Methanol-DME with 3 association sites for methanol and 2 association sites for DME. The 3-2 association scheme also gave fairly good predictions after including electrostatic interactions. However, Sadowski approach failed to give satisfactory predictions but after including electrostatic interactions in Sadowski approach it agrees satisfactorily with experimental data.

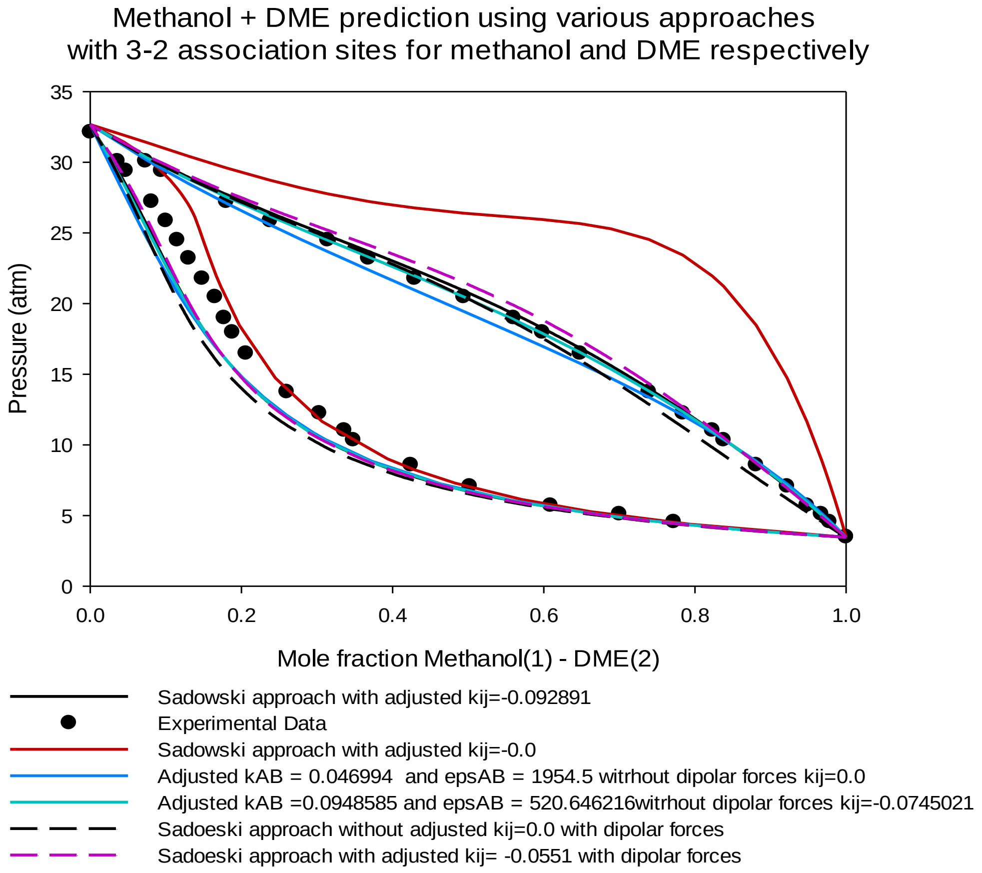

Figure 5-4 Prediction of DME-2-Methanol VLE at 373.15 K using Simplified SAFT model and Jog and Chapman (JC) dipolar by various approaches for 3-2 association sites for methanol and dimethyl ether respectively. Experimental data was obtained from [118]

Figure 5-5 provides a comparison of average absolute deviations in pressure for two different approaches of induced association. Sadowski vs adjusted association parameter approach with dipolar forces. The approach with adjusted association parameters including electrostatic interactions how remarkable level of improvements and hence it is successfully validated that after including dipole-dipole interaction the phase behavior prediction become excellent in agreement with experimental data

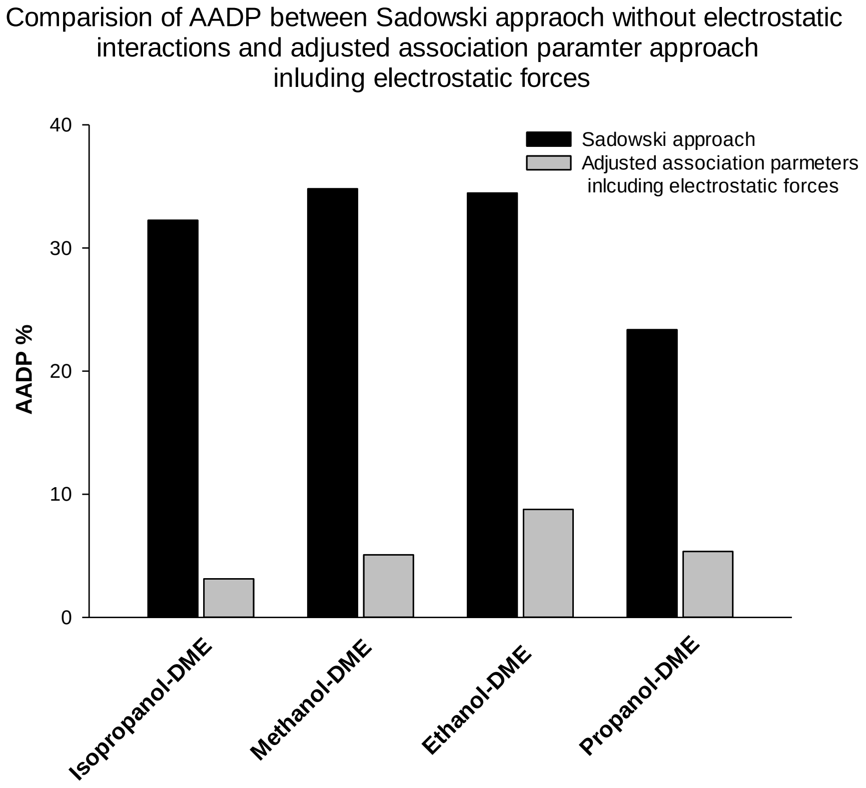

Figure 5-5 Comparison of average absolute deviation in pressure for between two different approach, Sadowski and adjusted association parameter approach, for different alcohol-DME mixtures

5.7 Prediction of Vapor liquid equilibrium of water-dimethyl ether (4 association sites water + 2 association sites for DME)

The prediction of VLE for DME-Water at 373.26K with 4 association sites for water and 2 cross induced association sites for dimethyl ether gave qualitatively good predictions. The DME-Water mixture exhibits liquid-liquid phase separation and the mixture critical line exhibits two separate branches. It is a class III system in the phase equilibrium classification scheme on Van Konyenburg and Scott [120,121].

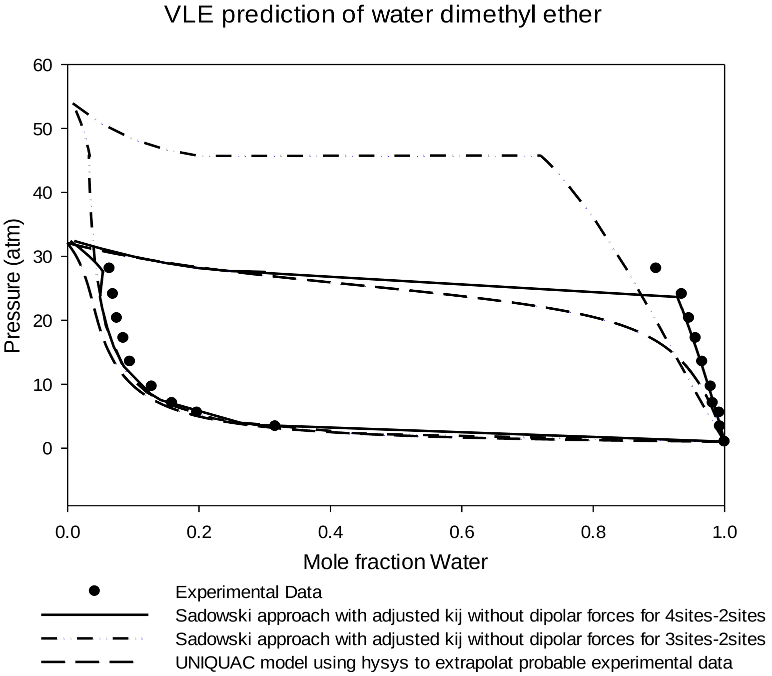

Figure 5-6 Vapor liquid equilibrium prediction for DME-Water at 373.26K using SSAFT-JC with 4 association sites for water and 2 association sites for DME.

5.8 Prediction of Excess molar enthalpy.

Excess molar enthalpy is evaluated from the proposed model for DME and methanol mixture using various approaches. Although the prediction of excess molar enthalpy is given for one mixture, the model is applicable to all mixtures studied so far and also to similar mixtures containing polar or associating species.

The method for calculating the excess molar enthalpy is based on, the expression developed by Fermeglia et al.(M. Fermeglia, 1984). It is a derived to calculate excess enthalpy from equation of states.

$$H^E = RT^2 \sum_i x_i \left(\frac{\partial ln\varphi_i^0}{\partial T} - \frac{\partial ln\varphi_i}{\partial T} \right)_{P,n}$$

φ_i^0 fugacity coefficient for pure component i in the liquid phase .

φ_i fugacity coefficient for component i in mixture in the liquid phase

The fugacity coefficients are calculated by solving the Helmholtz energy equation for both pure component and mixtures. Finally the excess enthalpy is calculated using finite difference formula for calculating the partial differentials.

Figure 5-8 illustrates the prediction of prediction of Excess molar enthalpy using the SSAFT-JC model for various approaches of cross induced association. It is observed that predictions are fairly and qualitatively following the actual experimental data. The best prediction obtained for approaches in which electrostatic interactions are accounted and hence evidently Sadowski and adjusted association parameter approach predicted molar excess enthalpies that agree well with the experimental data.

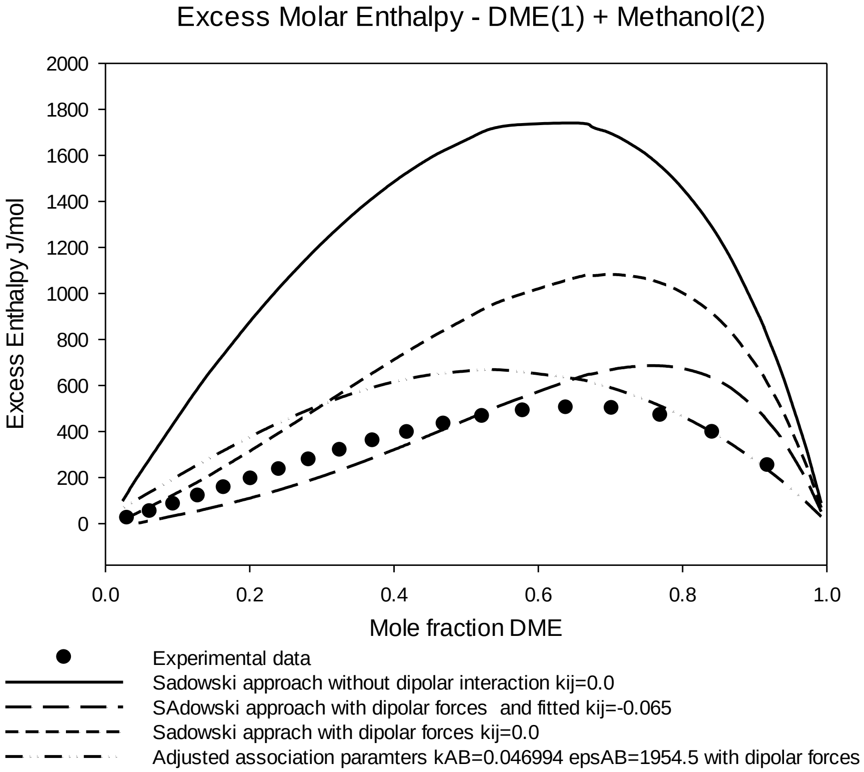

Figure 5-7 Prediction of Excess molar enthalpy of DME-Methanol system using various approaches of cross induced associations including long-ranged electrostatic interactions.

5.9 Conclusion

In this chapter extensive study was carried out to predict the vapor liquid equilibrium of mixtures containing dimethyl ether and alcohols. It was observed that cross association interaction play a significant role in the phase behavior of mixtures which are capable of cross associating. DME-Alcohols exhibit cross associations and these interactions are not trivial to study using traditional association interactions of SAFT. Several schemes of cross associations were evaluated and it was that best results were obtained in the case of adjusting the association parameters of polar-non-self-associating compound after employing log-ranged electrostatic interactions. The deviations are significantly less when compared to the Sadowski approach. It is successfully observed that inclusion of long ranged dipole-dipole interactions leads to significant improvement in the accurate predictive capability of the SSAFT model.

CHAPTER 6

VLE PREDICTION FOR DME-GASES

In the previous chapters, the dipole-dipole interactions were taken into consideration in the calculations of VLE of DME-hydrocarbons and DME-alcohols. Mixtures of DME and light gases are also commonly encountered in DME production processes. Hence, in this chapter, the focus is mainly on the prediction of the vapor-liquid equilibrium of DME-gases; more specifically DME-light gases. Various gases are considered such as hydrogen, nitrogen, carbon dioxide and sulfur dioxide. The study of these mixtures is not trivial due to several reasons. For instance hydrogen is a small molecule and exhibit significant quantum effects. Moreover, these light gases exhibit very high pressure in their VLE. As will be illustrated, the current model of SSAFT fails to give accurate predictions for these light gases systems without modifications. In fact, the pure parameters for hydrogen cannot be obtained using current SSAFT model. The present chapter proposes modification based on the fundamental structure of SSAFT and provides in depth study of mixtures containing DME and light gases emphasizing the improvements after modification.

The present chapter is divided into five sections. **Section 6.1** demonstrates the vapor-liquid equilibrium prediction using the SSAFT-JC for DME-SO_2 and DME-N_2. **Section 6.2** describes the reason for the failure of the model for the mixture of DME containing light gases. In **section 6.3,** proposed modification is discussed for making the model applicable to DME-light gases along with obtained pure compound parameters after modification. Vapor-liquid equilibrium predictions using the modified model are presented in s**ection 6.4**. Finally a brief conclusion about the present chapter is given in **section 6.4.**

6.1 VLE prediction of DME-Sulfur dioxide

Sulfur dioxide is not considered as a light gas; however, it is a polar compound. It would be necessary to evaluate the SSAFT in predicting VLE of DME-SO_2 system without any modification. The evaluation is considered with and without the dipolar forces for SO_2 while the DME is always considered a dipolar compound. The adjustable parameters of SSAFT-JC and SSAFT-GV for SO_2 are given in **Table 4.1** in Chapter 4 while the adjustable parameters for non-polar case were reported by Gross and Sadowski (2001). The VLE of DME-Sulfur dioxide is shown in **Figure 6-1.** As seen, the SSAFT-JC and SSAFT-GV gave satisfactory predication of VLE with adjusting binary interaction parameters. The average absolute deviations of SSAFT-JC with incorporating dipolar interactions for SO_2 are 2.79 % in pressure and 0.09 % in vapor mole fraction. On the other hand, if the dipolar interactions of SO_2 are ignored, these deviations in pressure and vapor mole fraction are 2.17 % and 0.07 %; respectively. Significant deviations were observed in case of Gross term for this mixture when SO_2 is considered as a polar compound as demonstrated in the figure. However, these deviations are reduced when the dipolar interactions of SO_2 are ignored. The inaccuracy of SSAFT-GV is surprising for this system. However, it should be noted that the SSAFT-GV doesn’t work and the adjusted binary interaction parameter is relatively high. This indicates that the SSAFT doesn't work very well for DME-SO_2 system.

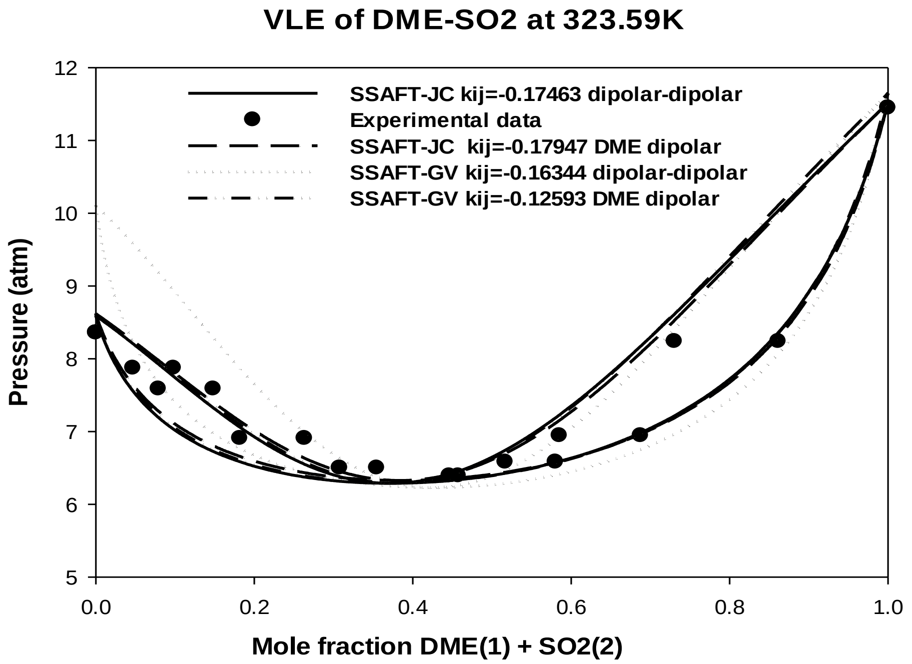

Figure 6-1 VLE of DME-SO2 using four different approaches. (1) SSAFT-JC with adjusted kij=0.17463 including dipole-dipole interactions for both DME and SO_2. (2) SSAFT-JC with adjusted kij=0.17947 including dipole-dipole interactions only for DME. (3) SSAFT-GV with adjusted kij=0.16344 including dipole-dipole interactions both for DME and SO_2. (4) SSAFT-GV with adjusted kij=0.12593 including dipole-dipole interactions only for DME. Experimental data was obtained from Cheric, Korean thermodynamic database.

Another example to evaluate the SSAFT for DME with gases is the system of DME-N_2. **Figure 6-2** gives the vapor-liquid equilibrium prediction of DME-nitrogen at 288.15 K. It is evident form the figure the SSAFT doesn't compare very well with the experimental data. The current model fails to describe the accurate phase behavior not only for DME-nitrogen but also for other systems such as DME-hydrogen, DME-CO and DME-CO_2. Indeed, for some light such as hydrogen, the SSAFT fails even to give adjustable parameters for correlating vapor pressure and liquid density. Therefore, the model need to be modified before it can become applicable to DME light gases. In the next section, the potential reasons for the failure of the SSAFT EOS are discussed. The evaluation of another SAFT version (PC-SAFT) is also made to see how other SAFT versions perform for light gases.

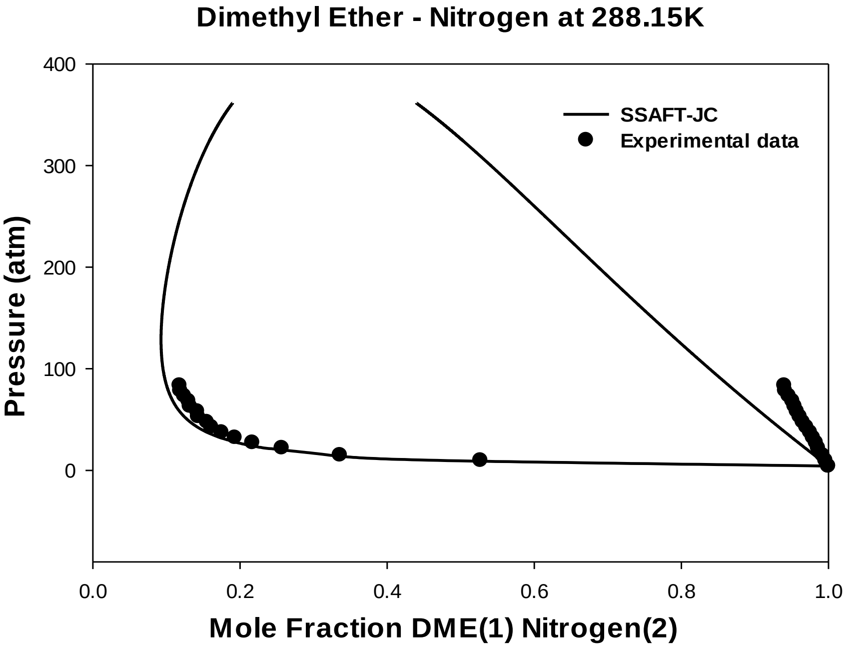

Figure 6-2 VLE of DME-Nitrogen at 288.15K using SSAFT-JC (dispersion constant originally based on ethane). Experimental data is obtained from [123]

6.2 Failure of SSAFT for light gases

The phase equilibrium of mixture containing light gases has been a big challenge for SSAFT EOS. As indicated in the previous section, it was not possible to estimate the pure hydrogen parameters using the SSAFT. The reason for such a failure is due to several reasons. For example, the quantum effects have not been considered in the original development of all SAFT EOSs. The de-Broglie wavelengths for light molecules such as hydrogen are considerably high. This is why these molecules exhibit wave-like properties. It should be noted that the thermal de-Broglie wavelength Λ is defined as follows:

$$\Lambda = \left(\frac{2\pi\beta\hbar}{m}\right)^{1/2}$$

$$\beta = \frac{1}{k_B T}$$

Where, m is mass of the atom, $\hbar$ is the Planck's constant, and k_B is the Boltzmann constant. Another reason for the failure of SSAFT is that DME-light gases mixtures exhibit very high pressure in VLE. It is usually more difficult to predict VLE at high pressures for any model.

Before proposing any modification, there is a question that might arise at this stage regarding the VLE prediction of light gases using other SAFT versions. Of course, it would be difficult to investigate the performance of all SAFT versions. However, the PC-SAFT, which is one of the most popular versions, is selected for this purpose. In particular, the PC-SAFT model was used to predict VLE of DME-H_2 at 306.15K by three different approaches, namely, PC-SAFT, PC-SAFT-JC and PC-SAFT-GV. The adjustable parameters of DME using PC-SAFT, PC-SAFT-JC and PC-SAFT-GV are given in **Table 6-1**. The PC-SAFT parameters for hydrogen are taken from [124] which are ($m=1.00$ $\sigma=2.9860$ $u^0/k=19.2775$). The VLE prediction of DME-H_2 (kij=0) using PC-SAFT, PC-SAFT-JC and PC-SAFT-GV shows deviations in bubble pressure equal to 77.83, 74.38 and 77.26 %; respectively. It is clear that the deviation is very high. It should be also noticed that the addition of the polar forces to DME doesn't improve the prediction. The pure component parameters for DME are obtained and are listed as follows.

Table 6-1 Pure component parameters for DME

	Pure DME Parameters				
Model	***m***	***σ***	***u_0/k***	***x_p***	**Temp range (K)**
PC-SAFT [94]	2.2963	3.2526	208.6	-	200-400
PC-SAFT-JC	2.0123	3.429	215.76	0.49694	200-400
PC-SAFT-GV	2.2634	3.2723	210.29	-	200-400

The failure of the current model of SAFT gives a strong suggestion that there is a need to modify it until it can be applied to DME-light gases. A proposed modification is presented in the next section to account for these shortcomings in SAFT.

6.3 Proposed modification for current SSAFT model

Although it is expected that the account of quantum effects would assist in improving SSAFT, it is not a trivial task and it will not be considered in this work. Therefore, any modification could be either in the repulsive term or in the dispersion term. However, it is well known that the repulsive term which is based on Carnahan and Starling term (1969) is very accurate. The dispersion term, on the other hand, was developed by Lee et al. (1985) and it gave fairly good comparison with simulation data. A potential place for improvement is to look at how the effective hard sphere diameter and square-well-potential depth depend on temperature for real molecules. As illustrated in Chapter 3, the effective hard sphere diameter (d) was defined in a similar way as proposed by Barker and

Henderson (1967) while the temperature dependence of the square-well-potential depth (u^0/kT) is given based on Chen and Kreglewski (1977):

$$d = \sigma\left[1 - ce^{\left(-3u^0/kT\right)}\right]$$

$$u = u^0[1 + (e/kT)]$$

Of course, the temperature dependency could be replaced by different models. For simplicity, the same models are utilized; however, the focus is on how the universal constants of *e/k* and *c* in these two models were obtained.

The universal constants in the original SSAFT were defined based on adjusting vapor pressure and liquid densities of ethane. To investigate why the ethane-based model fails to give a good approximation to hydrogen, it is necessary to study hydrogen without these universal parameters. In other words, it is necessary to see the values of the universal constants based on hydrogen. Therefore, the SSAFT model is adjusted to hydrogen to determine the three usual parameters for non-polar compounds (m, v00 and uk) plus the two universal constants (e/k and c). The results of the five parameters for ethane and hydrogen are given in **Table 6.2**. The adjustable parameters of argon is also added in **Table 6.2**.

Table 6-2 Pure Component parameters for SSAFT including addition universal constants for dispersion. Ethane parameters are obtained from [19]

Component	***m***	v^{00}	u_0/k	**c**	**e/k**	**Temp Range (K)**	**AADP (%)**	**AADL (%)**
Hydrogen	1	15.024	15.738	0.37244	-4.1060	13-31	5.65	1.987
Argon	1	16.807	66.675	0.27447	-4.1292	83-148	0.48	0.44
Ethane	2.022	16.236	90.529	0.333	-10	150-305.5	0.53	2.30

It is clear from the table that the universal constants of ethane don't compare well with those of hydrogen. This explains why the SSAFT is incapable to correlate vapor pressure and liquid density for hydrogen. An alternative compound that could be utilized for the determination of the universal constants is argon. In **Table 6.2**, it is evident that the universal constants of argon is a better approximation for hydrogen. The argon-based model is expected to work better for other small molecules such as N_2. For this reason, the model is now defined based on argon universal parameters.

Based on these modifications, it is found that the SSAFT model achieved significant improvements. The model now successfully estimates pure compound parameters for light gases such as H_2 and N_2. The VLE predictions from the model are improved significantly. The long ranged electrostatic interactions are still employed for polar components. The DME parameters are re-obtained based on argon and given in Table 6.3. The next section presents the results of VLE prediction for DME and light gases.

Table 6-3 Pure compound paramters using dispersion paramters based on Argon

Compound	**Model**	**Temp Range (K)**	**Parameters**						**AAD %**	
			m	σ	u_0/k	$1000\kappa^{AB}$	ε^{AB}/k	x_p	P	ρ^l
Argon	SSAFT	83-148	1.0	16.807	66.765	-	-	-	0.48	0.44
DME	SSAFT-JC	200-399	2.8141	13.022	94.479	-	-	0.2	2.22	0.84
DME	SSAFT-GV	200-399	2.6894	13.53	94.905	-	-	-	1.95	1.02
Hydrogen	SSAFT	13.8-31.0	1.0474	13.760	15.222	-	-		4.33	3.66
Nitrogen	SSAFT	66.1-126.2	2.1497	8.9045	35.306	-	-	-	5.01	1.22
Carbon dioxide	SSAFT	220-304	4.0413	4.5898	61.811	-	-	-	0.74	1.18
Carbon Monoxide	SSAFT	68-131	3.1844	6.2614	31.826	-	-	-	0.81	0.71

6.4 Prediction of vapor-liquid equilibrium of DME - light gases

In this section, the argon-based SSAFT is utilized to predict VLE for DME and light gases. **Figure 6.4** shows the prediction and correlation of SSAFT-JC and SSAFT-GV for DME-hydrogen at 288.15 K.

SSAFT-GV with kij=0.0 gives fairly accurate prediction for the system. The deviations are significantly reduced in comparison to the PC-SAFT-JC and PC-SAFT-GV. The average absolute deviation in pressure and vapor mole fraction are 14.14 % and 0.09 % respectively for SSAFT-GV with kij=0.0 and 9.21 % and 0.15 % when binary interaction parameter is adjusted (kij=-0.0859). The SSAFT-JC with kij=0.0 is surprisingly worse than that of SSAFT-GV with AADP of 26.07 % and AADY of 0.41. Slight improvement is achieved for SSAFT-JC with adjusting binary interaction parameter (kij=-0.2489). The AAD % in pressure and mole fraction are 14.47 and 0.30; respectively. It is clear from the figure that quantitative prediction is not possible for SSAFT-JC. However, fairly good results are obtained using SSAFT-GV.

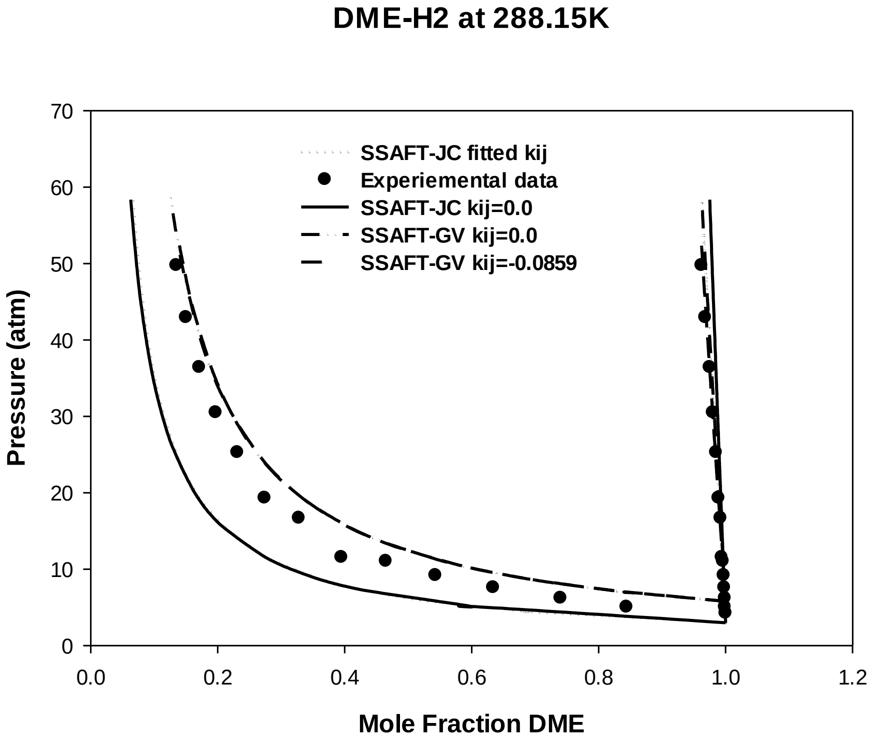

Figure 6-3 VLE prediction of DME - H_2 at 288.15 K e/k and c based on argon using different approaches (1) SSAFT-JC with adjusted kij DME (2) SSAFT-JC without adjusted (3) SSAFT-GV with adjusted kij (4) SSAFT-GV without adjusted. Experimental data was obtained from [125] .

Figure 6-4 illustrates the vapor-liquid equilibrium prediction of DME-H2 at 306.15K using two different approaches similar to the previous case. The best prediction are obtained by SSAFT-GV with adjusted kij=-0.1923 which gave 6.52 % and 0.10% deviations in AADP and AADY respectively. The deviations in pressure and vapor mole fraction using SSAFT-GV using kij=0.0 are 20.55% and 0.09% respectively. On the other hand SSFAT-JC model surprisingly exhibited higher deviation in comparison to GV term, AADP is 48.68% and AADY is 0.48 % while with adjusted kij= -0.4170 the deviation are 13.76 % and 0.26% respectively. So it is inferred that good results are obtained for SSAFT-GV.

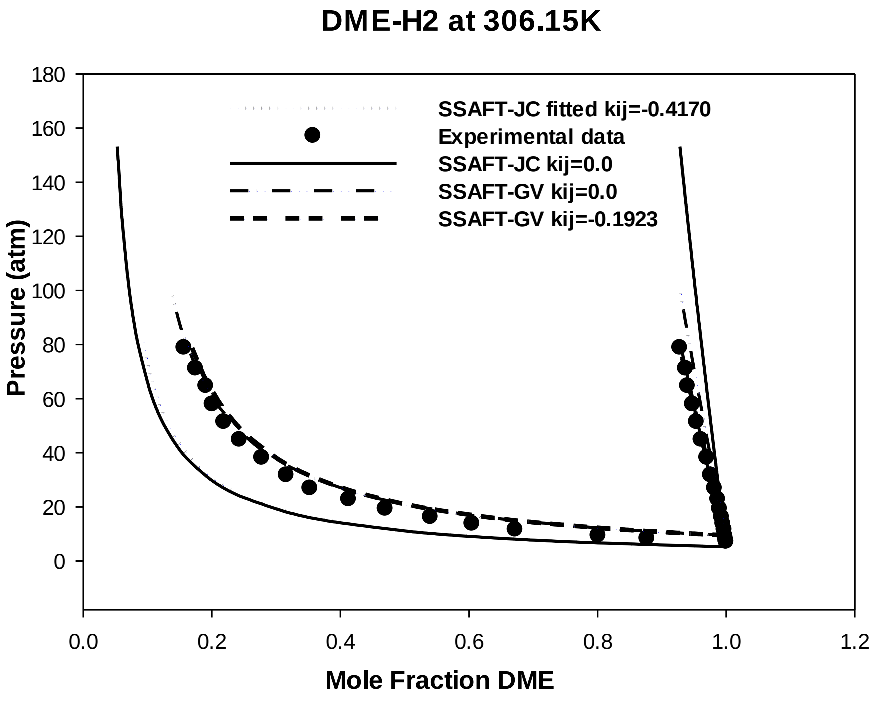

Figure 6-4 VLE prediction of DME - H_2 at 306.15 K e/k and c based on argon using different approaches (1) SSAFT-JC with adjusted kij DME (2) SSAFT-JC without adjusted (3) SSAFT-GV with adjusted kij (4) SSAFT-GV without adjusted. Experimental data was obtained from [125] .

Figure 6-5 represents vapor liquid equilibrium of DME-Nitrogen at 318.15K. The VLE of system of DME-N_2 exhibits very high pressure up to 600 atm. At such high pressure it becomes very difficult to predict the vapor liquid equilibrium because dispersion forces are predominant. The VLE for this system is predicted by two approaches using the dispersion parameters based on argon. The deviations are significantly small in comparison to those observed in PC-SAFT for H_2. The best predictions are obtained from SSAFT-GV with adjusted kij=0.1452 exhibited the least deviations 4.61 and 0.13 % AADP and AADY respectively whereas in case of SSAFT-JC at kij=0.0408 these deviations are 17.06 and 0.181%. The cases when binary interaction parameter is not adjusted remained at comparably at little higher deviations.

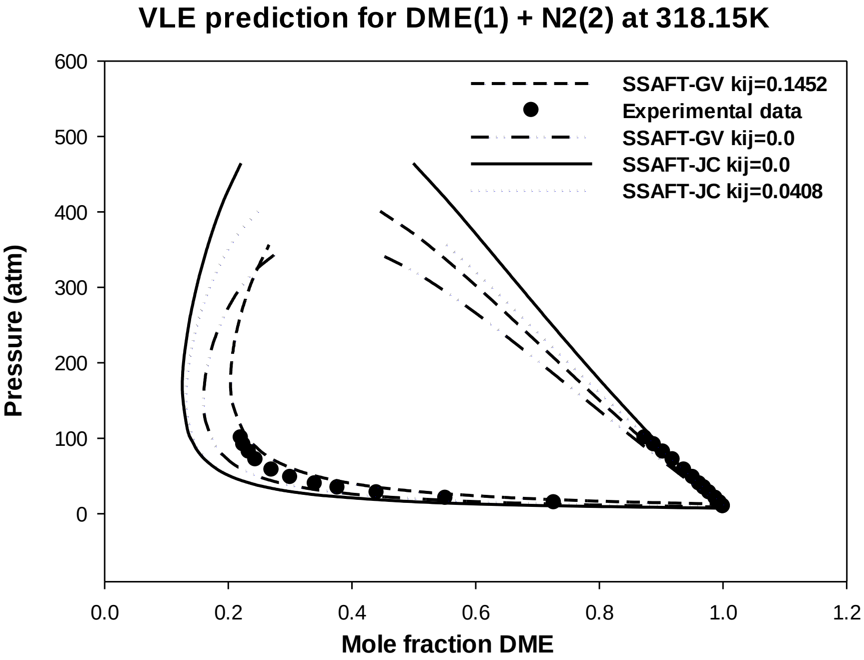

Figure 6-5 VLE prediction of DME - N$_2$ at 318.15 K e/k and c based on argon using different approaches (1) SSAFT-JC with adjusted kij DME (2) SSAFT-JC without adjusted (3) SSAFT-GV with adjusted kij (4) SSAFT-GV without adjusted. Experimental data was obtained from [123] .

Figure 6-6 represents the VLE of DME-Nitrogen at 308.15. The prediction is fairly accurate in case of SSAFT-GV with adjusted binary interaction parameter and by far the best case among. The deviations in this prediction are 4.01 % and 0.10 % in pressure and vapor mole fraction respectively using the SSAFT-GV at adjusted kij=0.1473. The other approaches like SSAFT-JC at kij=0.0 exhibits higher deviations for this system, AADP=17.40 % and AADY=0.20 % while its counterpart GV at kij=0.0 possess 15.13 and 0.25 % respectively.

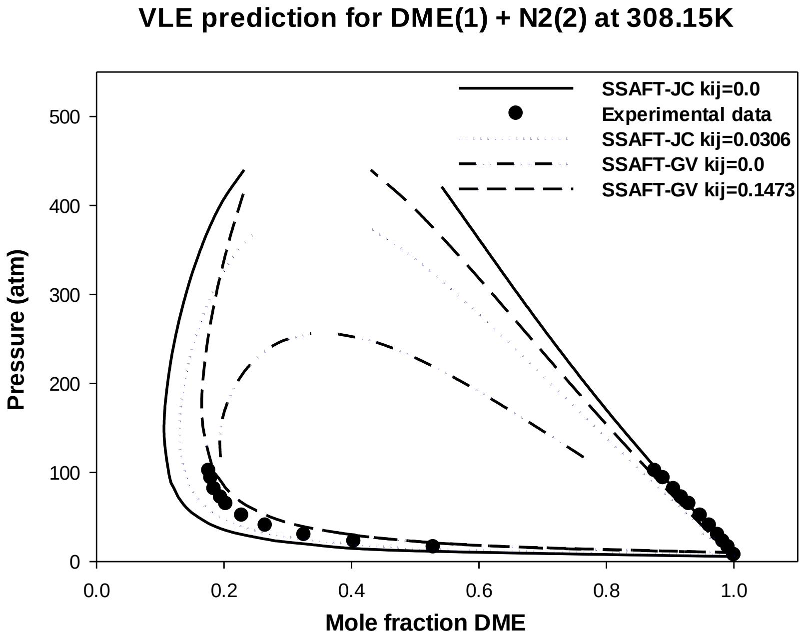

Figure 6-6 VLE prediction of DME - N_2 at 308.15 K e/k and c based on argon using different approaches (1) SSAFT-JC with adjusted kij DME (2) SSAFT-JC without adjusted (3) SSAFT-GV with adjusted kij (4) SSAFT-GV without adjusted. Experimental data was obtained from [123]

In the case of vapor liquid equilibrium of DME-Nitrogen illustrated in **Figure 6-7** similar trends like the previous predictions could be inferred. The SSAFT-JC kij=0.0 at 298.15K noted 17.0 % AAD in pressure while 0.23 % in vapor mole fraction, whereas its counterpart SSAFT-JC kij=0.0 deviated by 12.42 and 0.21 % respectively. In cases of adjusted binary interaction parameter these deviation reduced significantly, SSAFT-GV with kij=0.1539 had AAPD= 4.01 and AADY=0.10 % whereas SSAFT-JC with kij=0.0378 AADP=5.07 and AADY=0.19 %.

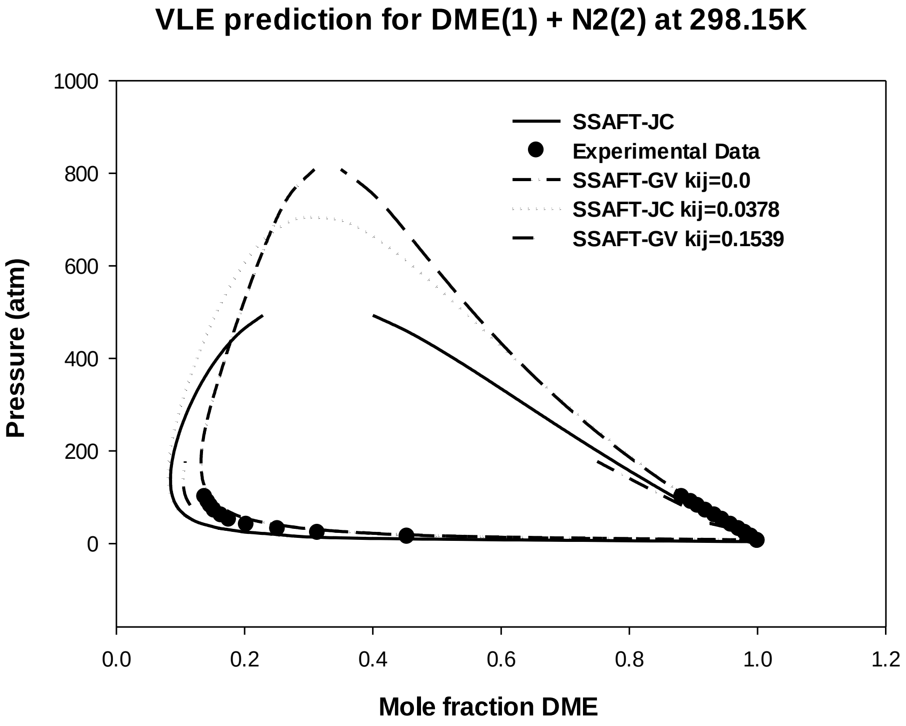

Figure 6-7 VLE prediction of DME - N_2 at 298.15 K e/k and c based on argon using different approaches (1) SSAFT-JC with adjusted kij DME (2) SSAFT-JC without adjusted (3) SSAFT-GV with adjusted kij (4) SSAFT-GV without adjusted. Experimental data was obtained from [123]

Figure 6-8 represents VLE of DME-Carbon dioxide at 273.15K using two different approaches. The prediction is very accurate and deviations are small. The inclusion of dipolar interaction and dispersion constants based on argon leads remarkable level of accuracy. The SSAFT-JC at kij=0.0 is able to achieve fairly accurate predictions with less deviations of 5.16 and 0.01 % in pressure and vapor mole fraction. The small deviation however are reduced by adjusting the binary interaction parameter (kij=0.00160) and deviation are then 1.32 and 0.01 % for AADP and AADY respectively. The case of SSAFT with Gross term was also accurate with deviations of 8.87 and 0.03 % respectively and in case of adjusted kij=0.01427 is 7.25 and 0.02 % respectively.

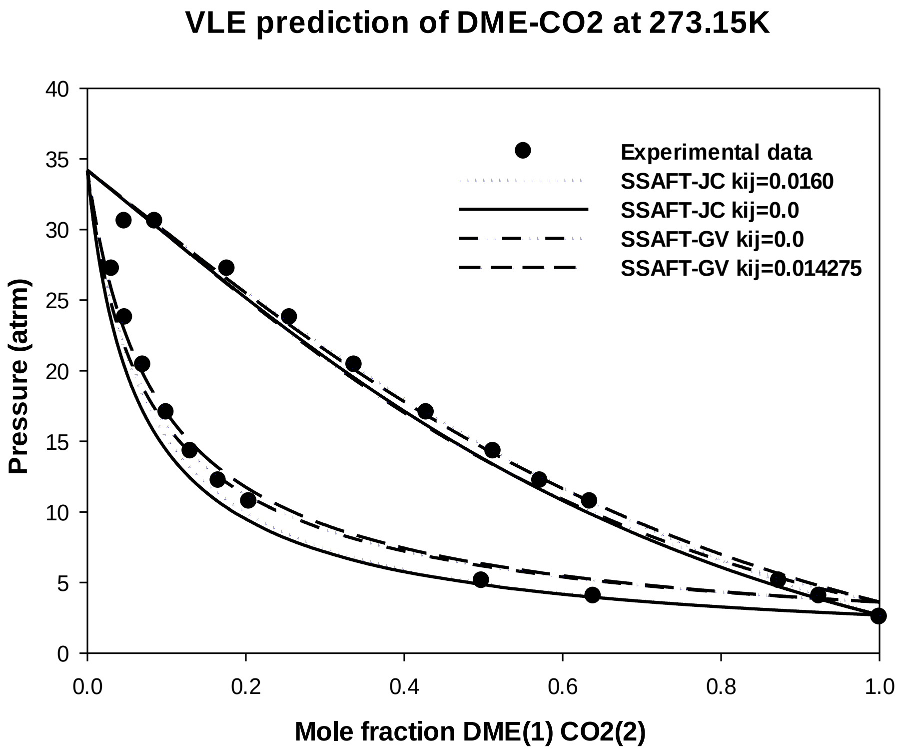

Figure 6-8 VLE prediction of DME - CO_2 at 273.15 K e/k and c based on argon using different approaches (1) SSAFT-JC with adjusted kij DME (2) SSAFT-JC without adjusted (3) SSAFT-GV with adjusted kij (4) SSAFT-GV without adjusted. Experimental data was obtained from [126]

The VLE prediction of DME-CO2 is shown in **Figure 6-9,** which is very accurate and follows the same trend as the precious one. The dispersion term constant based on argon are successfully able to describe the phase behavior of the system. The inclusion of dipole-dipole interactions also result in improved predictions. SSAFT-JC at k_{ij}=0.0 deviates by 6.0 and 0.02 % in pressure and vapor mole fraction whereby adjusting the binary interaction parameter these deviations are reduced to 0.97 and 0.02 % respectively. The case of SSAFT-GV at k_{ij}=0.0 deviates by 7.63 and 0.03 % in pressure and vapor mole fraction respectively whereas by adjusting kij these deviation are reduced to 5.89 and 0.0 % respectively.

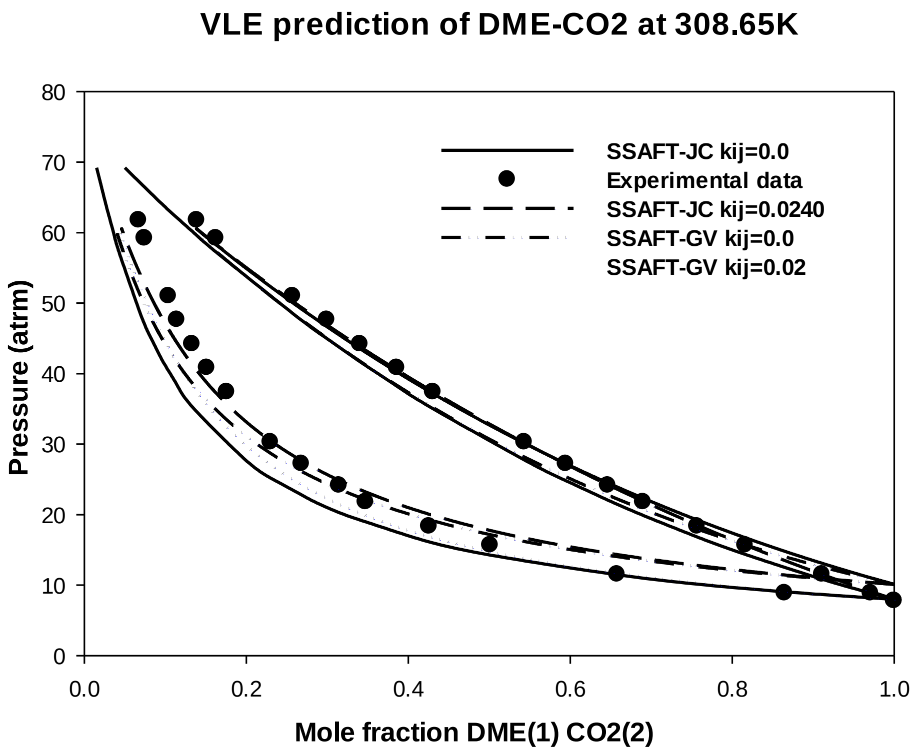

Figure 6-9 VLE prediction of DME - CO_2 at 308.65 K e/k and c based on argon using different approaches (1) SSAFT-JC with adjusted kij DME (2) SSAFT-JC without adjusted (3) SSAFT-GV with adjusted kij (4) SSAFT-GV without adjusted. Experimental data was obtained from [126]

Figure 6-10 presents the vapor liquid equilibrium of DME-Carbon monoxide. The prediction using SSAFT-JC is excellent and employment of dipolar interactions successfully describes the phase behavior of the system. SSAFT-JC with k_{ij}=0.0 deviates by 13.4 and 0.02 % respectively in pressure and vapor phase mole fraction whereas its counterpart SSFAT-GV deviates by 6.01 and 0.21 % respectively. After adjusting the binary interaction parameters the deviations are reduced to 7.80 and 0.02 % respectively for SSAFT-JC.

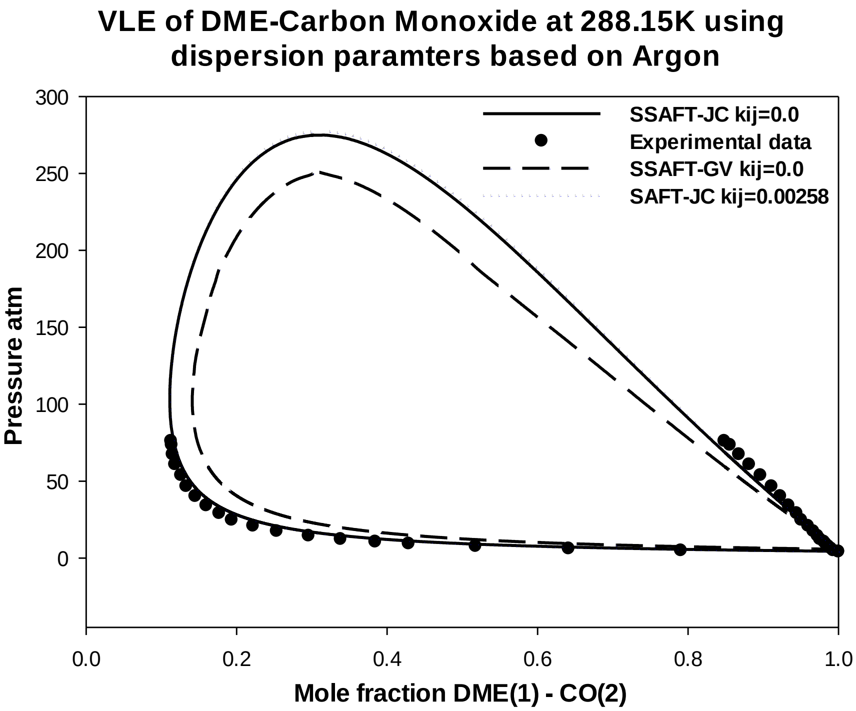

Figure 6-10 VLE prediction of DME - CO at 288.15 K e/k and c based on argon using different approaches (1) SSAFT-JC with adjusted kij DME (2) SSAFT-JC without adjusted (3) SSAFT-GV without adjusted. Experimental data was obtained from [127]

Table 6-3 provide the average absolute deviation in pressure and vapor phase mole fraction for each systems and each approach of predication studied in the present chapter. In **Figure 6-11** a comparison is made to illustrate the improvements in the current SSAFT-JC model with PC-SAFT-JC model. The improvements are remarkable and modification in the current model sustains high accuracy in comparison to PC SAFT version. **Figure 6-12** provide the comparison of average absolute deviation in pressure for each system among each approach

Table 6-4 Average absolute deviation in prediction of DME-light gases using various approach

Mixture	Model	T	AADP	AADY
DME-H_2	SSAFT-JC k_{ij}=-0.2489	288.15	14.47	0.30
DME-H_2	SSAFT-JC k_{ij}=0.0	288.15	26.07	0.41
DME-H_2	SSAFT-GV k_{ij}=0.0	288.15	14.14	0.09
DME-H_2	SSAFT-GV k_{ij}=-0.0859	288.15	9.21	0.15
DME-H_2	SSAFT-JC k_{ij}=-0.4170	306.15	13.76	0.26
DME-H_2	SSAFT-JC k_{ij}=0.0	306.15	48.68	0.48
DME-H_2	SSAFT-GV k_{ij}=0.0	306.15	20.55	0.09
DME-H_2	SSAFT-GV k_{ij}=-0.1923	306.15	6.52	0.10
DME-N_2	SSAFT-JC k_{ij}=0.0	298.15	17.0	0.23
DME-N_2	SSAFT-JC k_{ij}=0.0378	298.15	5.07	0.19
DME-N_2	SSAFT-GV k_{ij}=0.1539	298.15	4.01	0.10
DME-N_2	SSAFT-GV k_{ij}=0.0	298.15	12.42	0.21
DME-N_2	SSAFT-JC k_{ij}=0.0	308.15	17.40	0.20
DME-N_2	SSAFT-GV k_{ij}=0.0	308.15	15.13	0.25
DME-N_2	SSAFT-GV k_{ij}=0.1473	308.15	5.03	0.14
DME-N_2	SSAFT-JC k_{ij}=0.0306	308.15	14.41	0.08
DME-N_2	SSAFT-JC k_{ij}=0.0	318.15	10.01	0.24
DME-N_2	SSAFT-GV k_{ij}=0.0	318.15	17.04	0.05
DME-N_2	SSAFT-GV k_{ij}=0.1452	318.15	4.61	0.13
DME-N_2	SSAFT-JC k_{ij}=0.0408	318.15	17.06	0.18
DME-CO_2	SSAFT-GV k_{ij}=0.0	273.15	8.87	0.03
DME-CO_2	SSAFT-JC k_{ij}=0.0	273.15	5.16	0.01
DME-CO_2	SSAFT-GV k_{ij}=0.01427	273.15	7.25	0.02
DME-CO_2	SSAFT-JC k_{ij}=0.00160	273.15	1.32	0.01
DME-CO_2	SSAFT-GV k_{ij}=0.0	308.65	7.63	0.03
DME-CO_2	SSAFT-JC k_{ij}=0.0	308.65	6.00	0.02
DME-CO_2	SSAFT-GV k_{ij}=0.02	308.65	5.89	0.02
DME-CO_2	SSAFT-JC k_{ij}=0.0240	308.65	0.97	0.02
DME-CO	SSAFT-JC k_{ij}=0.0	288.15	13.4	0.02
DME-CO	SSAFT-JC k_{ij}=0.00258	288.15	7.80	0.02
DME-CO	SSAFT-GV k_{ij}=0.0	288.15	6.01	0.21

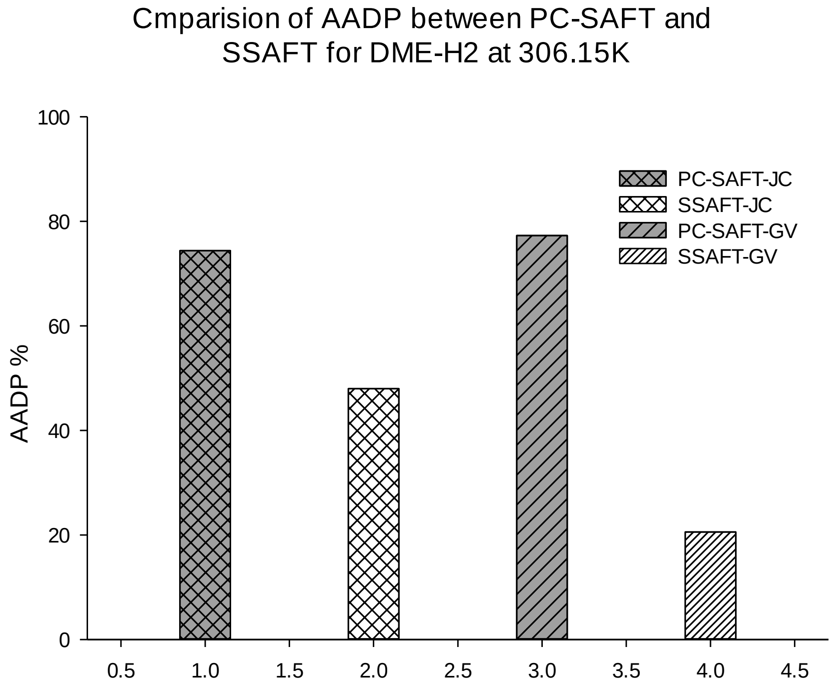

Figure 6-11Comparision of AADP between PC-SAFT-JC and SSAFT-JC and PC-SAFT-GV and SSAFT-GV

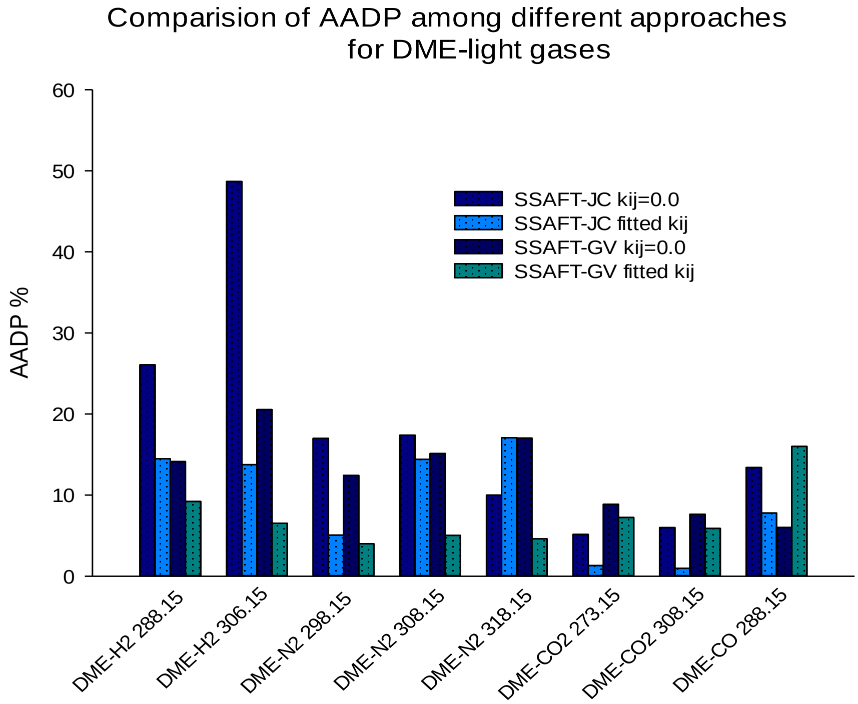

Figure 6-12 Comparison of Average absolute deviations in the prediction of DME-light gases using various approaches.

6.5 Conclusion

The present chapter covers an extensive study of mixtures containing dimethyl ether and light gases. SSAFT-JC was able to give accurate prediction for DME-Sulfur dioxide but when it comes to mixtures containing light gases, the present model failed abruptly. The reason was that small molecules of light gases do not behave the same way as the heavier molecules. The study of mixture of DME-light gases is not trivial and model needed basic modification. The dispersion term in the previous model was based on fitting the PVT data of ethane which is comparably a larger molecule. The dispersion term constants c and e/k were readjusted based on smaller molecule argon. The inclusion of these new dispersion constants based on adjusting over PVT of argon, showed remarkable improvements. After employing electrostatic interaction on the modified model was successfully able to give quantitative vapor liquid predictions with very good accuracy. It was interesting to note here that Gross and Vrabec term performed better in terms of accuracy than Jog & Chapman term. However as the size of the molecule increased in order from H_2, N_2, CO, CO_2 the accuracy increased from the Jog & Chapman term this proposition is also validated from the study in chapter 4, DME-hydrocarbons where greater accuracy was obtained for Jog & Chapman term. It was observed that by increasing temperatures the deviation increased in the prediction from polar SSAFT. The reason is owed to the fact that with the increase of temperature the polar forces begin to weaken however they are still substantially present, enough to be accounted for accurate predictions.

CHAPTER 7

CONCLUSION AND RECOMMENDATIONS FOR FUTURE WORK

7.1 Conclusion

The present work was carried out to improve the predictive capability of the Simplified SAFT model by including long ranged electrostatic interactions into the model. The work was successfully completed and achieved significant level of improvements in contrast to the actual model. Before providing the concluding remarks of outcomes, it is imperative to conclude the problems first. The research carried out in this work could be broadly classified into three challenging problems.

Problem 1: DME-hydrocarbons: DME is a polar compound and hydrocarbons are non polar, DME exhibits dipole-dipole interactions with its own molecules. Whereas dispersive interactions are present for both DME and hydrocarbons. Accounting for these interaction in such asymmetrical mixture was a challenging task.

Problem 2: DME-alcohols: DME and alcohols are both polar components in addition alcohols exhibit associations, however DME itself is non-associative. But, when DME comes in mixture phase with alcohols it exhibits cross associations with alcohols. It becomes a challenge to account for the association parameters for DME because DME does not have association parameters in its pure phase however in mixture phase it is associative so there is a need to account for such parameters. So in a nutshell, in such mixtures there are dipolar forces, association along with cross induced associations.

Problem 3: DME-light gases: Phase behavior of mixtures of DME-light gases such as DME-H_2 are very difficult to predict because small molecules of hydrogen exhibit significant quantum effects. SAFT however is based on comparatively larger molecules of ethane and does not account for such interactions. It even fails to obtain the pure component parameters of hydrogen. The model needed modification before it could be applied to such mixtures. Moreover electrostatic forces were still accounted in the modified model for DME and Carbon monoxide.

DME mixtures containing hydrocarbons, alcohols and light gases were extensively studied and predictions obtained ranged from excellent to very good, in agreement to the experimental data. It was observed that inclusion of dipole-dipole interactions were successfully able to describe the phase behavior of mixture containing DME (polar compound). Such inclusion made SSAFT close to the real behavior of the fluids and mostly eliminated the need for adjusting binary interaction parameter over experimental data. In most cases k_{ij} was set to 0.0 and predictions agreed well with the experimental data. However, in some cases kij for polar SSAFT were adjusted which evidently turned out to be a very small number in comparison to kij of non-polar SSAFT, to eliminate small deviations. In some case such as DME-hexane the prediction from polar-SSAFT was so accurate that was not even achieved through empirical adjustment in its non-polar counterpart. It was further observed that model worked well for various mixtures of DME-alkanes and alkenes. In case of alkenes, which are double bond unsaturated hydrocarbons, however SAFT is based on assuming molecules to singly bonded hard spheres. It was observed that accurate perdition were obtained by setting the value of mx_p=0.7. The reason for such setting could be to account for correction in chain length (m) for alkenes. It was further observed that with increase in temperatures the deviations in the prediction begin to increase slightly. The reason for such behavior is the fact that polar forces begin to weaken with increasing temperature due to increase in the kinetic energy of the molecules. However, polar forces are still predominant and their presence is still of enough magnitude that they must be accounted in order to achieve accurate prediction. It was also observed that Jog and Chapman dipolar term proved to be better in terms of accuracy than Gross and Vrabec dipolar term. VLE of DME-hydrocarbons are thus best obtained by SSAFT-JC at k_{ij}=0.0. In cases where there are small but noticeable deviation binary interaction parameter can be adjusted which is evidently a small number in comparison to k_{ij} of non-polar SSAFT.

DME-Alcohols were extensively studied along with induced cross associations along with hydrogen bonding associations and employing polar interactions. The case of DME-Alcohol becomes more complicated because of induced associations. Various schemes of induced association were thoroughly studied and it was inferred that the best approach among all was the one by adjusting the association parameters for DME along with polar interactions over the experimental data. The deviations for this approach were significantly small in comparison to the Sadowski approach of induced association.

DME-Gases more specifically DME-light gases system were studied in depth by introducing a modification in the basic model of SSAFT. The modified model was based on the dispersion term constant obtained by regressing the PVT of smaller molecule Argon instead of ethane which was comparably a larger molecule. The predictions obtained after such modification were remarkable and it is interesting to note here that Gross and Vrabec term performed better than Jog and Chapman term in terms of accuracy. However this trend fairly reversed with the increasing size of the gaseous molecule. In carbon monoxide and carbon dioxide mixtures with DME, better prediction were obtained from Jog & chapman term. DME-SO_2 was also studied including dipole-dipole interactions for both DME and Sulfur dioxide however it was observed that by including dipolar interactions in both molecules decreased the accuracy. The reason for such behavior is the fact that by including polar forces not only attractive but repulsive forces are also added, which however may be lesser in the real mixture and hence model overestimated the pressure.

It is finally concluded that SSAFT has shown excellent predictions for DME mixtures when electrostatic forces are incorporated. The Jog and Chapman dipolar exhibits higher accuracy for larger molecules whereas Gross & Vrabec dipolar term is more accurate for light gases and small molecules.

7.2 Recommendations for future work

The inclusion of electrostatic interaction are crucial for describing accurate phase behavior of mixtures containing polar components. The present work successfully incorporated electrostatic interaction of dipolar nature and thoroughly studied the vapor liquid of DME mixtures. The study of various mixture involving oxygenated hydrocarbon is not trivial and involves multifold level of complexities. Several association schemes need to be tested before a concluding argument can be provided for a valid scheme. Light molecules on the other hand needs to be treated differently because of their anomalous nature pertaining to significant quantum effects. Such as diverse nature of interactions and multifold level of behavior cannot be generalized in a simple model. Several addition and enhancements needs to studied and developed independently before an accurate predictive thermodynamic model can be obtained. The improvements however results in more complex terms that need to be dealt with different mathematical approaches than conventional.

Apart from vapor liquid equilibrium various thermo-physical properties may be evaluated using the current model by taking second or third order derivatives of the fundamental properties. Apart from DME, other polar-associating components and their various mixtures may be chosen for study from the present model. By employing appropriate polar forces and relevant association schemes accurate vapor liquid equilibrium could obtained.

Further enhancement/ addition in the model would be to include the electrolytic and ionic contributions and effects of solvation. Several phase equilibrium such as vapor-liquid vapor-liquid-liquid and liquid-liquid could be extensively studied to provide a conclusive support for the model.

APPENDIX – A

Various hydrogen bonding possibilities in water + dimethyl ether mixture.

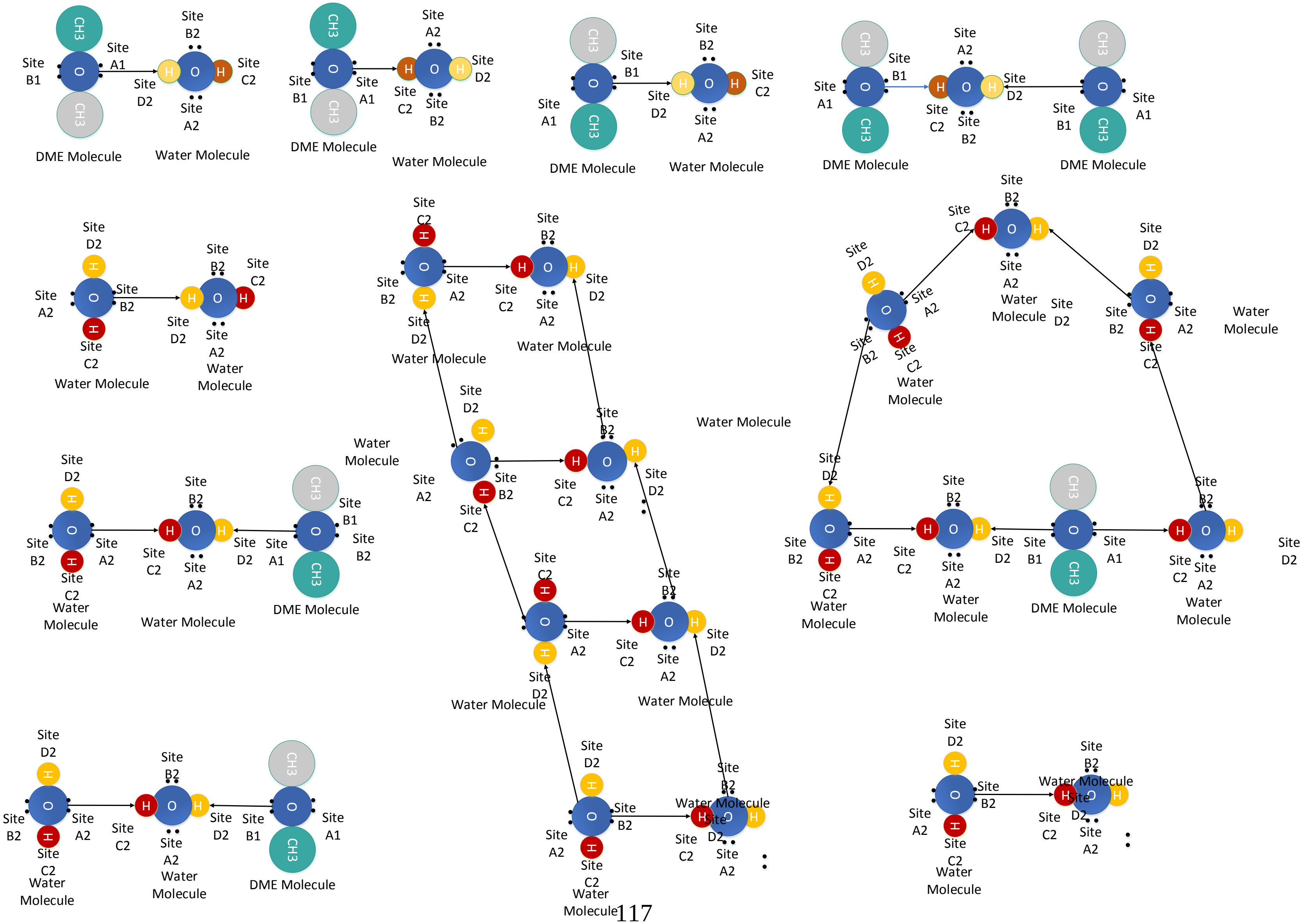

APPENDIX – B

Expansion of the association equation for a sample case of Water + ethanol + Dimethyl Ether

The case is studied using self-association and induced cross association, with 4-3-2 association sites for water + Ethanol + dimethyl ether respectively. The sites are labelled as follows.

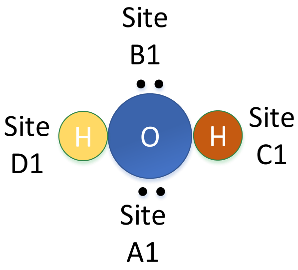

Water Molecule

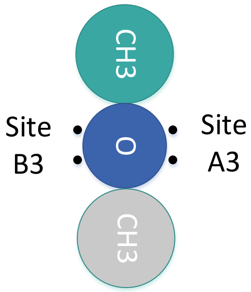

DME Molecule

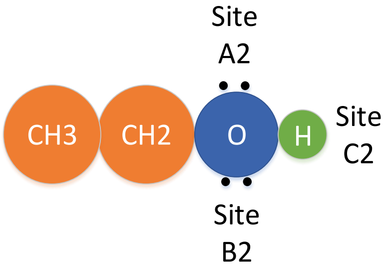

Ethanol Molecule

The equation are written accordingly (refer to **Section 2.5.2** for generalized form). The association will take place between sites capable of forming a hydrogen bond (refer to **section 2.6** for detailed illustration in **Figure 2.3 -2.4 and figure in Appendix A**). The association strength between all the interaction are indicated below either zero or non-zero, to indicate whether the site is interacting or non-interacting.

The sites labeled are A1, B1, C1 and D1 for water, A2, B2, C2 for methanol and A3, B3 of dimethyl ether. A lone pair on oxygen is labelled with A and B. hydrogen atom is given a letter C and D. The number indicates, the component number.

$\Delta^{A1B1}= 0$ $\Delta^{B1A1}= 0$ $\Delta^{A1B2}= 0$ $\Delta^{B2A1}= 0$ $\Delta^{A1A2}= 0$ $\Delta^{A2A1}= 0$ $\Delta^{A1B1}= 0$

$\Delta^{A1C1}\neq 0$ $\Delta^{C1A1}\neq 0$ $\Delta^{A1D1}\neq 0$ $\Delta^{D1A1}= 0$ $\Delta^{A1C2}\neq 0$ $\Delta^{C2A1}\neq 0$ $\Delta^{B1C1}\neq 0$ $\Delta^{C1B1}\neq 0$ $\Delta^{B1D1}\neq 0$ $\Delta^{D1B1}= 0$ $\Delta^{B1C2}\neq 0$ $\Delta^{C2B1}\neq 0$

All other cases are zero.

$$\begin{aligned}\frac{a^{assoc}}{RT} = \quad & x_1\left[\left(\ln X^{A1} - \frac{X^{A1}}{2}\right) + \left(\ln X^{B1} - \frac{X^{B1}}{2}\right) + \left(\ln X^{C1} - \frac{X^{D1}}{2}\right) + \left(\ln X^{D1} - \frac{X^{D1}}{2}\right) + 2\right] + \\ & x_2\left[\left(\ln X^{A2} - \frac{X^{A2}}{2}\right) + \left(\ln X^{B2} - \frac{X^{B2}}{2}\right) + \left(\ln X^{C2} - \frac{X^{C2}}{2}\right) + 3/2\right] + \\ & x_3\left[\left(\ln X^{A3} - \frac{X^{A3}}{2}\right) + \left(\ln X^{B3} - \frac{X^{B3}}{2}\right) + 1\right]\end{aligned}$$

$$X^{A1} = \frac{1}{1 + N_A[x_1\rho X^{C1}\Delta^{A1C1} + x_1\rho X^{D1}\Delta^{A1D1} + x_2\rho X^{C2}\Delta^{A1C2}]}$$

$$X^{B1} = \frac{1}{1 + N_A[x_1\rho X^{C1}\Delta^{B1C1} + x_1\rho X^{D1}\Delta^{B1D1} + x_2\rho X^{C2}\Delta^{B1C2}]}$$

$$X^{C1} = \frac{1}{1 + N_A[x_1\rho X^{A1}\Delta^{C1A1} + x_1\rho X^{B1}\Delta^{C1B1} + x_2\rho X^{A2}\Delta^{C1A2} + x_1\rho X^{B2}\Delta^{C1B2} + x_3\rho X^{A3}\Delta^{C1A3} + x_3\rho X^{B3}\Delta^{C1B3}]}$$

$$X^{D1} = \frac{1}{1 + N_A[x_1\rho X^{A1}\Delta^{D1A1} + x_1\rho X^{B1}\Delta^{D1B1} + x_2\rho X^{A2}\Delta^{D1A2} + x_1\rho X^{B2}\Delta^{D1B2} + x_3\rho X^{A3}\Delta^{D1A3} + x_3\rho X^{B3}\Delta^{D1B3}]}$$

$$X^{A2} = \frac{1}{1 + N_A[x_1\rho X^{C1}\Delta^{A2C1} + x_1\rho X^{D1}\Delta^{A2D1} + x_2\rho X^{C2}\Delta^{A2C2}]}$$

$$X^{B2} = \frac{1}{1 + N_A[x_1\rho X^{C1}\Delta^{B2C1} + x_1\rho X^{D1}\Delta^{B2D1} + x_2\rho X^{C2}\Delta^{B2C2}]}$$

$$X^{C2} = \frac{1}{1 + N_A[x_1\rho X^{A1}\Delta^{C2A1} + x_1\rho X^{B1}\Delta^{C2B1} + x_2\rho X^{A2}\Delta^{C2A2} + x_1\rho X^{B2}\Delta^{C2B2} + x_3\rho X^{A3}\Delta^{C2A3} + x_3\rho X^{B3}\Delta^{C2B3}]}$$

$$X^{A3} = \frac{1}{1 + N_A[x_1\rho X^{C1}\Delta^{A3C1} + x_1\rho X^{D1}\Delta^{A3D1} + x_2\rho X^{C2}\Delta^{A3C2}]}$$

$$X^{B3} = \frac{1}{1 + N_A[x_1\rho X^{C1}\Delta^{B3C1} + x_1\rho X^{D1}\Delta^{B3D1} + x_2\rho X^{C2}\Delta^{B3C2}]}$$

$$\Delta^{A1C2} = {\sigma_{12}}^3\kappa^{A1C2}g_{12}(d_{12})[exp(\epsilon^{A1C2}/kT) - 1]$$

$$\Delta^{B1C2} = {\sigma_{12}}^3\kappa^{B1C2}g_{12}(d_{12})[exp(\epsilon^{B1C2}/kT) - 1]$$

.

.

. The Δ^{AIBJ} is written for all the pair of interaction sites.

$${g_{ij}}^{hs}\left(d_{ij}\right) = \frac{1}{1-\zeta_3} + \frac{3d_{ii}d_{jj}}{d_{ii+}d_{jj}}\frac{\zeta_2}{(1-\zeta_3)^2} + 2\left[\frac{d_{ii}d_{jj}}{d_{ii+}d_{jj}}\right]^2\frac{{\zeta_2}^2}{(1-\zeta_3)^3}$$

$${g_{12}}^{hs}(d_{12}) = \frac{1}{1-\zeta_3} + \frac{3d_{11}d_{22}}{d_{11+}d_{22}}\frac{\zeta_2}{(1-\zeta_3)^2} + 2\left[\frac{d_{11}d_{22}}{d_{11+}d_{22}}\right]^2\frac{{\zeta_2}^2}{(1-\zeta_3)^3}$$

$${g_{23}}^{hs}(d_{23}) = \frac{1}{1-\zeta_3} + \frac{3d_{22}d_{33}}{d_{22+}d_{33}}\frac{\zeta_2}{(1-\zeta_3)^2} + 2\left[\frac{d_{22}d_{33}}{d_{22+}d_{33}}\right]^2\frac{{\zeta_2}^2}{(1-\zeta_3)^3}$$

.. written for all the pair of interaction sites.

$$d_{12} = \frac{d_{11} + d_{22}}{2}$$

$$\zeta_1 = \frac{\pi N_{AV}}{6}\left[x_1 m_1 (d_{11})^1 + \; x_2 m_2 (d_{22})^1 \; + \; x_3 m_3 (d_{33})^1 \right]$$

$$\zeta_k = \frac{\pi N_{AV}}{6}\sum_i x_i m_i (d_{ii})^k \qquad k = 0,1,2,3$$

$$\begin{aligned}
(H)_\rho = \frac{\partial H}{\partial \rho} = \Bigg[& x_1\left\{\left(\frac{1}{X^{A1}} - \frac{1}{2}\right)\frac{\partial X^{A1}}{\partial \rho} + \left(\frac{1}{X^{B1}} - \frac{1}{2}\right)\frac{\partial X^{B1}}{\partial \rho} + \left(\frac{1}{X^{C1}} - \frac{1}{2}\right)\frac{\partial X^{C1}}{\partial \rho} + \left(\frac{1}{X^{D1}} - \frac{1}{2}\right)\frac{\partial X^{D1}}{\partial \rho}\right\} \\
+ \quad & x_2\left\{\left(\frac{1}{X^{A2}} - \frac{1}{2}\right)\frac{\partial X^{A2}}{\partial \rho} + \left(\frac{1}{X^{B2}} - \frac{1}{2}\right)\frac{\partial X^{B2}}{\partial \rho} + \left(\frac{1}{X^{C2}} - \frac{1}{2}\right)\frac{\partial X^{C2}}{\partial \rho}\right\} \\
+ \quad & x_3\left\{\left(\frac{1}{X^{A3}} - \frac{1}{2}\right)\frac{\partial X^{A3}}{\partial \rho} + \left(\frac{1}{X^{B3}} - \frac{1}{2}\right)\frac{\partial X^{B3}}{\partial \rho}\right\} \Bigg]
\end{aligned}$$

$$\begin{aligned}
(H)_{x_1} = \frac{\partial H}{\partial x_1} = \frac{\partial (a^{assoc}/RT)}{\partial \rho} & \\
= \Bigg[& \left\{\left(lnX^{A1} - \frac{X^{A1}}{2}\right) + \left(lnX^{B1} - \frac{X^{B1}}{2}\right) + \left(lnX^{C1} - \frac{X^{C1}}{2}\right) + \left(lnX^{D1} - \frac{X^{D1}}{2}\right) + 2\right\} \\
+ \quad & x_1\left\{\left(\frac{1}{X^{A1}} - \frac{1}{2}\right)\frac{\partial X^{A1}}{\partial x_1} + \left(\frac{1}{X^{B1}} - \frac{1}{2}\right)\frac{\partial X^{B1}}{\partial x_1} + \left(\frac{1}{X^{C1}} - \frac{1}{2}\right)\frac{\partial X^{C1}}{\partial x_1} + \left(\frac{1}{X^{D1}} - \frac{1}{2}\right)\frac{\partial X^{D1}}{\partial x_1}\right\} \\
+ \quad & x_2\left\{\left(\frac{1}{X^{A2}} - \frac{1}{2}\right)\frac{\partial X^{A2}}{\partial x_1} + \left(\frac{1}{X^{B2}} - \frac{1}{2}\right)\frac{\partial X^{B2}}{\partial x_1} + \left(\frac{1}{X^{C2}} - \frac{1}{2}\right)\frac{\partial X^{C2}}{\partial x_1}\right\} \\
+ \quad & x_3\left\{\left(\frac{1}{X^{A3}} - \frac{1}{2}\right)\frac{\partial X^{A3}}{\partial x_1} + \left(\frac{1}{X^{B3}} - \frac{1}{2}\right)\frac{\partial X^{B3}}{\partial x_1}\right\} \Bigg]
\end{aligned}$$

Similarly the equations are also written for $\frac{\partial H}{\partial x_2}$ and $\frac{\partial H}{\partial x_3}$

$$\frac{\partial X^{A1}}{\partial x_1} = -\left(X^{A1^{2}}\right)\Bigg[\rho\{X^{C1}\Delta^{A1C1} + X^{D1}\Delta^{D1C1} + x_1\left(\frac{\partial X^{C1}}{\partial x_1}\Delta^{A1C1} + \frac{\partial X^{D1}}{\partial x_1}\Delta^{A1D1}\right) + x_2\left(\frac{\partial X^{C2}}{\partial x_1}\Delta^{A1C2}\right)$$
$$+ x_1\left(X^{C1}\frac{\partial \Delta^{A1C1}}{\partial x_1} + X^{D1}\frac{\partial \Delta^{A1D1}}{\partial x_1}\right) + x_2\left(X^{C2}\frac{\partial \Delta^{A1C2}}{\partial x_1}\right)\Bigg]$$

Similarly equation are written for $\frac{\partial X^{A2}}{\partial x_1}$ $\frac{\partial X^{B1}}{\partial x_1}$…..$\frac{\partial X^{B3}}{\partial x_1}$and $\frac{\partial X^{A1}}{\partial x_2}$….$\frac{\partial X^{B1}}{\partial x_2}$…$\frac{\partial X^{B3}}{\partial x_3}$

$$\frac{\partial X^{A1}}{\partial \rho} = -\left(X^{A1^{2}}\right)\Bigg[\{x_1(X^{C1}\Delta^{A1C1} + X^{D1}\Delta^{D1C1}) + x_2\, X^{C2}\Delta^{A1C2}$$
$$+ \qquad x_1\left(\frac{\partial X^{C1}}{\partial \rho}\Delta^{A1C1} + \frac{\partial X^{D1}}{\partial \rho}\Delta^{A1D1}\right) + x_2\left(\frac{\partial X^{C2}}{\partial \rho}\Delta^{A1C2}\right)$$
$$+ \qquad x_1\left(X^{C1}\frac{\partial \Delta^{A1C1}}{\partial \rho} + X^{D1}\frac{\partial \Delta^{A1D1}}{\partial \rho}\right) + x_2\left(X^{C2}\frac{\partial \Delta^{A1C2}}{\partial \rho}\right)\Bigg]$$

APPENDIX – C

Calculation Procedure

The vapor liquid equilibrium calculations used in this work are made by simultaneously solving the non-linear equations. The equilibrium calculations were made by satisfying the three equilibrium criterion namely, chemical, thermal and mechanical. The fugacity and Pressure equation used for calculation are provided below.

The purpose of phase equilibrium thermodynamics is to predict conditions (temperature, pressure, composition) which exist when two or more phases are in equilibrium.

- ☐ Equality of Temperature $T^{\alpha} = T^{\beta}$ (Thermal equilibrium)
- ☐ Equality of Pressure $P^{\alpha} = P^{\beta}$ (Mechanical equilibrium)
- ☐ Equality of chemical potential $\mu_i^{\alpha} = \mu_i^{\beta}$ (Chemical equilibrium)

$$f_i^{\alpha} = f_i^{\beta}$$

(Each component i)

$$RT\ln\varphi_i = RT\ln\frac{f_i}{y_iP} = \left(\frac{\partial A^{res}}{\partial n_i}\right)_{T,V,n_j} - RT\ln Z$$

$$Z = \frac{PV}{nRT}$$

$$P = \frac{nRT}{V} - \left(\frac{\partial A^{res}}{\partial V}\right)_{T,n}$$

The generalized model was coded in MATLAB® which is developed not only for dimethyl ether mixtures but for any polar hydrocarbon mixtures. The model includes various configurations for polar and associating components and hence depending on the nature of the mixture it can be used for quantitative predictions by altering those configurations. The final form of the developed code is easily extensible and could be used for calculating various other thermodynamic properties.

NOMENCLATURE

A : Helmholtz free energy

d_{ij} : Average diameter of segments i and j

f : Fugacity

k : Boltzmann constant (J/K)

k_{ij} : Binary interaction parameter

m : Number of segments

M : Weight-average molar mass (g/mol)

N : Number of particles

P : Pressure

T : Absolute temperature (K)

v^{00} : Segment molar volume

x_p : Fraction of dipole segment in a molecule

φ : Fugacity coefficient

u^0/k : Temperature independent square well depth

k^{AB} : Association volume

ε^{AB} : Association energy

μ_i^{*2} : Squared dimensionless dipole moment

$J_{2,ij}^{DD}$: The intergral on the 2-body correlation function

$J_{3,ij}^{DD}$: The intergral on the 3-body correlation function

η : Dimensionless density.

ω_i : A set of two molecular orientation angles $\{\theta_i$ and $\varphi_i\}$

$r_{\alpha\beta}$: The distance between two LJ sites of different molecules i and j

μ_i : Dipole moment

θ_i : Polar angle of the dipole formed with the vector r_{ij}

φ_i : Azimuthal angle

N : Total number of molecules and

A^{2CLJ} : Residual Helmholtz energy of the 2CLJ reference fluid.

A^{DD} : Contribution from the dipole-dipole interaction

ϱ_s : The molar density of hard sphere fluid.

d : Effective hard sphere diameter of segment.

N_{AV} : Avogadro number.

R : Gas constant, T denotes the temperature.

c : Adjusted parameter, taken to be 0.333

a_0^{disp} : Segment's dispersive Helmholtz energy

D_{ij} : The segment-segment attraction is assumed to be the square well potential

Z_M : Maximum coordination number which is taken to be 36

$g^{hs}(d)$: The radial distribution function for the hard sphere.

X^A : The fraction of un-bonded associations sites A

M : The number of association sites in a molecule.

M_i : Total number of association sites in a component i

Δ^{AB} : The association strength between two sites A and B.

k_{ij} : Adjustable binary interaction parameter

L^{*} : Dimensionless molecular elongation

Superscripts

assoc	association term
chain	chain term
DD	dipole-dipole
disp	dispersion term
hs	hard sphere

Subscripts

ijk	components
cal.	calculated
exp.	experimental

REFERENCES

[1] M. S. Dresselhaus and I. L. Thomas, “Alternative energy technologies,” Nature, vol. 414, no. 6861, pp. 332–337, Nov. 2001.

[2] B. L. Salvi, K. A. Subramanian, and N. L. Panwar, “Alternative fuels for transportation vehicles: A technical review,” Renew. Sustain. Energy Rev., vol. 25, pp. 404–419, Sep. 2013.

[3] D. J. Santini, Encyclopedia of Energy. Elsevier, 2004, pp. 203–219.

[4] S. Moka, M. Pande, M. Rani, R. Gakhar, M. Sharma, J. Rani, and A. N. Bhaskarwar, “Alternative fuels: An overview of current trends and scope for future,” Renew. Sustain. Energy Rev., vol. 32, pp. 697–712, Apr. 2014.

[5] S. Bezergianni and A. Dimitriadis, “Comparison between different types of renewable diesel,” Renew. Sustain. Energy Rev., vol. 21, pp. 110–116, May 2013.

[6] G. Knothe, “Biodiesel and renewable diesel: A comparison,” Prog. Energy Combust. Sci., vol. 36, no. 3, pp. 364–373, Jun. 2010.

[7] T. A. Semelsberger, R. L. Borup, and H. L. Greene, “Dimethyl ether (DME) as an alternative fuel,” J. Power Sources, vol. 156, no. 2, pp. 497–511, Jun. 2006.

[8] W. Cho, T. Song, A. Mitsos, J. T. McKinnon, G. H. Ko, J. E. Tolsma, D. Denholm, and T. Park, “Optimal design and operation of a natural gas tri-reforming reactor for DME synthesis,” Catal. Today, vol. 139, no. 4, pp. 261–267, Jan. 2009.

[9] I. H. Kim, S. Kim, W. Cho, and E. S. Yoon, 20th European Symposium on Computer Aided Process Engineering, vol. 28. Elsevier, 2010, pp. 799–804.

[10] F. REN, J.-F. WANG, and H.-S. LI, “Direct mass production technique of dimethyl ether from synthesis gas in a circulating slurry bed reactor,” Stud. Surf. Sci. Catal., pp. 489–492.

[11] “National Center for Biotechnology Information,” PubChem Open Chemistry Database. p. CID 8254, 2015.

[12] J. G. Speight, Perry’s Standard Tables and Formulas for Chemical Engineers,. New York: McGraw-Hill, 2003.

[13] H. S. H. M.Q. Wang, “A full fuel-cycle analysis of energy and emission impacts of transportation fuels produced form natural gas,” 1999.

[14] H. S. B. John, “Fuels and Fuel Processing Options for Fuel Cells,” 2004.

[15] D. J. W. D.A. Good, J.S. Francisco, A.K. Jain, “No Title,” J. Geophys. Res, vol. 103, pp. 28181–28186, 1998.

[16] D.-Y. Peng and D. B. Robinson, “A New Two-Constant Equation of State,” Ind. & Eng. Chem. Fundam., vol. 15, no. 1, pp. 59–64, 1976.

[17] J. Wu and J. M. Prausnitz, “Phase Equilibria for Systems Containing Hydrocarbons, Water, and Salt: An Extended Peng−Robinson Equation of State,” Ind. & Eng. Chem. Res., vol. 37, no. 5, pp. 1634–1643, 1991.

[18] W. G. Chapman, K. E. Gubbins, G. Jackson, and M. Radosz, “New reference equation of state for associating liquids,” Ind. Eng. Chem. Res., vol. 29, no. 8, pp. 1709–1721, Aug. 1990.

[19] Y.-H. Fu and S. I. Sandler, “A Simplified SAFT Equation of State for Associating Compounds and Mixtures,” Ind. Eng. Chem. Res., vol. 34, no. 5, pp. 1897–1909, May 1995.

[20] P. K. and W. C. Jog, “Application of Wertheim’s thermodyncamic perturbation theory to dipolar hard sphere chains,” Mol. Phys., vol. 97, no. 3, pp. 307–319, 1999.

[21] J. Gross and J. Vrabec, “An equation-of-state contribution for polar components: Dipolar molecules,” AIChE J., vol. 52, no. 3, pp. 1194–1204, Mar. 2006.

[22] M. S. Wertheim, “Fluids with highly directional attractive forces. II. Thermodynamic perturbation theory and integral equations,” J. Stat. Phys., vol. 35, no. 1–2, pp. 35–47, 1984.

[23] M. S. Wertheim, “Fluids with highly directional attractive forces. I. Statistical thermodynamics,” J. Stat. Phys., vol. 35, no. 1–2, pp. 19–34, 1984.

[24] M. S. Wertheim, “Fluids with highly directional attractive forces. III. Multiple attraction sites,” J. Stat. Phys., vol. 42, no. 3–4, pp. 459–476, 1986.

[25] M. S. Wertheim, “Fluids with highly directional attractive forces. IV. Equilibrium polymerization,” J. Stat. Phys., vol. 42, no. 3–4, pp. 477–492, 1986.

[26] W. G. Chapman, G. Jackson, and K. E. Gubbins, “Phase equilibria of associating fluids,” Mol. Phys., vol. 65, no. 5, pp. 1057–1079Molecular Physics, Dec. 1988.

[27] W. G. Chapman, K. E. Gubbins, G. Jackson, and M. Radosz, “SAFT: Equation-of-state solution model for associating fluids,” Fluid Phase Equilibria, vol. 52. pp. 31–38, 1989.

[28] J. G. and Gabriele Sadowski, "Perturbed-Chain SAFT: An Equation of State Based on a Perturbation Theory for Chain Molecules," Ind. Eng. Chem. Res., vol. 40, no. 2, p. 1244, 2001.

[29] C. J. Gregg, S. Chen, F. P. Stein, and M. Radosz, "Phase behavior of binary ethylene-propylene copolymer solutions in sub- and supercritical ethylene and propylene," Fluid Phase Equilib., vol. 83, pp. 375–382, Feb. 1993.

[30] S. J. Chen, I. G. Economou, and M. Radosz, "Density-tuned polyolefin phase equilibria. 2. Multicomponent solutions of alternating poly(ethylene-propylene) in subcritical and supercritical olefins. Experiment and SAFT model," Macromolecules, vol. 25, no. 19, pp. 4987–4995, Sep. 1992.

[31] S. H. Huang and M. Radosz, "Equation of state for small, large, polydisperse, and associating molecules: extension to fluid mixtures," Ind. Eng. Chem. Res., vol. 30, no. 8, pp. 1994–2005, Aug. 1991.

[32] S. H. Huang and M. Radosz, "Phase behavior of reservoir fluids III: Molecular lumping and characterization," Fluid Phase Equilibria, vol. 66. pp. 1–21, 1991.

[33] S. H. Huang and M. Radosz, "Equation of state for small, large, polydisperse and associating molecules," Ind. Eng. Chem. Res., vol. 29, pp. 2284–2294, 1990.

[34] C.-S. Wu and Y.-P. Chen, "Calculation of vapor-liquid equilibria of polymer solutions using the SAFT equation of state," Fluid Phase Equilib., vol. 100, pp. 103–119, Sep. 1994.

[35] S.-J. Chen, I. G. Economou, and M. Radosz, "Phase behavior of LCST and UCST solutions of branchy copolymers: experiment and SAFT modelling," Fluid Phase Equilib., vol. 83, pp. 391–398, Feb. 1993.

[36] S. -j. Chen, Y. C. Chiew, J. A. Gardecki, S. Nilsen, and M. Radosz, "P-V-T properties of alternating poly(ethylene-propylene) liquids," J. Polym. Sci. Part B Polym. Phys., vol. 32, no. 10, pp. 1791–1798, Jul. 1994.

[37] S. Chen, M. Banaszak, and M. Radosz, "Phase Behavior of Poly(ethylene-1-butene) in Subcritical and Supercritical Propane: Ethyl Branches Reduce Segment Energy and Enhance Miscibility," Macromolecules, vol. 28, no. 6, pp. 1812–1817, Mar. 1995.

[38] G. K. F. Georgios M. Kontogeorgis, Thermodynamic Models for Industrial Applications: From Classical and Advanced Mixing Rules to Association Theories. Wiley, 2010, p. 710.

[39] T. Kraska and K. E. Gubbins, "Phase Equilibria Calculations with a Modified SAFT Equation of State. 1. Pure Alkanes, Alkanols, and Water," Ind. Eng. Chem. Res., vol. 35, no. 12, pp. 4727–4737, Jan. 1996.

[40] T. Kraska and K. E. Gubbins, “Phase Equilibria Calculations with a Modified SAFT Equation of State. 2. Binary Mixtures of n-Alkanes, 1-Alkanols, and Water,” Ind. Eng. Chem. Res., vol. 35, no. 12, pp. 4738–4746, Jan. 1996.

[41] D. NguyenHuynh, J.-P. Passarello, P. Tobaly, and J.-C. de Hemptinne, “Application of GC-SAFT EOS to polar systems using a segment approach,” Fluid Phase Equilib., vol. 264, no. 1–2, pp. 62–75, Mar. 2008.

[42] A. N. B. A. Gil-Vilegas, A. Galindo, P.J. Whitehead, S.J. Mills, G. Jackson, “No Title,” J Chem Phys, vol. 106, p. 4168, 1997.

[43] G. J. C. McCabe, A. Gil-Vilegas, “No,” Chem Phys Lett., vol. 303, no. 27, 1999.

[44] L. F. V. F.J. Blas, “No Title,” 1998, vol. 37, no. 360.

[45] M. L. M. A. Tihic, G.M. Kontogeorgis, N. von Solms, “No Title,” Fluid Phase Equilib., vol. 248, p. 29, 2006.

[46] G. M. K. N. von Solms, M.L. Michelsen, “No Title,” Ind. Eng. Chem. Res., vol. 42, p. 1098, 2003.

[47] E. M. H. M.L. Michelsen, “No Title,” Fluid Phase Equilib., vol. 180, no. 1–2, p. 165, 2001.

[48] S. Tamouza, J.-P. Passarello, P. Tobaly, and J.-C. de Hemptinne, “Group contribution method with SAFT EOS applied to vapor liquid equilibria of various hydrocarbon series,” Fluid Phase Equilib., vol. 222–223, pp. 67–76, Aug. 2004.

[49] S. Tamouza, J.-P. Passarello, P. Tobaly, and J.-C. de Hemptinne, “Application to binary mixtures of a group contribution SAFT EOS (GC-SAFT),” Fluid Phase Equilib., vol. 228–229, pp. 409–419, Feb. 2005.

[50] T. X. Nguyen Thi, S. Tamouza, P. Tobaly, J.-P. Passarello, and J.-C. de Hemptinne, “Application of group contribution SAFT equation of state (GC-SAFT) to model phase behaviour of light and heavy esters,” Fluid Phase Equilib., vol. 238, no. 2, pp. 254–261, Dec. 2005.

[51] F. S. Emami, A. Vahid, J. R. Elliott, and F. Feyzi, “Group Contribution Prediction of Vapor Pressure with Statistical Associating Fluid Theory, Perturbed-Chain Statistical Associating Fluid Theory, and Elliott−Suresh−Donohue Equations of State,” Ind. & Eng. Chem. Res., vol. 47, no. 21, pp. 8401–8411, 2008.

[52] C. Le Thi, S. Tamouza, J.-P. Passarello, P. Tobaly, and J.-C. de Hemptinne, “Modeling Phase Equilibrium of H2 + n-Alkane and CO2 + n-Alkane Binary Mixtures Using a Group Contribution Statistical Association Fluid Theory Equation of State

(GC−SAFT−EOS) with a kij Group Contribution Method," Ind. & Eng. Chem. Res., vol. 45, no. 20, pp. 6803–6810, 2006.

[53] D. N. Huynh, M. Benamira, J.-P. Passarello, P. Tobaly, and J.-C. de Hemptinne, "Application of GC-SAFT EOS to polycyclic aromatic hydrocarbons," Fluid Phase Equilib., vol. 254, no. 1–2, pp. 60–66, Jun. 2007.

[54] A. Tihic, G. M. Kontogeorgis, N. von Solms, M. L. Michelsen, and L. Constantinou, "A Predictive Group-Contribution Simplified PC-SAFT Equation of State: Application to Polymer Systems," Ind. Eng. Chem. Res., vol. 47, no. 15, pp. 5092–5101, Dec. 2007.

[55] G. J. A. Lymperiadis, C.S. Adjiman, A. Galindo, "A group contribution method for associating chain molecules based on the statistical associating fluid theory (SAFT-γ)," J Chem Phys, vol. 127, p. 234903, 2007.

[56] P. Paricaud, A. Galindo, and G. Jackson, "Recent advances in the use of the SAFT approach in describing electrolytes, interfaces, liquid crystals and polymers," Fluid Phase Equilib., vol. 194–197, pp. 87–96, Mar. 2002.

[57] E. a Müller and K. E. Gubbins, "Molecular-based equations of state for associating fluids: A review of SAFT and related approaches," Ind. Eng. Chem. Res., vol. 40, pp. 2193–2211, 2001.

[58] I. G. Economou, "Statistical Associating Fluid Theory: A Successful Model for the Calculation of Thermodynamic and Phase Equilibrium Properties of Complex Fluid Mixtures," Ind. & Eng. Chem. Res., vol. 41, no. 5, pp. 953–962, 2002.

[59] Y. S. Wei and R. J. Sadus, "Equations of state for the calculation of fluid-phase equilibria," AIChE J., vol. 46, no. 1, pp. 169–196, 2000.

[60] M. R. S.P. Tan, H. Adidharma, "No Title," Ind. Eng. Chem. Res., vol. 47, p. 8063, 2008.

[61] A. K. W. Arlt, O. Spuhl, "No Title," Chem. Eng. Process., vol. 43, p. 221, 2004.

[62] G. M. K. N. Von Solms, I. Kouskoumvekaki, M.L. Michelsen, "No Title," Fluid Phase Equilib., vol. 241, p. 344, 2006.

[63] R. I. J.C. De Hemptinne, P. Mougin, A. Barreau, L. Ruffine, S. Tamouza, "No Title," Oil Gas Sci Technol-Rev, vol. 61, p. 363, 2006.

[64] A. G. C. G. B. Behzadi, B.H. Patel, "No Title," Fluid Phase Equilib., vol. 236, p. 241, 2005.

[65] G. C. M. B.H. Patel, P. Paricaud, A. Galindo, “No Title,” Ind. Eng. Chem. Res., vol. 42, p. 3809, 2003.

[66] J. M. M. L.F. Cameretti, G. Sadowski, “No Title,” Ind. Eng. Chem. Res., vol. 44, p. 3355, 2005.

[67] G. S. D. Fuchs, J. Fischer, F. Tumakaka, “D. Fuchs, J. Fischer, F. Tumakaka, G. Sadowski,” Ind. Eng. Chem. Res., vol. 45, p. 6578, 2006.

[68] Y. Lin, K. Thomsen, and J. de Hemptinne, “Multicomponent equations of state for electrolytes,” AIChE J., vol. 53, no. 4, pp. 989–1005, 2007.

[69] I. G. Economou and C. Tsonopoulos, “Associating models and mixing rules in equations of state for water/hydrocarbon mixtures,” Chem. Eng. Sci., vol. 52, no. 4, pp. 511–525, Feb. 1997.

[70] F. J. Blas and L. F. Vega, “Prediction of Binary and Ternary Diagrams Using the Statistical Associating Fluid Theory (SAFT) Equation of State,” Ind. Eng. Chem. Res., vol. 37, no. 2, pp. 660–674, Jan. 1998.

[71] L. R. Pratt and D. Chandler, “Theory of the hydrophobic effect ,” J. Chem. Phys., vol. 67, no. 8, p. 3683, 1977.

[72] N. M. Alsaifi, G. N. Patey, and P. Englezos, “A General Treatment of Polar-Polarizable Systems for an Equation of State,” Chem. Eng. Res. Des., vol. Special Ed, p. Accepted, 2014.

[73] N. M. Alsaifi and P. Englezos, “Prediction of multiphase equilibrium using the PC-SAFT equation of state and simultaneous testing of phase stability,” Fluid Phase Equilib., vol. 302, no. 1–2, pp. 169–178, 2011.

[74] P. K. Jog, S. G. Sauer, J. Blaesing, and W. G. Chapman, “Application of Dipolar Chain Theory to the Phase Behavior of Polar Fluids and Mixtures,” Ind. Eng. Chem. Res., vol. 40, no. 21, pp. 4641–4648, Sep. 2001.

[75] F. Tumakaka and G. Sadowski, “Application of the Perturbed-Chain SAFT equation of state to polar systems,” Fluid Phase Equilib., vol. 217, no. 2, pp. 233–239, Mar. 2004.

[76] F. Tumakaka, J. Gross, and G. Sadowski, “Thermodynamic modeling of complex systems using PC-SAFT,” Fluid Phase Equilib., vol. 228–229, pp. 89–98, Feb. 2005.

[77] S. G. Sauer and W. G. Chapman, “A Parametric Study of Dipolar Chain Theory with Applications to Ketone Mixtures,” Ind. Eng. Chem. Res., vol. 42, no. 22, pp. 5687–5696, Oct. 2003.

[78] I. G. E. E.K. Karakatsani, “No Title,” J. Phys. Chem., vol. 110, p. 9252, 2006.

[79] I. G. E. E.K. Karakatsani, T. Spyriouni, “No Title,” AIChE J., vol. 51, no. 2328, 2005.

[80] I. G. E. E.K. Karakatsani, G.M. Kontogeorgis, “No Title,” Ind. Eng. Chem. Res., vol. 45, no. 17, p. 6063, 2006.

[81] J. V. J. Gross, “No Title,” AIChE J., vol. 52, p. 1194, 2006.

[82] J. Gross, “No Title,” AIChE J., vol. 51, no. 2556, 2005.

[83] J. G. M. Kleiner, “No Title,” AIChE J., vol. 52, no. 1951, 2006.

[84] I. G. E. E.K. Karakatsani, “No Title,” Fluid Phase Equilib., vol. 261, p. 265, 2007.

[85] P. D. KIM, CH.: Vimalchand, “Composition of model for chain like molecules: A new simplified version of perturbed hard chain theory.,” AIChE J., vol. 32, pp. 1726–1734, 1986.

[86] F. Tumakaka and G. Sadowski, “Application of the Perturbed-Chain SAFT equation of state to polar systems,” Fluid Phase Equilib., vol. 217, no. 2, pp. 233–239, Mar. 2004.

[87] A. Dominik, W. G. Chapman, M. Kleiner, and G. Sadowski, “Modeling of Polar Systems with the Perturbed-Chain SAFT Equation of State. Investigation of the Performance of Two Polar Terms,” Ind. Eng. Chem. Res., vol. 44, no. 17, pp. 6928–6938, Aug. 2005.

[88] J. Gross, “An equation-of-state contribution for polar components: Quadrupolar molecules,” AIChE J., vol. 51, no. 9, pp. 2556–2568, Sep. 2005.

[89] E. K. Karakatsani, T. Spyriouni, and I. G. Economou, “Extended statistical associating fluid theory (SAFT) equations of state for dipolar fluids,” AIChE J., vol. 51, no. 8, pp. 2328–2342, Aug. 2005.

[90] J. Vijande, M. M. Piñeiro, D. Bessières, H. Saint-Guirons, and J. L. Legido, “Description of PVT behaviour of hydrofluoroethers using the PC-SAFT EOS,” Phys. Chem. Chem. Phys., vol. 6, no. 4, pp. 766–770, 2004.

[91] J. S. RUSHBROOKE, G. S. STELL, G., HOYE, “Molecular Physics: An International Journal at the Interface Between Chemistry and Physics,” Mol. Phys., vol. 26, no. 1199, 1973.

[92] J. A. B. and D. Henderson, “Perturbation Theory and Equation of State for Fluids. II. A Successful Theory of Liquids,” J Chem Phys, vol. 47, no. 4714, 1967.

[93] K. E. Gubbins and C. H. Twu, “Thermodynamics of polyatomic fluid mixtures—I theory,” Chem. Eng. Sci., vol. 33, no. 7, pp. 863–878, Jan. 1978.

[94] J. Gross and G. Sadowski, “Perturbed-Chain SAFT: An Equation of State Based on a Perturbation Theory for Chain Molecules,” Ind. Eng. Chem. Res., vol. 40, pp. 1244–1260, 2001.

[95] B. Saager and J. Fischer, “Construction and application of physically based equations of state,” Fluid Phase Equilib., vol. 72, pp. 67–88, Mar. 1992.

[96] T. Boublik, “Perturbation theory of pure quadrupolar hard gaussian overlap fluids,” Mol. Phys., vol. 69, no. 3, pp. 497–505, 1990.

[97] M. Lupkowski and P. A. Monson, “Structure and thermodynamics of polar interaction site fluids,” Mol. Phys., vol. 63, no. 5, pp. 875–890, 1988.

[98] D. B. McGuigan, M. Lupkowski, D. M. Paquet, and P. A. Monson, “Phase diagrams of interaction site fluids,” Mol. Phys., vol. 67, no. 1, pp. 33–52, 1989.

[99] B. Saager, J. Fischer, and M. Neumann, “Reaction Field Simulations of Monatomic and Diatomic Dipolar Fluids,” Mol. Simul., vol. 6, no. 1–3, pp. 27–49, 1991.

[100] J. F. Berthold Saager, “Construction and application of physically based equations of state: Part II. The dipolar and quadrupolar contributions to the Helmholtz energy,” Fluid Phase Equilib., vol. 72, pp. 67–68, 1992.

[101] N. H. Stell G, Rasaiah JC, “Thermodyncamic petrurbation theory for simpler fluids,” Mol. Phys., vol. 27, pp. 1393–1414, 1974.

[102] M. G. K. F Stephnopolous, “No Title,” Mol. Phys., vol. 30, p. 1649, 1975.

[103] R. A. M. Nelder, J.A., “No Title,” Comput J., vol. 7, p. 308, 1965.

[104] N. . Vargaftik, Table on Thermophysical properties of liquid and gases. New York: John Wiley & Sons, Inc., 1975.

[105] S. Glos, R. Kleinrahm, and W. Wagner, “Measurement of the (p,ρ,T) relation of propane, propylene, n-butane, and isobutane in the temperature range from (95 to 340) K at pressures up to 12 MPa using an accurate two-sinker densimeter,” J. Chem. Thermodyn., vol. 36, no. 12, pp. 1037–1059, Dec. 2004.

[106] J. H. Weber and A. C. E. Journal, “THERMODYNAMIC PROPERTIES OF 1-BUTENE,” AIChE J., vol. 730, pp. 210–214, 1955.

[107] E. C. Morris and R. G. Wylie, “The PVT properties of nitrogen from −20 to +35 °C and 200 to 570 MPa, and some comparisons with argon and the Lennard-Jones (6-12) fluid,” J. Chem. Phys., vol. 79, no. 6, p. 2982, 1983.

[108] D. W. G. R. Perry, Perrys Chemical Engineering Hadbook, 8th ed. McGraw-Hill, 2008, pp. 2–302.

[109] Thermodynamic-Tables-TexasAM, Thermodynamic tables for non-hydrocarbon. Themodyncamic research rcentre Texas AM university.

[110] Y. Takiguchi and M. Uematsu, “P V T Measurements of Liquid Ethanol in the Temperature Range from 310 to 363 K at Pressures up to 200 MPa ~,” vol. 14, no. 1, 1995.

[111] D. T.E., Data Compilation Tables of properties of Pure compunds. New York: Design Institute for physical property data, AMerical Institute of Chemical Engineers, 1985.

[112] Car L Yaws, Yaws handbook of thermodynamic and physical properties of chemical compunds. Gulf publishing company, 2003.

[113] D. M. J.M. Junquera-Hernandez J. Sanchez-Mar, “Molecular electric quadrupole moments calculated with matrix dressed SDCI,” Chem Phys Lett., vol. 359, pp. 343–348, 2002.

[114] A. T. Sundberg, P. Uusi-Kyyny, M. Pakkanen, and V. Alopaeus, “Vapor−Liquid Equilibrium for Methoxymethane + Methyl Formate, Methoxymethane + Hexane, and Methyl Formate + Methanol,” J. Chem. & Eng. Data, vol. 56, no. 5, pp. 2634–2640, 2011.

[115] S. Horstmann, G. Birke, K. Fischer, and Ag, “Vapor - Liquid Equilibrium and Excess Enthalpy Data for the Binary at Temperatures from (298 to 323) K,” J. Chem. Eng. Data, vol. 49, pp. 38–42, 2004.

[116] W. B. Streett, “Vapor-liquid equilibria in the binary system dimethyl ether + n-butane from 282 . 9 to 414 . 5 K at pressures to 4 . 82 MPa,” Fluid Phase Equilib., vol. 74, pp. 289–302, 1992.

[117] M. M. Elbaccouch and J. R. Elliott, “High-Pressure Vapor - Liquid Equilibrium for Dimethyl Ether + 2-Propanol and Dimethyl Ether + 2-Propanol + Water,” J. Chem. Eng. Data, pp. 675–678, 2001.

[118] E. Chang, J. C. Calado, and W. B. Stroett, “Vapor-Liquid Equilibrium in the System Dimethyl Ether / Methanoi from 0 to 180 “ C and at Pressures to 6 . 7 MPa,” J. Chem. Eng. Data, vol. 27, pp. 293–298, 1982.

[119] S. Park and K. Han, “Vapor - Liquid Equilibria and H E for Binary Systems of Dimethyl Ether (DME) with C 1 - C 4 Alkan-1-ols at 323 . 15 K and Liquid - Liquid Equilibria for Ternary System of DME + Methanol + Water at 313 . 15 K,” J. Chem. Eng. Data, vol. 52, pp. 230–234, 2007.

[120] M. E. Pozo and W. B. Streett, “Fluid phase equilibria for the system dimethyl ether/water from 50 to 220.degree.C and pressures to 50.9 MPa,” J. Chem. Eng. Data, vol. 29, no. 3, pp. 324–329, 1984.

[121] R. L. F. Van Konynenberg, P. H.; Scott, “Critical lines and phase equilibria in binary van der Waals mixtures,” Trans. R. SOC, vol. 298, no. 1442, pp. 495–590, 1980.

[122] I. K. M. Fermlia, “Excess enthalpy calculation y means of equation of state,” jounal Therm. Anal., vol. 29, pp. 687–695, 1984.

[123] M. Teodorescu and P. Rasmussen, “High-Pressure Vapor−Liquid Equilibria in the Systems Nitrogen + Dimethyl Ether, Methanol + Dimethyl Ether, Carbon Dioxide + Dimethyl Ether + Methanol, and Nitrogen + Dimethyl Ether + Methanol,” J. Chem. & Eng. Data, vol. 46, no. 3, pp. 640–646, 2001.

[124] A. Ghosh, W. G. Chapman, and R. N. French, “Gas solubility in hydrocarbons—a SAFT-based approach,” Fluid Phase Equilib., vol. 209, no. 2, pp. 229–243, Jul. 2003.

[125] A. Jonasson and O. Persson, “High-pressure Solubility of Hydrogen in Dimethyl Ether,” J. Chem. Eng. Data, no. 1, pp. 1209–1210, 1996.

[126] C. Y. Tsangt and W. Streett, “Vapor-Liquid Equilibrium in the System Carbon Dioxide/Dimet h yl Ether,” J. Chem. Eng. Data, vol. 26, pp. 155–159, 1981.

[127] A. Jnasson, O. Persson, and A. Fredenslund, “High Pressure Solubility of Carbon dioxide and Carbon Monoxide in Dimethyl Ehter,” J. Chem. Eng. Data, vol. 40, no. 1, pp. 296–300, 1995.

Vitae

Name : SAIFUDDIN AHMED

Nationality : INDIAN

Date of Birth : 17-Dec-1991

Email : saifuddin.ahmed@live.com

Address : 536 Kha/65
Makkaganj, Lucknow
Uttar Pradesh - India

Academic Background : MS Chemical Engineering,
KFUPM, Saudi Arabia – Feb 2015
B.Tech Petrochemical Engineering,
AMU, India - June 2012

Papers

Saifi, Nayef Al, and **Saifuddin Ahmed**. *Prediction of Dissociation Pressure of Gas Hydrates for Gas Mixtures Using Theory-Based Equation of State*. Proc. of Gas Hydrate In Flow Assurance, UAE, 2014

Conference

Middle East Process Engineering Conference 2013, Bahrain, winner of the Process simulation competition organized by AIChE.